RELIABILITY EVALUATION OF POWER SYSTEMS CONSIDERING ELECTRIC VEHICLE CHARGING

NINGZHOU XU

Ph.D

The Hong Kong Polytechnic University

2015

The Hong Kong Polytechnic University
Department of Electrical Engineering

RELIABILITY EVALUATION OF POWER SYSTEMS CONSIDERING ELECTRIC VEHICLE CHARGING

NINGZHOU XU

A thesis submitted in partial fulfillment of the requirements for the degree of
Doctor of Philosophy

October, 2014

Certificate of Originality

I hereby declare that this thesis is my own work and that, to the best of my knowledge and belief, it reproduces no material previously published or written, nor material that has been accepted for the award of any other degree or diploma, except where due acknowledgement has been made in the text.

NINGZHOU XU

To my dear mother Qiu and father Yang

Abstract

Three issues in regard to reliability evaluation of power systems incorporating electric vehicles (EVs) are addressed in this thesis: Well-being analysis of generating systems considering EVs grid participation as interruptible load and spinning reserves; The uncertainties of EV charging and their effects on the well-being analysis of generating systems; Reliability evaluation of distribution systems incorporating EVs grid contribution.

With increasing demand for EV charging, power grids can take advantage of the distinctive features of EV charging load. In response to outages, the charging load can be interrupted with no penalty until additional generation becomes available, as long as charging requirements can be fulfilled, to improve system health. Moreover, EVs can further provide emergency capacities back to the grid (i.e. vehicle-to-grid (V2G)). The generating system operating health analysis is extended by taking EV charging into consideration. This is the first work that proposes the idea of EV charging being treated as interruptible load and serving as emergency units to improve system well-being. Numerical results show that V2G is more effective for well-being improvement than the interruptible EV charging. In the V2G enabled scenario, EVs are able to provide more capacities to help the system.

The contribution of EVs is uncertain because they serve both the power system and the transportation sector. Scheduled EV charging can be affected either by failures of components such as charging facilities, or by human errors such as punc-

tuality, rounding of time and errors in forecast of energy consumption. Moreover, with the introduction of the aggregator, the realization of EVs grid services also plays an important role. Major uncertainties that can affect EV charging are identified. They are punctuality, rounding of time, forecast error of energy consumption, charging component failure and EV absence, and aggregator failure and grid realization. Methodologies are developed to consider these elements in well-being analysis. As expected, results show the uncertainties identified directly affect EVs contribution to the system well-being.

The evaluation of reliability of the classical distribution system is also extended to incorporate the grid contribution of EVs in different modes of operation. For each load point, two topologies—centralized and dispersed EV charging—are considered. During the islanding mode of operation, household demand can be supported by vehicle-to-home (V2H) and/or local V2G, depending on the charging topologies applied. In grid connected mode of operation, energy not supplied can be further reduced by interregional V2G, which allows energy exchange among load points through healthy mains and laterals by sectionalizing the failure parts of the grid. Evaluation methods are proposed to determine the capacity contribution of EVs for each scenario. For the scenario of interregional V2G, optimal power flow is conducted to maximize the energy exchange. From the results of a case study, V2H and V2G, on both local and system levels, show great promise for reliability enhancement.

Acknowledgements

At the end of my normal study period, my supervisor, Prof. C. Y. Chung, left Hong Kong for his new position in Saskatchewan. Nearly two weeks have passed and I am writing this part as a final expedition in composing the thesis. As I was collecting thoughts for the past two weeks, memories kept flooding back.

Trust—I can not thank Prof. Chung enough for believing in me and giving me the chance to study as a research student. I am never good at examinations and my language skills were extremely poor at the beginning. It was Prof. Chung who took a chance on me so that I could prove myself worthy. It was also Prof. Chung who during the course of my pursuing the degree trusted me and allowed me with no hesitation to flexibly manage my own schedule, from which I really benefited in terms of study and living.

Wisdom—I am beholden to Prof. Chung for teaching me not only the expertise I needed but also the wisdom for problem solving. Every time he reviewed my work, each single grammatical mistake and spelling error was meticulously checked. On top of that, he taught me how to better the work with his judicious perception, grand vision and his surgically precise opinion. Very often reviewers' comments could be difficult to deal with or even harsh. Without Professor's brilliant solutions, I could not survive those hardships. I do and always will remember his teaching, such as "Think before doing!"

Patience—Just as Prof. Chung is passionate about power system research, he cares for his apprentices like his own children. Life hits us hard sometimes. With my capricious nature, situations worsened. I would rush to Professor's office rudely and hoped to seek some advice desperately. Despite his busy schedules 24/7, not one time had Professor complained. he never loses his patience. Instead, he would help me to track down the problem, peel layers of the onion off and offer suggestions rationally. Learning to be steady, is probably the most precious gift I have received from Professor.

Critical thinking—As I am sure many of his students would agree, Prof. Chung does not confine his efforts to conducting research. Throughout the years he was teaching numerous courses, giving lectures and presentations. Yet teaching materials were conscientiously prepared. "An equation is meaningless," he often said in the class,"unless you understand the physical meaning behind it!"

To put it rather crassly, I am deeply indebted to Prof. C. Y. Chung for the invaluable teaching, support and inspiration throughout the years. Words are not enough to express my gratitude and I can only say proper thanks to him through my future work.

Contents

List of Tables

List of Figures

List of Abbreviations and Symbols

Abbreviations (*in alphabetical order*)

Indices and Parameters

ACCI	Average customer curtailment index.
AENS	Average energy not supplied.
ASCI	Average system curtailment index.
ASAI	Average service availability index.
ASUI	Average service unavailability index.
CAIDI	Customer average interruption duration index.
CAIFI	Customer average interruption frequency index.
EIR	Energy index of reliability.
EIU	Energy index of unreliability.
ENS	Energy not supplied.
EENS	Expected energy not supply.
FOR	forced outage rate.
F&D	Frequency and duration.
LOEE	Loss of energy expectation.
LOLE	Loss of load expectation.
LOLP	Loss of load probability.
MTBF	Mean time between failures.
MTTF	Mean time to failure.

MTTR	Mean time to repair.
ORR	Outage replacement rate.
SAIDI	System average interruption duration index.
SAIFI	System average interruption frequency index.
UCR	Unit commitment risk.
UCRC	Unit commitment risk criterion.

Others

COPT	Capacity outage probability table.
DG	Distributed generation.
DLC	Direct load control.
DSM	Demand-side management.
EV	Electric vehicle.
GSOSR	Generating system operating state rick, identical to the unit commitment risk obtained by the basic PJM method.
HLI and HLI	Hierarchical Level I and II.
IEEE-RTS	IEEE Reliability Test System.
ISO	Independent system operator.
LFU	Load forecast uncertainty.
MCS	Monte Carlo simulation.
NHTS	National Household Travel Survey
PEV or PHEV	Plug-in electric vehicle or plug-in hybrid electric vehicle.
PJM	Pennsylvania-New Jersey-Maryland (USA) interconnected system.
PV	Photovoltaic.
RBTS	Roy Billinton Test System.
SAPS	Small autonomous power system.

SIPS	Small isolated power system.
SOC	State-of-charge of battery packs.
UPS	Uninterruptible power supply.
V2G	Vehicle-to-grid.
V2H	Vehicle-to-home.
VPP	Virtual power plant.
WT	Wind Turbine.

Symbols (*in order of appearance*)

Chapter 1

λ	Expected failure rates.
μ	Expected repair rates.
T	Cycle time.
λ_{s}	Average failure rate of a distribution system.
r_{s}	Average outage time of a distribution system.
U_{s}	Average annual outage time of a distribution system.
λ_{i}	Average failure rate of section i in a radial distribution system.
r_{i}	Average outage time of section i in a radial distribution system.
U_{i}	Average annual outage time of section i in a radial distribution system.

Chapter 2

P_{H}	Probability of healthy state.
P_{M}	Probability of marginal state.
P_{R}	Probability of at risk state.
P_{EH}	Equivalent probability of healthy state.
P_{EM}	Equivalent probability of marginal state.

P_{ER}	Equivalent probability of at risk state.
R_{a}	Partial risk between 0 and T_1 in an area risk curve.
R_{b}	Partial risk between T_1 and T_2 in an area risk curve.
R_{c}	Partial risk between T_3 and T_3 in an area risk curve.
$f(R)$	Risk function or area risk curve.
T_1	Lead times of interruptible load.
T_2	Lead times of rapid start units.
T_3	Lead times of additional generating units.
D_{r}	Total risk reduction.
t^i_{HA}	Home arrival time of EV i.
t^i_{HD}	Home departure time of EV i.
E^i_{D}	Energy depleted of EV i during its daily driving.
m	Number of EVs.
n	Number of time intervals in a calendar day.
p_{I}	Interruptible capacity for a period of interruption.
E_{I}	Maximum allowable energy loss of EV charging during charging interruption.
T_{I}	Duration for which EVs to be interrupted.
$e_{\mathrm{IC},i}$	Maximum energy loss of EV i due to interrupted charging.
$e_{\mathrm{SC},i}$	Maximum energy provided by supplementary charging for EV i.
$\mathbf{1}$	$1 \times 2n$ row matrix having all elements equal to one.
$\boldsymbol{t}_{\mathbf{I}}$	$1 \times 2n$ binary row matrix representing time period of charging interruption.
$\boldsymbol{e}_{\mathbf{IC}}$	$m \times 1$ column matrix representing maximum energy loss of EVs due to interrupted charging.
$\mathbf{P}_{\mathbf{OC}}$	$m \times 2n$ matrix representing power levels applied for original charging arrangement of EVs.

$\boldsymbol{e}_{\mathbf{SC}}$ — $m \times 1$ column matrix representing maximum energy provided by supplementary charging for EVs.

p_{O} — Power level of charging outlets (i.e. maximum EV charging level).

$\mathbf{T_A}$ — $m \times 2n$ binary matrix representing available charging periods of EVs.

$\boldsymbol{t}_{\mathbf{AI}}$ — $1 \times 2n$ binary row matrix representing time period after charging interruption.

p_{V2G} — Capacity for V2G.

E_{V2G} — Maximum allowable energy for V2G.

E_{EI} — V2G-equivalent maximum allowable energy loss during the interruption.

$e_{\mathrm{EIC},i}$ — V2G-equivalent maximum energy loss of EV i due to interrupted charging.

$\boldsymbol{e}_{\mathbf{EIC}}$ — $m \times 1$ column matrix representing V2G-equivalent energy loss of EVs due to interrupted charging.

$\boldsymbol{e}_{\mathbf{R}}$ — $m \times 1$ column matrix representing reverse energy of EVs available for V2G.

p_{R} — Capacity limit for reverse power flow.

$\boldsymbol{e}_{\mathbf{EV}}$ — $m \times 1$ column matrix representing state-of-charge (SOC) of EVs when interruption begins.

$\boldsymbol{e}_{\mathbf{F}}$ — $m \times 1$ column matrix representing full energy capacity of EVs.

$\boldsymbol{e}_{\mathbf{D}}$ — $m \times 1$ column matrix representing energy of EVs depleted for daily driving.

$\boldsymbol{t}_{\mathbf{BI}}$ — $1 \times 2n$ binary row matrix representing time period before charging interruption.

M^i — Daily mileage of EV i.

$\overline{S_{\mathrm{A}}}$ — Upper limit of daily average speed of EV i.

$\underline{S_{\mathrm{A}}}$ — Lower limit of daily average speed of EV i.

R_{A} — Average rate of electricity consumption of EVs.

L_{EV}	Penetration level of EV.
p_{syst}	System capacity.

Chapter 3

$P(.)$	Probability distribution function.
λ and μ	Failure and repair rates.
$f(R)$	Risk function.
m	Number of EVs.
n	Number of time intervals in a calendar day.
p_{I}	Interruptible capacity for a period of interruption.
E_{I}	Maximum allowable energy loss of EV charging during charging interruption.
T_{I}	Duration for which EVs to be interrupted.
$e_{\mathrm{IC},i}$	Maximum energy loss of EV i due to interrupted charging.
$e_{\mathrm{SC},i}$	Maximum energy provided by supplementary charging for EV i.
$\mathbf{1}$	$1 \times 2n$ row matrix having all elements equal to one.
$\boldsymbol{t}_{\mathbf{I}}$	$1 \times 2n$ binary row matrix representing time period of charging interruption.
$\boldsymbol{e}_{\mathbf{IC}}$	$m \times 1$ column matrix representing maximum energy loss of EVs due to interrupted charging.
$\mathbf{P}_{\mathbf{OC}}$	$m \times 2n$ matrix representing power levels applied for original charging arrangement of EVs.
$\boldsymbol{e}_{\mathbf{SC}}$	$m \times 1$ column matrix representing maximum energy provided by supplementary charging for EVs.
p_{O}	Power level of charging outlets.
$\mathbf{T}_{\mathbf{A}}$	$m \times 2n$ binary matrix representing available charging periods of EVs.
$\boldsymbol{t}_{\mathbf{AI}}$	$1 \times 2n$ binary row matrix representing time period after charging interruption.

p_{V2G}	Capacity for V2G.
E_{V2G}	Maximum allowable energy for V2G.
E_{EI}	V2G-equivalent maximum allowable energy loss during the interruption.
$e_{\mathrm{EIC},i}$	V2G-equivalent maximum energy loss of EV i due to interrupted charging.
$\boldsymbol{e}_{\mathbf{EIC}}$	$m \times 1$ column matrix representing V2G-equivalent energy loss of EVs due to interrupted charging.
$\boldsymbol{e}_{\mathbf{R}}$	$m \times 1$ column matrix representing reverse energy of EVs available for V2G.
p_{R}	Capacity limit for reverse power flow.
$\boldsymbol{e}_{\mathbf{EV}}$	$m \times 1$ column matrix representing state-of-charge (SOC) of EVs when interruption begins.
$\boldsymbol{e}_{\mathbf{F}}$	$m \times 1$ column matrix representing full SOC of EVs.
$\boldsymbol{e}_{\mathbf{D}}$	$m \times 1$ column matrix representing energy of EVs depleted for daily driving.
$\boldsymbol{t}_{\mathbf{BI}}$	$1 \times 2n$ binary row matrix representing time period before charging interruption.
t^i_{ETA}	Expected time of arrival of EV i.
t^i_{ETD}	Expected time of departure of EV i.
t^i_{ATA}	Actual time of arrival of EV i.
t^i_{ATD}	Actual time of departure of EV i.
$t^i_{\mathrm{Err,A}}$	Error of expected time of arrival of EV i.
$t^i_{\mathrm{Err,D}}$	Error of expected time of departure of EV i.
E^i_{FD}	Forecast value of daily energy depleted of EV i.
E^i_{AD}	Actual value of daily energy depleted of EV i.
M^i_{S}	Daily mileage reported in schedule of EV i.
M^i_{Err}	Error of reported daily mileage of EV i.
R_{FA}	Forecast value of average consumption rate of EVs.

R^{i}_{AA}	Actual value of average consumption rate of EV i.

Chapter 4

m	Number of EVs/households.
n	Number of time intervals in a calendar day.
k	Number of load points.
E_{B}	Total amount of energy backed up by EVs.
η	Efficiency of vehicle-to-grid (V2G) and vehicle-to-house (V2H).
$e_{\mathrm{R},i}$	Amount of reversible energy from EV i during the period of interruption.
$e_{\mathrm{lim},i}$	Upper limit for reversible energy of EV i during the period of interruption.
$\boldsymbol{e}_{\mathbf{R}}$	$m \times 1$ column matrix representing amounts of reversible energy from EVs.
$\boldsymbol{e}_{\mathbf{SC}}$	m column matrix representing amounts of energy that can be provided for supplementary charging of EVs.
p_{R}	Capacity limit for reverse power flow.
$\mathbf{T_A}$	$m \times n$ binary matrix representing available charging periods of EVs.
$\boldsymbol{t}_{\mathbf{I}}$	$1 \times n$ binary row matrix representing the time period of charging interruption.
$\boldsymbol{e}_{\mathbf{EV}}$	$m \times 1$ column matrix representing state-of-charge (SOC) of EVs when interruption begins.
$\boldsymbol{e}_{\mathbf{F}}$	$m \times 1$ column matrix representing full energy capacities of EVs.
$\boldsymbol{e}_{\mathbf{D}}$	$m \times 1$ column matrix representing energy of EVs depleted during daily driving.
$\mathbf{P_{OC}}$	$m \times n$ matrix representing power levels applied for original charging arrangement of EVs.
$\boldsymbol{t}_{\mathbf{BI}}$	$1 \times n$ binary row matrix representing the time period before charging interruption.

p_{O}	Power level of charging outlets (i.e. maximum EV charging level).
$\boldsymbol{t}_{\mathbf{AI}}$	$1 \times n$ binary row matrix representing the time period after charging interruption.
$\mathbf{1}$	$1 \times n$ row matrix having all elements equal to one.
$\boldsymbol{e}_{\mathbf{lim}}$	$m \times 1$ column matrix representing upper limits for reversible energy from EVs.
$\mathbf{P}_{\mathbf{H'}}$	$m \times n$ matrix representing trimmed power consumption profiles of households.
$\mathbf{P}_{\mathbf{H}}$	$m \times n$ matrix representing originally planned power consumption profiles of households.
$E_{\mathrm{B}}^{\mathrm{V2H}}$	Total amount of energy backed up through V2H.
$e_{\mathrm{V2H},i}$	Amount of energy backed up by EV through V2H.
$\boldsymbol{e}_{\mathbf{V2H}}$	$m \times 1$ column matrix representing amounts of energy of households backed up by EVs through V2H.
$E_{\mathrm{B}}^{\mathrm{LV2G}}$	Amount of energy backed up through local V2G.
$\mathrm{P}_{\mathrm{H'},ij}$	Power consumption level of household i at time j after the modification (i.e. the i, j entry of $\mathbf{P}_{\mathbf{H'}}$).
$\mathrm{T}_{\mathrm{A},ij}$	The i, j entry of $\mathbf{T}_{\mathbf{A}}$.
$\overline{E_{\mathrm{ex}}^{x}}$	Amount of energy can be exported from node x.
$\overline{s_{\mathrm{ex},j}^{x}}$	Power capacity left in node x for export at time j.
$\overline{E_{\mathrm{im}}^{x}}$	Energy not supplied in node x despite local V2G.
E_{im}^{x}	Amount of energy imported to node x.
$s_{\mathrm{im},j}^{x}$	Apparent power imported to node x at time j.
$s_{\mathrm{ex},j}^{x}$	Apparent power exported from node x at time j.
$p_{\mathrm{im},j}^{x}$	Active power imported to node x at time j.
$p_{\mathrm{ex},j}^{x}$	Active power exported from node x at time j.
$q_{\mathrm{im},j}^{x}$	Reactive power imported to node x at time j.
$q_{\mathrm{ex},j}^{x}$	Reactive power exported from node x at time j.

$\underline{p^x}$ and $\overline{p^x}$	Lower and upper limits of active power at node x.
$\underline{q^x}$ and $\overline{q^x}$	Lower and upper limits of reactive power at node x.
v^x	Voltage at node x.
$\underline{v^x}$ and $\overline{v^x}$	Lower and upper limits of voltage at node x.

1

Introduction

1.1 Backgrounds

The reliability of power supply is maintained by reserve generation capacity, i.e. spinning reserve or non-synchronized generation, which is also known as stand-by generation capacity comprising rapid start and hot reserve units [21]. In response to outages, a time delay (i.e. system lead time) is required before additional generation can be made available. On the other hand, electric vehicle (EV) charging is growing and has come to play a more influential role in the system nowadays. One of the distinctive features of EV charging is that it can be stopped during the lead time with no penalty as long as the charging can be compensated afterwards when additional generation is in service. Moreover, if vehicle-to-grid (V2G) is enabled, EVs are able to act like rapid start units for neutralizing the generation shortage. However, how much capacity can be freed by interrupting EV charging or how much power can be injected back into the grid and to what extent can this help improve the system reliability are yet to be discovered.

The electricity load becomes more flexible than before due to the rise of smart meters and proliferation of EVs population [97, 52, 98, 64]. Beyond being treated as interruptible load, EVs can even serve as standby units to improve system reliability through V2G. However, component failures as well as errors in travel schedule making and energy consumption forecasting makes EV charging uncertain, which have direct effects on EVs' capability as a provider of grid services. What the uncertain elements are and how they affect on EVs' role to improve system reliability are need to be found out.

EVs can serve as a source of energy for the grid in the forms of both V2H (vehicle-to-home) and V2G [85, 98, 64, 52]. During outages, an EV can power the house of its owner with its stored energy, i.e. V2H, and the surplus energy that goes to the grid can serve other houses within the local community or even in other regions, i.e. V2G. How EV charging can contribute to distribution system reliability in different modes of operation is yet to be known.

1.2 Introductions and Literature Reviews

1.2.1 Generating Capacity

The determination of the required amount of system generating capacity to ensure an adequate supply is an important aspect of power system planning and operating. The total problem can be divided into two conceptually different areas designed as static and operating capacity requirements. The fundamental difference between static and operating capacity evaluation is in the time period considered. The study of the static capacity requirements relates to the long-term evaluation of this overall system requirement. The study of the operating capacity relates to the short-term evaluation of the actual capacity required to meet a given load level. Both areas must be examined at the planning level as alternative facilities are evaluated. Once the decision has been made, however, the short-term requirement becomes an operating problem. As the thesis focuses on the short-term evaluation of the actual generating capacity, the assessment of operating capacity reserves is reviewed in the Subsection 1.2.2.

Static Capacity

The static requirement can be considered as the installed capacity that must be planned and constructed in advance of the system requirements. The static reserve must be sufficient to provide for the overhaul of generating equipment, outages that are not planned or scheduled and load growth requirements in excess of the estimates. A practice that has developed over many years is to measure the adequacy of both the planned and installed capacity in terms of a percentage reserve. An important objection to the use of the percentage reserve requirements criterion is the tendency to compare the relative adequacy of capacity requirements provided for totally different systems on the basis of peak loads experienced over the same time period for each system. Large differences in capacity requirements to provide the same assurance of service continuity may be required in two different systems with peak load of the same magnitude. This situation arises when the two systems being compared have different load characteristics and different types and sizes of installed or planned generating capacity.

The percentage reserve criterion also attaches no penalty to a unit because of size unless this quantity exceeds the total capacity reserve. The requirement that a reserve should be maintained equivalent to the capacity of the largest units on the system plus a fixed percentage of the total system capacity is a more valid adequacy criterion and calls for larger reserve requirements with the addition of larger units to the system. This characteristic is usually found when probability techniques are used. The application of probability methods to the static capacity problem provides an analytical basis for capacity planning which can be extended to cover partial or complete integration of systems, capacity of interconnections, effects of unit size and

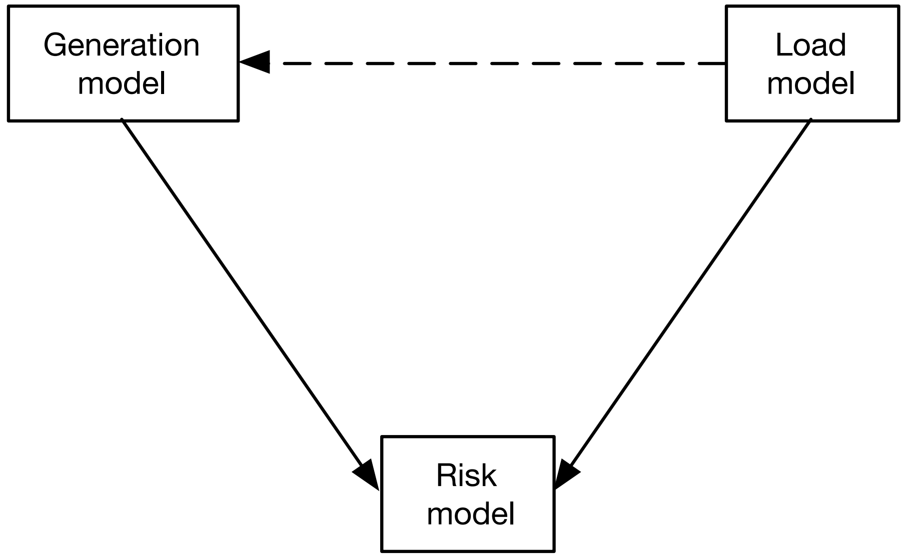

FIGURE 1.1: Conceptual tasks in generating capacity reliability evaluation

design, effects of maintenance schedules and other system parameters.

The Generation System Model

The basic approach to evaluating the adequacy of a particular generation configuration is fundamentally the same for any technique. It consists of three parts as shown in Figure 1.1 The generation and load models shown in the figure are combined (convolved) to form the appropriate risk model.

Generating Unit Unavailability

The basic generating unit parameter used in static capacity evaluation is probability of finding the unit on forced outage at some distant times in the future. This probability was defined as the unit unavailability, and historically in power system applications it is known as the unit forced outage rate (FOR).

$$\begin{aligned}
\text{Unavailability(FOR)} &= \frac{\lambda}{\lambda+\mu} \\
&= \frac{\text{MTTR}}{\text{MTTF}+\text{MTTR}} = \frac{\text{MTTR}}{\text{MTBF}} \\
&= \frac{\sum[\text{down time}]}{\sum[\text{down time}]+\sum[\text{up time}]}
\end{aligned} \tag{1.1}$$

$$\begin{aligned}
\text{Availability} &= \frac{\mu}{\lambda+\mu} \\
&= \frac{\text{MTTF}}{\text{MTTF}+\text{MTTR}} = \frac{\text{MTTF}}{\text{MTBF}} \\
&= \frac{\sum[\text{up time}]}{\sum[\text{down time}]+\sum[\text{up time}]}
\end{aligned} \tag{1.2}$$

where,

$$\text{MTTF} = \frac{1}{\lambda}$$

$$\text{MTTR} = \frac{1}{\mu}$$

$$\text{MTBF} = \text{MTTF} + \text{MTTR} = T$$

The concepts of availability and unavailability as illustrated in (1.1) and (1.2) are associated with the simple two state model as shown in Figure 1.2, which is directly applicable to a base load generating unit which is either operating or forced out of service. In the case of generating equipment with relative long operating cycles, the unavailability (FOR) is an adequate estimator of the probability that the unit under similar conditions will not be available for service in the future.

1.2.2 Operating Capacity

As discussed in above subsections, the time span for a power system is divided into two sectors: the planning phase and operating phase. In power system operation,

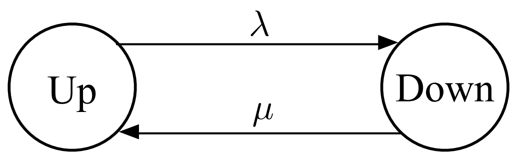

FIGURE 1.2: Two-state model

the expected load must be predicted (short-term load forecasting) and sufficient generation must be scheduled accordingly. Reserve generation must also be scheduled in order to account for load forecast uncertainties and possible outage of generating plant. Once this capacity is scheduled and spinning, the operator is committed for the period of time it takes to achieve output from other generating plant; this time may be several hours in case of thermal units but only few minutes in the case of gas turbines and hydroelectric plant.

A generally accepted definition of spinning reserve is that this is the rotating capacity in excess of the system load which is synchronized and immediately available to take up load. Some utilities include only this spinning reserve in their assessment of system adequacy, whereas others also include one or more of the following factors: rapid start units such as gas turbines and hydro-plant, interruptible loads, assistance from interconnected systems, voltage and/or frequency reductions. These additional factors add to the effective spinning reserve and the total entity is known as operating reserve.

Historically, operating reserve requirements have been done by *ad hoc* or rule-of-thumb methods, the most frequently used method being a reserve equal to one or more largest units. In the operational phase, it could lead to overscheduling which, although more reliable, is uneconomic, or to underscheduling which, although less costly to operate, can be very unreliable.

A more consistent and realistic method would be one based on probabilistic methods. A risk index based on such methods would enable a consistent comparison to be made between various operating strategies and the economic of such strategies. Generally two values of risk can be evaluated: unit commitment risk and response risk. Unit commitment risk (UCR) is associated with the assessment of which units to commit in any given period of time whilst the response risk is associated with the dispatch decisions of those units that have been committed. The acceptable risk level is and must remain a management decision based on economic and social requirements. An estimate of a reasonable level can be made by evaluating the probabilistic risk index associated with existing operational reserve assessment methods. Once a risk level has been define, sufficient generation can be scheduled to satisfy this risk level [18]. Baisc probability criteria and indices used in power system reliability evaluation are summarized in Appendix A.

1.2.3 Reliability Evaluation of Generating Systems—UCR and Well-Being Framework

PJM Methods and Modified PJM Methods

As reviewed in Subsection 1.2.2, operating reserve requirements have been estimated by deterministic methods, the most frequently used method being a reserve equal to one or more of the largest units, which does not take into account the probabilistic or stochastic nature of system behavior and can lead to overscheduling [18]. A more comprehensive and realistic method would be one based on probabilistic methods. The PJM approach [7], the first major probabilistic technique, was proposed in 1963 for analysis of UCR.

It has been considerably refined and enhanced since then but still remains a basic method for evaluating unit commitment risk. In its more enhanced form, it is probably the most versatile and readily implementable method for evaluating operational reserve requirements.

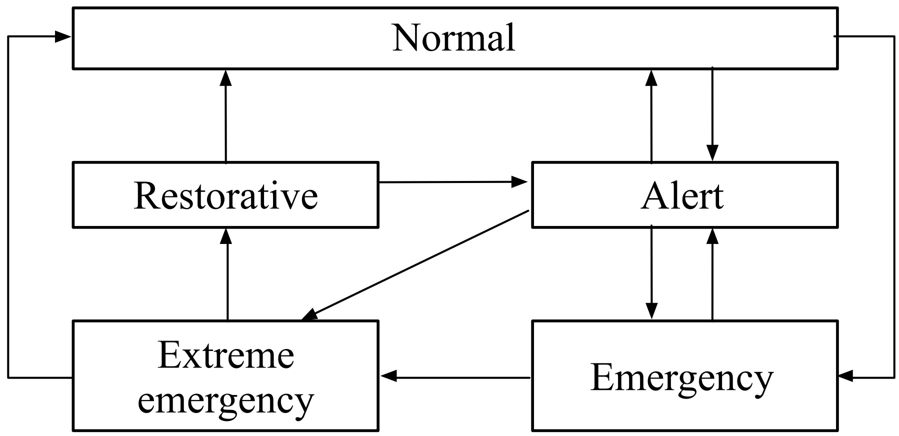

FIGURE 1.3: Operating states of system

The basis of the PJM method is to evaluate the probability of the committed generation just satisfying or failing to satisfy the expected demand during the period of time that generation cannot be replaced. This time period is known as the lead time. The operator must commit himself at the beginning of this lead time knowing that he cannot replace and units which fail or start other units, if the load grows unexpectedly, until the lead time has elapsed. The risk index therefore represents the risk of just supplying or not supplying the demand during the lead time and can be re-evaluated continuously through real time as the load and status of generating units change.

Billinton *et al* [18, 16] proposed a modified PJM approach, which allows the inclusion of rapid start and hot reserve units, interruptible load and postponable outages during the lead time into the risk assessment to compensate the generation shortage. Fotuhi-Firuzabad *et al* [44] evaluated the economic benefits of the existence of interruptible load. Recently, the idea of UCR has been extended for analysis of systems with wind power penetration [23].

Well-Being Framework

To address the difficulty of interpreting the numerical risk index and inadequacy of information provided by a single index, a modified framework for the operating states and associated definitions based on the security constraints in composite system reliability evaluation was proposed in [27] and is illustrated in Figure 1.3. In that paper, the framework was examined for application to operating reserve assessment in generating systems. In this approach the generation system is classified into different operating states designated as normal, alert, emergency and extreme emergency. A system can transfer into the alert, emergency and extreme emergency states from the normal state due to the loss of certain operating capacity or due to a sudden increase in the system load. The state definitions are structured to include deterministic criteria used by many operating utilities. Utilization of these operating states to assess operating reserve requirements can alleviate some of the difficulty often encountered in interpreting a single risk index and provide useful and comprehensive information for the system operator.

The operating state framework was then transformed into the well-being analysis framework [19]. In the well-being analysis framework, the system performance is evaluated using deterministic consideration and quantified by probabilistic indices. The overall well-being of the generation system is identified as being healthy, marginal or at risk using the designations shown in Figure 1.4 and can be quantified by system operating state probabilities. A system is identified as being healthy (normal), marginal (alert) or at risk [19]. The healthy and marginal states were formerly recognized as a single state of success or comfort [7]. In the healthy state (normal state) the generation is adequate to supply the existing total load demand. In this state there is enough margin such that the loss of any generating unit, specified by the deterministic criterion, e.g. any single unit outage, will not result in load curtailment.

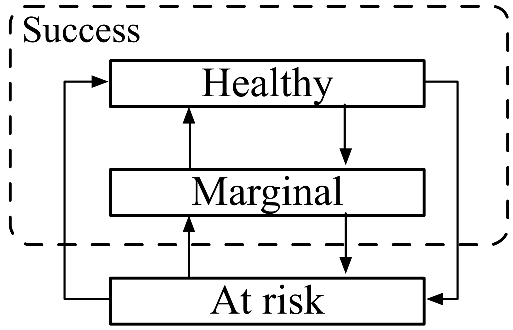

Figure 1.4: Model for system well-being analysis

The marginal state (alert state) is similar to the healthy state in that the system no longer has sufficient margin to withstand the loss as specified by the deterministic criterion. In the state of risk the system load is either equal to (emergency state) or greater than (extreme emergency state) the available generation capacity.

Literature Review

Until recently, the well-being analysis framework has been widely applied to generating systems [19, 25], operating reserve assessment [26, 3], bulk power systems [27, 61, 89], wind power integrated systems [50, 22], autonomous systems [24, 59] and generating systems with energy storage [13].

The revised well-being framework introduced in [3] was utilized to evaluate the optimal value of health probability based on the cost/benefit analysis. In [3], an approach was presented which has a similar structure as conventional well-being method, but it uses a different algorithm to determine healthy and marginal state probabilities. In the proposed architecture, the severity associated with each contingency was used to classify healthy and marginal states in identifying the degree of system well-being and can be implemented in practical systems.

There is growing interest in combining deterministic considerations with probabilistic assessment in order to evaluate the "system well-being" of a composite generation and transmission system and to evaluate the likelihood not only of entering a complete failure state but also the likelihood of being very close to trouble. To classify the success operating states into healthy and marginal, an artificial neural network based on group method data handling techniques was used in [61] to capture the patterns of these state classes, during the beginning of the simulation process. The idea is to provide the simulation process with an intelligent memory, based on polynomial parameters, to speed up the evaluation of the operating states. A bulk electric system well-being analysis using sequential Monte Carlo simulation (MCS) was presented in [89]. The approach provides accurate frequency and duration assessments and the index probability distributions associated with the mean values. The basic N-1 security criterion was used in [89] as the requirement for incorporating a deterministic consideration in a probabilistic assessment to monitor system well-being.

Two of the many challenges facing the electric power industry are the uncertainty associated with the demand for electrical energy and the emergence of renewal energy sources and particularly wind power. A large number of studies incorporating wind power or load forecast uncertainty in generating system reliability evaluation [Hierarchical Level I (HLI)] assessment have been conducted. Relatively little work has been done on composite generation and transmission system [Hierarchical Level II (HLII)] reliability assessment incorporating wind power and particularly in the well-being framework. Literature [50] was focused on examining the impacts of wind power, load forecast uncertainty (LFU) and their interactive effects on system reliability in HLII well-being analysis. An approach was presented in [22] for calculating well-being indices which gives much faster results than previously published methods. It extended the application of probabilistic techniques in operating reserve evaluation and determination. The method can be useful in the decision making process of choosing an appropriate unit commitment risk criterion (UCRC).

A relatively high renewable energy penetration can significantly reduce the system fuel costs but can also have considerable impact on the system reliability. Small isolated power systems (SIPSs) routinely plan their generating facilities using deterministic adequacy techniques that cannot incorporate the highly erratic behaviour of renewable energy sources. Deterministic and probabilistic techniques were combined using a system well-being approach in [24] to provide useful reliability indices for SIPS containing renewable energy, which facilitates an evaluation of the contribution from photovoltaics (PVs) and wind energy sources to SIPS reliability. In [59], a computationally efficient analytical method was presented for system well-being assessment and for production costing analysis of the small autonomous power systems (SAPSs) containing distributed generation (DG), PV, and wind turbine (WT) units. The developed method requires much less amount of meteorological data in comparison to MCS. Suitable probability distributions were used in that literature to model the system load and renewable resources, and the forced outages of various generating units were also accounted for.

A simulation technique was presented in [13] which extended the conventional well-being approach to generating systems using energy storage. This approach combines probabilistic indices with commonly used deterministic criteria in generating systems with storage facilities to assess the well-being of these systems. Multiple system configurations with different energy compositions and battery storage capacity levels were examined in the literature. The approach can be useful in the planning and design of generating systems for remote locations.

1.2.4 Reliability Evaluation of Generating Systems Considering Demand-side Participants

Traditionally electric utilities have been primarily interested in supply-side initiatives in their power system planning. Demand-side options such as demand-side management (DSM) initiatives were not extensively considered. This situation is no longer the case as electric utilities are responding to public concern regarding the environment and desire to conserve natural resources by placing increased attention on the customer side of the meter. Nowadays both supply- and demand-side options are integral elements in system planning and operation. A handful of works were devoted to seeking resources from demand side to help improve system reliability. Salehfar *et al* [79] evaluated the reliability effects of direct load control. Direct load control (DLC) is a form of load management in which portions of the system load are under the direct operational control of the utility. Thus, the load can be modified, within limits, to match the available generating capacity thereby minimizing events of uncontrolled load loss. Salehfar *et al* recognized the importance of the temporal correlation of load and generating capacity for accurate assessment and recommended Monte Carlo simulation as a way. The contribution from interruptible load was considered in the well-being analysis [16]. The presence of interruptible loads can affect the generating system operating state rick (GSOSR) and the system operating state probabilities. Load curtailment can be considered as a means of reducing system risk when the system operates at a risk higher than is desirable and stand-by units are unavailable [16]. The ability of a system to interrupt its load can be considered as an ability to bring ready reserve into the system depending on the allowable time delay of the load interruption. It is usually assumed that a utility has prior knowledge regarding the various loads that can be interrupted with minimum or no penalty. The magnitude of curtailable load and the corresponding time of interruption depend on agreements between the utility and its consumers.

Billinton *et al* [17] conducted a reliability cost/worth analysis to quantify the effects of DSM. DSM, in general, refers to any activity adopted by a utility that ultimatelt changes the utilitiy's total system load curve. The proposed models can be used as the basic framework in the design and implementation of a utility DSM program. Fotuhi-Firuzabad *et al* [44] evaluated the economic benefits of interruptible load involvement. A framework was developed in the literature for a comprehensive evaluation of possible scenarios for the implementation of interruptible load into demand-side management. A procedure was presented to calculate the total societal cost which includes system operating cost and the customer interruption cost. Customer interruption cost is the monetary losses incurred by customers due to generating unit or transmission line outages. The study results indicate that the load model reflecting the interruptible load initiative has the greatest cost-savings in terms of reducing the total societal cost of electricity. It was also concluded in the literature that having interruptible load at specific buses has more effect on the customer interruption cost than other buses. Hirst [49] identified the reliability benefits of demand-side participation in different markets. Huang *et al* [51] applied load shifting to seven load sectors, including agricultural, large Users, residential, government, industrial, commercial, and office, to study the effects of DSM on system reliability. As noted in the literature, there is relatively little reliability or monetary benefit in terms of decreased customer outage costs associated with demand response initiatives in the agricultural, residential, government, and office load sectors, in the IEEE Reliability Test System (IEEE-RTS). Under these conditions, it is unlikely that a large scale implementation of smart meters in the residential sector would provide a significant benefit to assist in justifying this course of action. The results show that the largest reliability benefits occur with the application of load shifting in the large user sector followed by the industrial user and commercial user sectors.

1.2.5 Applications of V2G and V2H

The basic idea behind the V2G and V2H technology is that electric vehicles can provide power to the grid when parked and plugged in [56]. Figure 1.5 shows the basic concept of the V2G technology. As depicted, electric vehicles can be connected

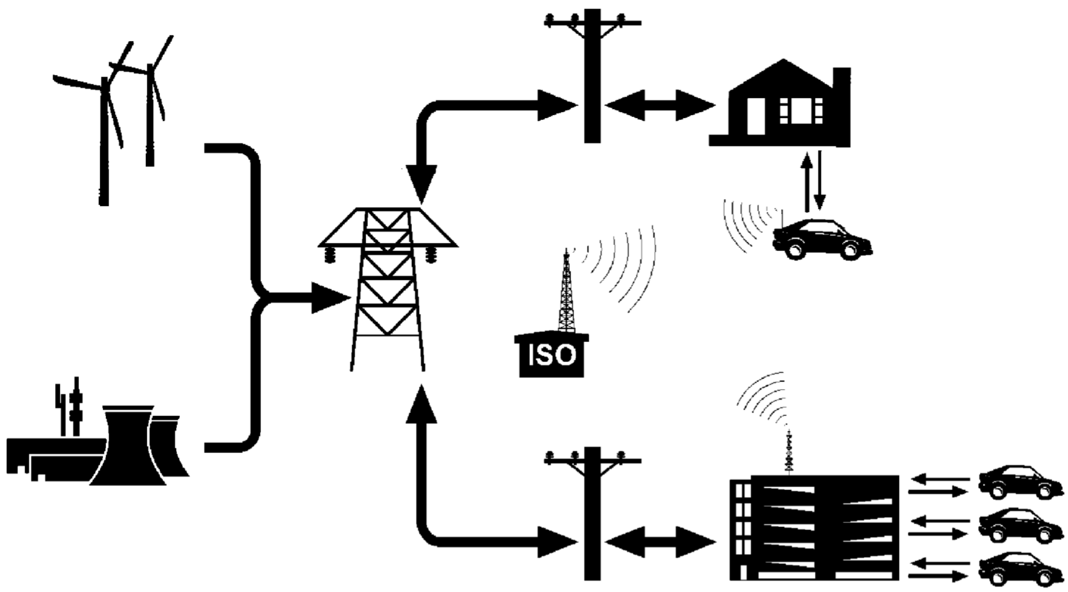

FIGURE 1.5: Illustrative schematics of the V2G implementation [56]

either to the house (one or more vehicles) or to the facility (fleet of vehicles) and perform the V2G operation. Charging and discharging of the vehicle's battery can be performed according to the remote commands from the grid operator or independent system operator (ISO). The ISO must continuously tune the balance between the production and consumption of power in specific control areas since the mismatch might cause the grid frequency to deviate from the nominal operating point of the utility frequency. Also, by getting demands for reactive power from the ISO, vehicles can perform the voltage regulation at certain points and even maintain the unity power factor at the house or other facility power terminals [91].

The most significant electric service markets include base load, peak power, spinning reserve and regulation. V2G appears unsuitable for the first two, since they are accomplished by base-load power plants (nuclear and coal-fired) and peaking power plants (gas turbines and hydroelectric plants) respectively. But in the fast response power service markets, like spinning reserve and regulation, V2G could be a very promising technology [91].

Though it has been speculated that unidirectional V2G will be implemented first [81], it has several limitations. One of which is that the regulation and reserves capacities bid with unidirectional V2G are significantly less than those that can be bid in bidirectional V2G [84]. Unidirectional V2G also cannot provide the system with the energy stored in the EV batteries.

In order to function in bidirectional V2G mode, the EV has to be equipped with a bidirectional power converter and additional battery pack. Having this, two way energy flow is possible—when the power demand is low, EV's batteries can be charged and when high, batteries can be discharged and thus perform voltage and frequency regulation by matching generation with the load demand [30]. Madawala *et al* [66] presented a novel bidirectional inductive power transfer system, which is particularly suitable for applications such as plug-in electric vehicles (PEVs) and V2G systems, where two-way power transfer is advantageous.

for Frequency Regulation and Spinning Reserves

In recent years, extensive efforts have been involved in understanding as well as implementing V2G as a source of spinning reserve and regulation service in power systems [37, 31, 38, 82, 48]. Brooks *et al* [31] touched on some background requirements for demand dispatch and how the Internet can be used for communication and control. They showed how loads that meet the communication and control requirements can be aggregated and dispatched—turned on or off—to help manage the grid. Aggregated loads are able to perform many of the same ancillary services for the grid that are provided by power plants today. In that literature a concrete example of demand dispatch was given as it can be applied to EVs: smart charging. In [82] a V2G algorithm was developed to optimize energy and ancillary services (load regulation and spinning reserves) scheduling. The algorithm can be used by an aggregator, which may be a utility or a third party. It maximizes profits to the aggregator while providing additional system flexibility and peak load shaving to the utility and low costs of EV charging to the customer. Han *et al* [48] proposed an aggregator that makes efficient use of the distributed power of electric vehicles to produce the desired grid-scale power. In that literature they investigated the cost arising from the battery charging and the revenue obtained by providing the regulation. The cost was then represented mathematically.

In order to participate in energy markets, the V2G capabilities of many EVs are combined by aggregators and then bid into the appropriate markets [47, 74, 48, 65, 45]. Economic aspects of V2G services have been analyzed in a number of studies [57, 58, 90, 84, 6]. Most studies identified benefits for V2G vehicle owners in the range of a few to several hundred dollars per month.

for Voltage Support and Voltage Power Compensation

Existing and forthcoming devices at the residential level have the ability to provide reactive power support. Inverters which connect distributed generation such as solar panels and plug-in hybrid electric vehicles (PHEVs) to the grid are an example. Such devices are not currently utilized by the power system. Roger *et al* [77, 76] put forth the vision that residential-level devices can be called upon to correct voltage violations in their local area, using secure, authenticated messaging to coordinate the control. In [76] they investigated the integration of these end-user reactive-power-capable devices including PHEV to provide voltage support to the grid via a secure communications infrastructure. They determined effective locations in the transmission system and showed how reactive power resources connected at those buses can be controlled. Kisacikoglu *et al* [60] examined a PHEV charger system to utilize it for reactive power support to the grid. The authors investigated different scenarios to deliver the stored energy from V2G and explained the effects of this usage on the vehicle traction battery and the charger dc link capacitor.

Other Applications

Some of the research works are devoted to EV's application as a form of uninterruptible power supply (UPS). Cvetkovic *et al* [37] presented the structure and capabilities of a small, grid-interactive distributed energy resource system comprised of a PV source, PHEV, and various local loads. Implemented at the residential level, the system, with a plug-in hybrid electrical vehicle, has the ability to isolate a house from the utility grid (intentionally due to a fault or other abnormal grid conditions), work in the standalone mode, synchronize and reconnect to the utility grid, without load power interruptions.

Uncontrolled and random EV charging can cause increased power losses, overloads and voltage fluctuations, which are all detrimental to the reliability and security of newly developing smart grids. On the other side, expanding functionalities from demand side enables smart grids to rapidly self-regulate and heal, improve system reliability and security, and more efficiently manage energy delivery and consumption [70, 78, 68, 71, 32, 33, 43]. A real-time smart load management control strategy was proposed in [39] and developed for the coordination of PEV charging based on real-time (e.g., every 5 min) minimization of total cost of generating the energy plus the associated grid energy losses. The approach reduces generation cost by incorporating time-varying market energy prices and PEV owner preferred charging time zones based on priority selection.

1.2.6 EV's Inclusion for Reliability Improvement and Its Consideration

Up to now limited number of attempts have been made to discover the EV's inclusion in to power systems as a source of reliability improvement. Compared to other applications such as V2G regulation, utilizing energy stored in EVs during system outages has following advantages:

1. Outages occur much less frequently in a typical system than it calls for ancillary services such as frequency regulation and spinning reserves. As a result, heavy burdens such as real time communication, monitoring, and scheduling are lifted when EVs are used for system reliability improvement.

2. Battery wear and tear is EV users' concern specially in the application of V2G regulation service, since it requires battery packs being charged (in unidirectional V2G) or charged and discharged (in bidirectional V2G) constantly with wide ranges of power capacities.

3. It is every EV user's full responsibility to rigidly follow his/her daily schedules (driving and parking) once the EV participates in services such as frequency regulation. In real life, however, errors in daily schedules are inevitable since a large amount of population is involved and just a traffic jam can simply make the schedule go awry. In the application for reliability improvement, as will be put forth in Chapter 3, those unavoidable uncertainties can be accounted for.

For a resource from the demand side, basic information such as its capacity is required to be known before its participation [46]. Conventional resources, i.e. generating units and purchased power, historically have possessed attributes which allow the system operator to operate the electrical system in a reliable and economical mannier. Also, these resources are supported by sufficient documentation to assist schedulers in their planning environment. For DSM programs such as EV charging to be considered as resources, in the conventional sense, they must meet similar criteria to assure that the operations personnel can maintain control of the electrical system. It should be noted that even though some of the DSM programs may not meet the requirements to be a resource, they may have positive effects on the shape of our daily load curve, thus being considered "negative" load vs. a resource, and may provide benefit to the corporation [46].

To study EVs' capability of improving the well-being of generating systems, a method was given in [94] for evaluating capacities contributed from EVs in terms of both interruptible EV charging and V2G capacities. It was found that the involvement of EVs in the grid services not only compensates the risk increase due to EVs' penetration but also further improves the system well-being. Wang [88] showed that uncertainties in either the unit model or load forecast can affect results of reliability evaluation and concluded that the greater the uncertainty in the input, the weaker the assessment results become. In addition to the availability of hardware component, commitment of EVs in grid services depends heavily on individuals' travel and charging plans [94]. Human actions such as auto-driving would not go exactly the same as planned so the accuracy of reliability evaluation may be affected. A new reliability evaluation method is therefore needed to consider the uncertainties of EV charging.

1.2.7 Reliability Evaluation of Distribution Systems

Historically, distribution systems have received considerably less of the attention devoted to reliability modeling and evaluation than have generating systems. The main reasons for this are that generating stations are individually very capital intensive and that generation inadequacy can have widespread catastrophic consequences for both society and its environment. Consequently great emphasis has been placed on ensuring the adequacy and meeting the needs of this part of a power system.

A distribution system, however, is relatively cheap and outages have a very localized effect. Therefore less effort has been devoted to quantitative assessment of the adequacy of various alternative designs and reinforcements. On the other hand, analysis of the customer failure statistics of most utilities shows that the distribution system makes the greatest individual contribution to the unavailability of supply to a customer. The statistics reinforce the need to be concerned with the reliability evaluation of distribution systems, to evaluate quantitatively the merits of various reinforcement schemes available to the planner and to ensure that the limited capital resources are used to achieve the greatest possible incremental reliability and improvement in the system.

Several other aspects must also be considered in the need to evaluate the reliability of distribution systems. Firstly, although a given reinforcement scheme may be relatively inexpensive, large sums of money are expended collectively on such systems. Secondly, it is necessary to ensure a reasonable balance in the reliability of the various constituent parts of a power system, i.e. generation, transmission and distribution. Thirdly, a number of alternatives are available to distribution engineer in order to achieve acceptable customer reliability, including alternative reinforcement schemes, allocation of spares, improvements in maintenance policy, alternative operating policies. It is not possible to compare quantitatively the merits of such alternatives nor to compare their effect per monetary unit expended without utilizing quantitative reliability evaluation [18].

These problems have been fully recognized and utilities throughout the world are routinely using quantitative reliability techniques. The techniques required to analyze a distribution system depend on the type of system being considered and the depth of analysis needed. In this work, radial systems, the most common type of distribution systems, are considered.

Basic Techniques

A radial distribution system consists of a set of series components, including lines, cables, disconnects (or isolators), busbars, etc. A customer connected to any load point of such a system requires all components between himself and the supply point to be operating. Consequently the principle of series systems can be applied directly to these systems. The three basic reliability parameters of average failure rate, λ_{s}, average outage time, r_s, and average annual outage time, U_s, are given by

$$\lambda_\mathrm{s} = \sum_i \lambda_i \tag{1.3}$$

$$U_\mathrm{s} = \sum_i \lambda_i r_i \tag{1.4}$$

$$r_\mathrm{s} = \frac{U_\mathrm{s}}{\lambda_\mathrm{s}} = \frac{\sum_i \lambda_i r_i}{\sum_i \lambda_i} \tag{1.5}$$

These three indices in many literatures are generally referred to as failure rate, outage duration and annual outage time. It should be noted that they are not deterministic values but are the expected or average values of an underlying probability distribution and hence only represent the long-run average values. Although the three primary indices are fundamentally important, they do not always give a complete representation of the system behavior and response. In those cases, additional indices are required, which are summarized in Appendix B.

1.2.8 Reliability Evaluation of Distribution Systems Considering Emerging Energy Sources

Techniques for reliability assessment have evolved over the last decade as the distribution system embraces various newcomers. Among them, DG, especially fueled by renewable energy, has been considered extensively, from diverse perspectives. Solar and wind DG were included in the adequacy assessment of distribution systems [8, 9]. In [8], the adequacy of a radial distribution system including different types of DG units was assessed during different modes of operation. It was found that integrating DG units with the system has a notable impact on the improvement of the system adequacy, and allowing islanding mode of operation adds more improvement to this adequacy. A technique for modeling solar irradiance chronologically using MCS was later proposed in [9]. The connection matrix was proposed in [11, 12] to neatly represent system configuration and restoration order. The traditional reliability indices cover only sustained interruptions. The time necessary to start-up the DG should be taken into account for the reliability evaluation of the distribution system including DG. If this time is sufficiently short, the customers suffer a momentary interruption, while, if not, they suffer a sustained interruption. Various resources recovering loads have an influence on the reliability indices, such as duration and frequency of sustained or momentary interruption, depending on the operation mode of DG. In [11], an analytical technique was developed which involves the system versatility with time-varying parameters, and its accuracy was verified as almost comparable to that of MCS. For the customers contracted with microgrid, a recursive algorithm to compose a connection matrix of DG in microgrid was proposed in [12] using a matrix which represents the connection between sections. The work also added PV systems and the fuse devices to the analytical technique for the generalized application.

Customer interruption can be reduced by optimizing the positions of DG and protection devices in distribution systems [72]. If islanded operation of these DG sources is allowed on a feeder subjected to a disturbance, DG may reduce the number of interruptions and/or durations for customers residing within their protection zones, thus increasing the reliability of service. A procedure for finding optimal positions for DG and protection devices was presented in [72] for a feeder equipped with capacity-constrained distributed generators, using a custom-tailored genetic algorithm, and the improvement in reliability was demonstrated on a test feeder.

Energy storage and its intelligent operation strategy were made use of to improve system reliability and economy [96, 95]. In [96], the reliability and economy of a radial distribution system integrated with electric energy storage and renewable energy resources were evaluated. Proposed reliability and economy assessment framework was applied to evaluate the impact on reliability and economy brought by proposed operation strategies, and electric energy storage and renewable energy resources integration. Later, the same authors [95] presented the communication and control structure for implementing the operation strategy for energy storage to better manage its energy procurement and distributed renewable energy generation. The communication network also allowed the energy storage coordination during loss of load event in the bulk power system.

Telecontrolled switches and microgrids were being taken into consideration in [36]. Conti *et al* [36] presented a systematic and analytical method to investigate the influence of switches' telecontrol/automation and microgrids' islanding on systems reliability, accounting for their combined effect as well. Not fully reliable switches were also considered.

A two-hierarchy procedure for minimal path search and state evaluation was proposed in [14]. A major contribution is that the concept of the virtual power plant (VPP) was introduced to model microgrids connected with intermittent sources. The VPP offers a simplified equivalent model to be used at distribution grid level. It can be easily combined with the multi-state reliability model obtained by the generalized capacity outage tables.

Recently, a risk analysis was conducted in [62] for distribution systems under severe weather conditions. The authors found that: 1) wind storms have significant effects on distribution system reliability and it is indispensable to involve extreme weather in the reliability evaluation; and 2) reliability evaluation considering wind storm classifications provides the change trend of the reliability indices and reveals some severe but rare events.

A distribution system with DG units can be operated in two modes: islanding mode and grid connected mode. During islanding mode of operation, the system fails when there is a deficit in power generation of DG [8]. By making use of smart sensors, advanced switches and andppropriate control methods [55], excess load can be curtailed or interrupted to maintain partial load during islanding. Use of V2H, which means EVs function as energy sources to supply household demand, is envisioned in [63]. The feasibility to control each household appliance through home computer networks is shown in [67]. Unlike conventional energy sources, EVs are primarily used in the transportation sector. As a result, the amount of energy available from EVs depends on their travel patterns, charging requirements, and time and duration of outages. In an attempt to assess EVs' contribution to the generating system reliability, a method has been proposed to evaluate the capacities available from EVs in terms of interruptible charging and V2G [94].

1.3 Primary Contributions

1.3.1 Reliability Evaluation of Generating Systems Incorporating EV Charging

The first intention of this thesis is to extend the well-being analysis of generating systems by incorporating EV charging in the assessment. To assess individual EVs' contribution and incorporate them into the system, methods for evaluating the aggregate capacity are proposed, so that with data input from the demand side, capacity contribution from EVs can be easily obtained while the daily travel and charging requirements of EVs are not comprised. Two scenarios are considered—the interruptible EV charging scenario and V2G enabled scenario. In the former scenario, charging load of an EV is considered interruptible as long as charging requirements can be fulfilled afterwards. In the V2G enabled scenario, in addition to the interruptible capacity, energy stored in EVs is allowed to feed back to the grid. With the capacity evaluated, the aggregated population of V2G enabled EVs can be regarded as a rapid start unit adding to the system. Besides, since usage of EVs is strongly dependent on time of the day [92] and most of the short-term generation schedule is based on the calendar day, the study of this thesis is conducted on a daily basis, in order to get the whole picture. To facilitate the capacity evaluation and make it fit with daily generating schedules, the idea of equivalent EV charging period is proposed. Also, indices used in conventional well-being analysis, where only one single load level and emergency capacity are considered, are no longer sufficient. Thus, indices such as the daily risk reduction are provided to have the insights. The effects on the system health of EV charging are analyzed using the Roy Billinton Test System (RBTS) [28]. It is found from the results that with the interruptible and V2G service enabled, EV charging is able to not only compensate for any lowering of reliability due to its penetration but can also improve the system well-being.

1.3.2 Uncertainties of EV Charging and Its Impact on Reliability Evaluation of Generating Systems

Secondly, uncertainties of EV charging are identified, such as punctuality, rounding of time, forecast error of daily energy consumption and charging failure. Any of these elements can cause errors in evaluation of EVs' capacity contribution, which may lead to unreliable results of the well-being assessment. For instance, punctuality and rounding of time describe people's inclination toward being early or late [41], causing the actual charging arrangement differ from the scheduled one. People have tendencies in estimating their daily mileages [83] and this can affect the charging plan as well if the energy consumption is changed.

How the EV charging and its grid services are organized and realized is also important. There is a consensus that aggregators are required to enable EVs' participation into load management programs [93, 47]. An aggregator serves as a representative of a group of EVs because the limited capacity of an individual EV is not negotiable and the sheer number of EVs introduces scalability problem. However, a side effect is that grid services from EVs will cease with the failure of aggregator. Besides, the number of aggregators deployed in a system is indeterminate. This thesis takes into account the failure of aggregator with two potential grid realizations: the one with a single aggregator and multiple aggregators. Fig. 1.6 shows the framework of well-being analysis of generating systems considering EV charging and its uncertainties.

Since system load as well as capacity contribution of EVs varies during the day, the operating well-being of generating systems for each load level of the day is examined.

1.3.3 Reliability Evaluation of Distribution Systems Including V2G and V2H

As the third contribution, this thesis incorporates EVs as active components into the classical distribution system reliability evaluation [29]. During outages, EVs can reduce the load interruption through V2H and V2G. To illustrate, a fault is assumed in the first section of the main feeder (2 miles) in a typical distribution system (Fig. 1.7). In such an instance, load points A, B and C would not be recovered until repaired. With EVs serving as energy sources at each load point, however, load can be backed up in islanding mode of operation. Moreover, if excess power is available, load points B and C can exchange power to further reduce the loss caused by the fault by sectionalizing the fault component and maintaining the connection between B and C.

Two topologies for EV charging are considered at each load point: centralized and

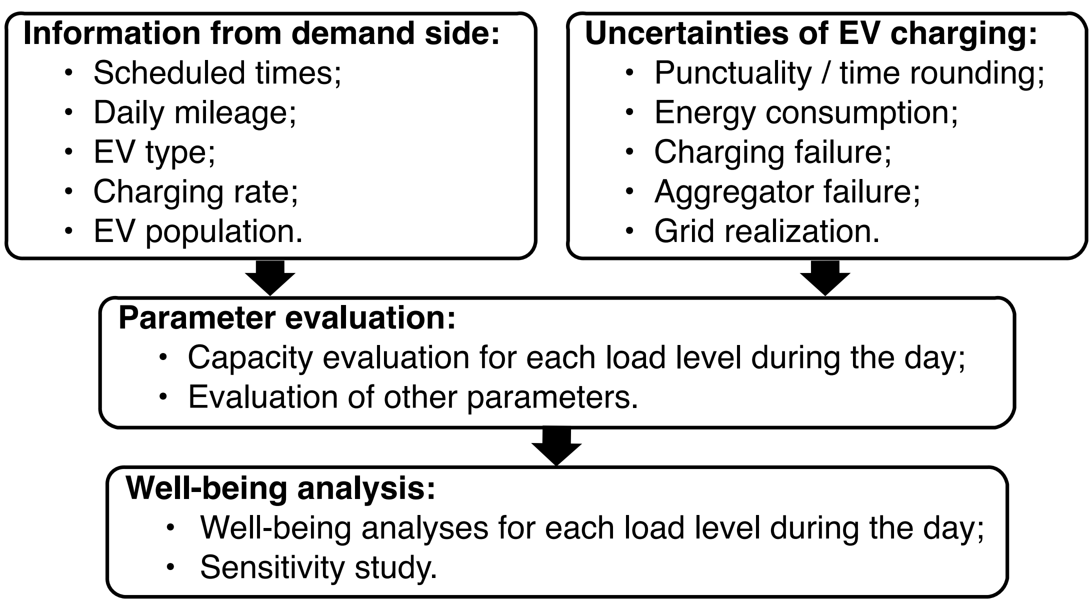

Figure 1.6: Well-being analysis considering EV charging and its uncertainties

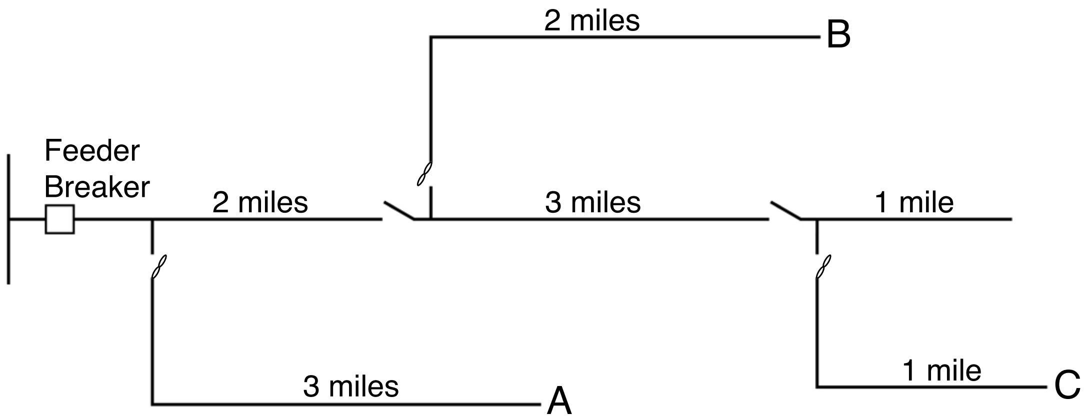

FIGURE 1.7: A typical configuration of distribution systems [29]

dispersed EV charging (Fig. 1.8). In the context of distribution system, the network topology, which has a direct impact on EVs' capacity contribution in both islanding and grid connected mode of operation, has to be scrutinized. Since the topology on the system level of a specific distribution circuit is given, much emphasis should be put on the local charging network. The topology of centralized EV charging is favored in densely populated areas with existing parking lots, whereas dispersed EV charging is more practical in suburban or rural areas.

Therefore ensuing from diversities of different modes of operation and topologies of local charging networks are five possible scenarios: a). *"local V2G"* and b). *"interregional V2G"* for the topology of centralized EV charging; and c). *"V2H"*, d). *"V2H + local V2G"* and e). *"interregional V2G"* for the topology of dispersed EV charging (Table 1.1).

Table 1.1: Scenarios considered

		Charging topology	
		Centralized	Despersed
Mode of operation	Islanding	a. *Local V2G*	c. *V2H* d. *V2H + local V2G*
	Grid connected	b. *Interregional V2G*	e. *Interregional V2G*

In this thesis, the term "V2H" is used to indicate EVs directly backing up their households, which can happen only in the topology of dispersed EV charging. Two types of V2G—local V2G and interregional V2G—are introduced. The former is confined to each load point, while the latter entails energy exchanges within working sections of the main feeder. As for the latter, calculation of power flow is required since power loss along distribution lines has to be considered. Note that for dispersed EV charging, each house can choose to either isolate itself from the local circuit (i.e. V2H) or remain connected to take part in local V2G or interregional V2G.

1.4 Organization of the Thesis

Chapter 2 provides models to analyze EVs to improve reliability of the generating system as interruptible load and additional generating units. Chapter 3 studies the uncertainties of aggregated EVs and their effects on well-being of generating systems. Chapter 4 presents models to adopt both V2G and V2H into the reliability evaluation of distribution systems. Chapter 5 concludes the thesis.

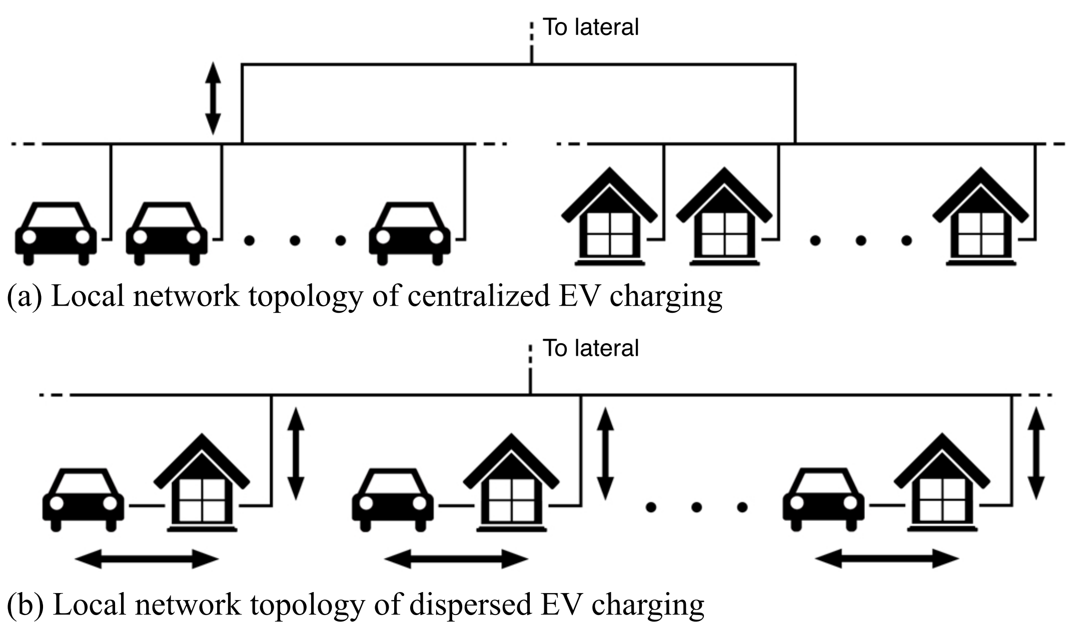

Figure 1.8: Different topologies for local networks

1.5 List of Publication

[1] N. Z. Xu, M. Ding, and C. Y. Chung, "Control strategies of BESS for compensating renewable energy fluctuations," in *Advances in Power System Control, Operation and Management (APSCOM 2012), 9th IET International Conference on*, Nov. 2012, pp. 1-5.

[2] N. Z. Xu, Huazhang Huang, and C. Y. Chung, "A comprehensive framework for unidirectional vehicle-to-grid regulation services," in *Power and Energy Engineering Conference (APPEEC), 2014 IEEE PES Asia-Pacific*, Dec. 2014, pp. 1-5.

[3] N. Z. Xu, C. Y. Chung, "Well-being analysis of generating systems considering electric vehicle charging," *IEEE Trans. on Power Syst.*, vol. 29, no. 5, pp.2311-2320, Sep. 2014.

[4] N. Z. Xu, C. Y. Chung, "Challenges in future competition of electric vehicle charging management and solutions," *IEEE Trans. on Smart Grid*, vol. 6, no. 3, pp.1323-1331, May 2015.

[5] N. Z. Xu, C. Y. Chung, "Uncertainties of EV charging and effects on well-being analysis of generating systems," *IEEE Trans. on Power Syst., Early Access.*

[6] N. Z. Xu, C. Y. Chung, "Reliability evaluation of distribution systems including vehicle-to-home and vehicle-to-grid," *IEEE Trans. on Power Syst., Early Access.*

2

Well-Being Analysis of Generating Systems Considering EV Charging

This chapter is organized as follows. The analytical method for well-being evaluation is briefly reviewed in Section 2.1. Section 2.2 illustrates the methodologies for examining the interruptible capacity and the V2G capacity that EVs could contribute to the system. The analysis procedure is also provided in Section 2.2. Numerical results are analyzed in Section 2.3. Finally, sensitivity analyses are presented in Section 2.4 to reveal the impact of parameters of concern such as energy capacity and charging/discharging limits of EV, penetration of EVs and lead time of EV charging.

2.1 Well-Being of Generating Systems

The relationship between the probabilities of the system being in healthy, marginal or at risk state is given by (2.1):

$$P_{\mathrm{H}} + P_{\mathrm{M}} + P_{\mathrm{R}} = 1 \tag{2.1}$$

where the three probabilities can be determined by looking up the capacity outage probability table (COPT). A detailed algorithm for developing a COPT is presented in [18]. It should be noted that in well-being analysis, the COPT is created using ORR instead of FOR. The ORR represents the probability that a unit fails and is not replaced during the lead time. UCR from a COPT has a discrete nature due to the individual unit capacities [23]. For calculation of ORR, the reader is referred to [23].

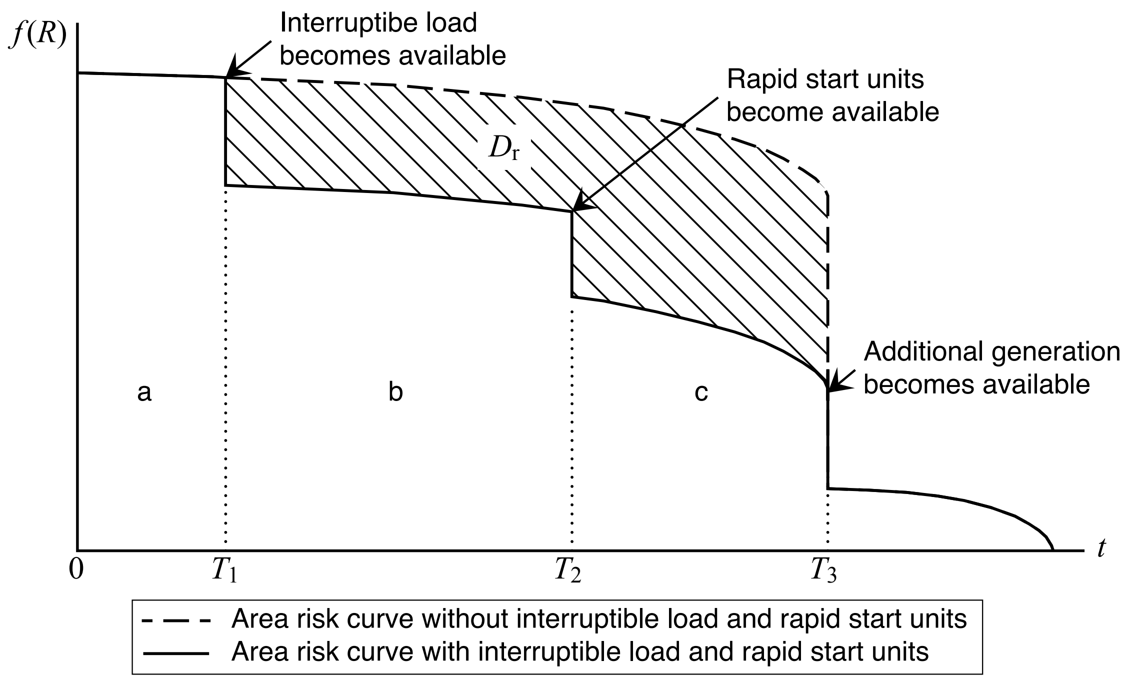

FIGURE 2.1: Area risk curves with and without interruptible load and rapid start units

The upper and lower curves in Figure 2.1 are typical area risk curves (or risk functions $f(R)$ [18]) without and with the inclusion of interruptible load and rapid start units, respectively. T_1, T_2 and T_3 are lead times associated with interruptible load, rapid start units and conventional thermal units, respectively. The total risk decreases by D_{r} as shown by the shaded area. Calculation of the equivalent UCR (i.e. the area under the lower curve of Figure 2.1) and equivalent probabilities of the normal and marginal states are summarized as follows:

$$P_{\mathrm{ER}} = R_{\mathrm{a}} + R_{\mathrm{b}} + R_{\mathrm{c}} \tag{2.2}$$

$$P_{\mathrm{EH}} = P_{\mathrm{H}} \cdot (1 + D_{\mathrm{r}}) + P_{\mathrm{R}} \cdot D_{\mathrm{r}} \tag{2.3}$$

$$P_{\mathrm{EM}} = P_{\mathrm{M}} \cdot (1 + D_{\mathrm{r}}) \tag{2.4}$$

where R_{a}, R_{b} and R_{c} are partial risks represented by corresponding areas under the lower area risk curves in Figure 2.1 and D_{r} is given by (2.5):

$$D_{\mathrm{r}} = P_{\mathrm{R}} - P_{\mathrm{ER}} \tag{2.5}$$

Given the tiny capacity a single EV has, normally EVs need to be aggregated before they can interact directly with the grid [31]. In this thesis, we assume charging/discharging capacities of EVs are aggregated. So available capacities can be called on in the same lead time.

If we substitute (2.5) into (2.3) and (2.4) and add , and together, (2.6) can be obtained and the relationships among the three state probabilities remain the same as (2.1):

$$P_{\mathrm{EH}} + P_{\mathrm{EM}} + P_{\mathrm{ER}} = 1 \tag{2.6}$$

For details of calculation of the equivalent risk with interruptible load consideration and rapid start units, the reader is referred to [16] and [18], respectively.

2.2 Methodologies

2.2.1 Information Required

Daily activities of EVs should not be affected by the interruption of EV charging so daily charging requirements of daily charging should be obtained before the interruptible capacity can be evaluated. Travel times of EV driving and SOC of EVs are the two basic requirements of EV charging. Every EV should have sufficient

SOC to cover its daily mileage the next day. This thesis assumes EV charging takes place only at home, where the daily travel starts and ends. The time period between arrival of an EV at home and its departure is thus the available charging period, during which temporary interruption of EV charging is acceptable. Once data from demand side, such as home arrival time (t^i_{HA}), home departure time (t^i_{HD}) and energy depleted during daily driving (E^i_{D}) of every EV are obtained, the evaluation procedure can begin.

2.2.2 Interruptible Capacity Evaluation

Normally the period of a conventional daily generation schedule is one calendar day, which starts and ends at midnight. It can be expected, however, that an available charging period (i.e. the parking period) of an EV is usually across two days. This causes inconvenience as a complete EV charging period is split by the study period of one calendar day. For instance, given the time of departure and arrival of an EV is 7:00 and 16:00, respectively, the study period of one calendar day, which is from 0:00 to 23:59, essentially includes two separate available charging periods: on one hand the period from 0:00 to 6:59 is from the available charging period of the day before and on the other hand, the period from 16:00 to 23:59 is a part of the available charging period which is supposed to last until 7:00 of the next day. To avoid separate periods available for charging while retaining the conventional study period for generation schedule, we first expand the study period to 48 hours (two calendar days) to have a complete charging period available for each EV; the period between and would not exceed 48 hours. Figure 2.2 illustrates the idea of the extended study period, where only the complete period available for charging (from 16:00 to 31:00) is preserved. The period of interruption in Figure 2.2 is the period of interest, during which the system well-being is to be examined. As long as fixed daily charging requirements are assumed, results from the extended study period are equal to the ones from

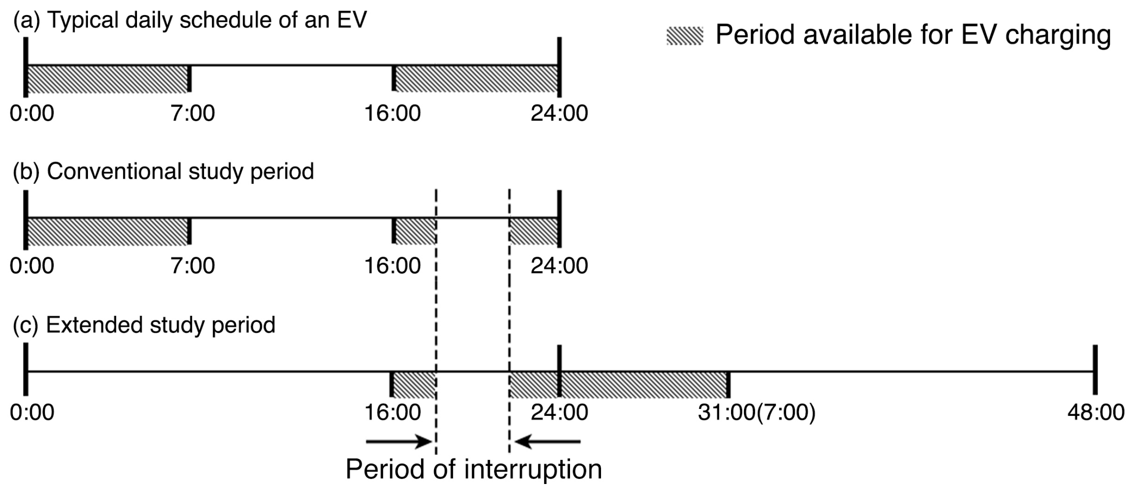

FIGURE 2.2: Illustration of the extended study period

the conventional study period. By splitting back into two single calendar days and superimposing them, the results can be simply converted back to the daily basis. For example, interruptible capacities evaluated for the period from 24:00 to 31:00 in the extended study period are equal to the capacities for the period from 0:00 to 7:00 in a single calendar day, as illustrated in Figure 2.2(c). With the continuous period available for charging, evaluation of interruptible capacity as well as basic EV charging simulations can be done in an easier and convertible way.

Basically, the interruptible capacity (p_I) is dependent on the quantum of interruptible charging energy and duration of the interruption (T_I), equal to the system lead time less the lead time of EV charging:

$$p_\mathrm{I} = \frac{E_\mathrm{I}}{T_\mathrm{I}} \tag{2.7}$$

where,

$$E_\mathrm{I} = \min\left(\sum_i^m e_{\mathrm{IC},i}\,,\, \sum_i^m e_{\mathrm{SC},i}\right) \tag{2.8}$$

$$T_\mathrm{I} = \mathbf{1} \cdot \boldsymbol{t_\mathrm{I}}^\mathsf{T} \tag{2.9}$$

where $e_{\mathrm{IC},i}$ and $e_{\mathrm{SC},i}$ can be derived from (2.10) and (2.11), respectively; $\boldsymbol{t}_{\mathbf{I}}$ represents the period during which EV charging is to be interrupted. For example, if the system lead time is 1 hour, lead time of EV charging is 10 minutes and the outage takes place from 7:00, then $\boldsymbol{t}_{\mathbf{I}}$ should represent a period from 7:10 to 7:59.

The fundamental premise of the evaluation is that the requirements of EV charging should not be compromised by the interruption. The maximum allowable energy loss (E_{I}) is restrained by two variables: the maximum energy loss due to the interruption and maximum energy provided by supplementary charging. The maximum energy loss due to the interruption is equal to the energy supposed to be charged originally during the period of interruption, given by (2.10). Energy provided by supplementary charging is defined as the amount of energy that can be delivered to an EV, in addition to its original charging arrangement, after the interruption, as defined by (2.11). For instance, if there is no additional time period left for charging an EV after the interruption, then the EV cannot provide any capacity during the interruption. Similarly, no capacity can be provided if the interruption happens when no charging is planned in the original charging arrangement. In this chapter, it is assumed that only EVs whose charging requirements can be fulfilled by the original charging arrangements are considered and the original charging starts right at the home arrival time, charges EV with maximum charging level and lasts until the required SOC is reached.

$$\boldsymbol{e}_{\mathbf{IC}} = \mathbf{P}_{\mathbf{OC}} \cdot {\boldsymbol{t}_{\mathbf{I}}}^{\mathsf{T}} \tag{2.10}$$

$$\boldsymbol{e}_{\mathbf{SC}} = \left(p_{\mathrm{O}} \mathbf{T}_{\mathbf{A}} - \mathbf{P}_{\mathbf{OC}}\right) {\boldsymbol{t}_{\mathbf{AI}}}^{\mathsf{T}} \tag{2.11}$$

where two $m \times 2n$ matrices $\mathbf{P}_{\mathbf{OC}}$ and $\mathbf{T}_{\mathbf{A}}$ are used to represent the charging of every EV during each time interval. For example, if the time interval is 1h, then the corresponding matrices are $m \times 48$; if the home arrival and departure time of EV i are assumed to be 16:00 and 7:00, respectively, then the 16th to 31st elements in the

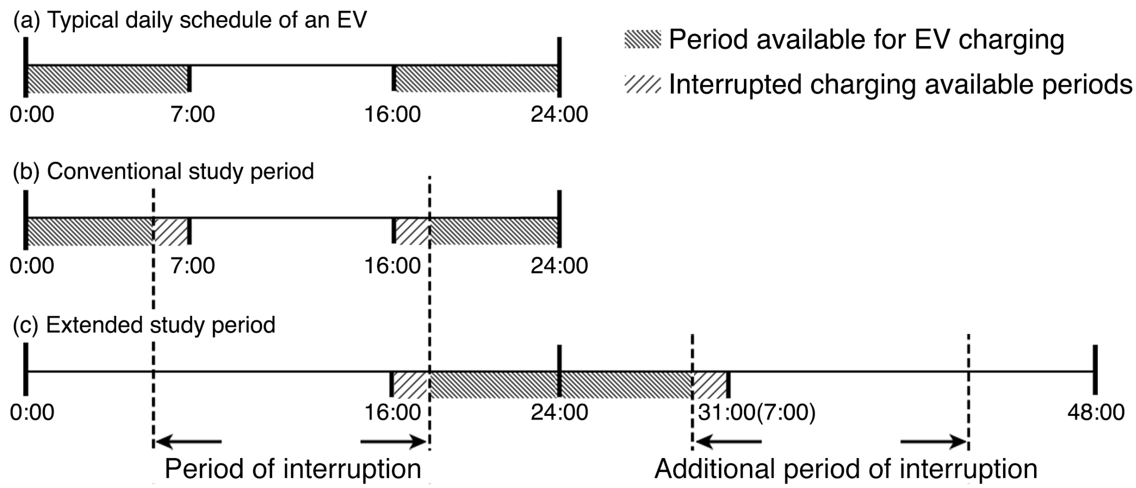

FIGURE 2.3: Illustration of the additional period of interruption for the extended study period

ith row of $\mathbf{T_A}$ are 1 (hour) and the other elements in the row are 0; if the required SOC for charging is 20 kWh and maximum charging rate is 5 kW, then the 16th to 19th elements in the ith row of $\mathbf{P_{OC}}$ are equal to 5 kW. Similarly, if the interruption takes place at 16:00 and the lead time of back-up units is two hours, then the 16th and 17th columns of row matrix $\boldsymbol{t_I}$ and the 18th to 48th columns of $\boldsymbol{t_{AI}}$ are 1 with the other elements in the matrices equal to 0. It should be noted that with the extended study period, the charging interruption should be considered twice in the calculation. This is because, as illustrated by Figure 2.3, in a one-calendar-day based study period, interruption may affect the separate available charging periods. It can be seen from Figure 2.3 that an additional period of interruption is applied to achieve equivalence.

Consequently, the above calculation ((2.7)$-$(2.11)) should be carried out twice for the equivalent periods of interruption and the final solution of the interruptible capacity for the period of interruption is the sum of the two results.

2.2.3 Capacity of V2G

When V2G is enabled, EVs are allowed to give their stored energy back to the grid. The basic idea of evaluating the capacity for V2G is similar to evaluating the interruptible capacity of EV charging. The idea of equivalent interruptible capacity for V2G is introduced here to implement this. With the V2G-equivalent interruptible capacity, which can be derived without changing the calculation procedure used in the previous subsection too much, the capacity for V2G (p_{V2G}) can be obtained by subtracting the interruptible capacity from the V2G-equivalent. For example, in addition to interruptible capacity of 5 kW for a given period, if an EV can provide another 5 kW back to the grid during the same period, then the equivalent interruptible capacity for that period is 10 kW:

$$p_{\mathrm{V2G}} = \frac{E_{\mathrm{V2G}}}{T_{\mathrm{I}}} \tag{2.12}$$

$$E_{\mathrm{V2G}} = E_{\mathrm{EI}} - E_{\mathrm{I}} \tag{2.13}$$

where T_{I} is the same as in (2.9) and we assume EVs have the same lead time for both being interrupted and providing V2G capacity; the calculation of E_{EI} is similar to E_{I}, except for the V2G-equivalent maximum energy loss ($\boldsymbol{e}_{\mathbf{EIC}}$):

$$E_{\mathrm{EI}} = \min\left(\sum_{i}^{m} e_{\mathrm{EIC},i}\,,\ \sum_{i}^{m} e_{\mathrm{SC},i}\right) \tag{2.14}$$

where the V2G equivalence ($e_{\mathrm{EIC},i}$) is obtained by (2.15):

$$\boldsymbol{e}_{\mathbf{EIC}} = \mathbf{P}_{\mathbf{OC}} \cdot {\boldsymbol{t}_{\mathbf{I}}}^{\mathsf{T}} + \boldsymbol{e}_{\mathbf{R}} \tag{2.15}$$

where the amount of reverse energy ($\boldsymbol{e}_{\mathbf{R}}$) is subject to SOC at the time when interruption takes place and the capacity limits of the reverse power:

$$\boldsymbol{e}_{\mathbf{R}} = \min\left(\mathbf{e}_{\mathbf{EV}}\,,\ p_{\mathrm{R}}\mathbf{T}_{\mathbf{A}} \cdot {\boldsymbol{t}_{\mathbf{I}}}^{\mathsf{T}}\right) \tag{2.16}$$

where the SOC ($\boldsymbol{e}_{\mathbf{EV}}$) is dependent on energy consumed for daily travel and energy charged by the original charging arrangement:

$$\boldsymbol{e}_{\mathbf{EV}} = \boldsymbol{e}_{\mathbf{F}} - \boldsymbol{e}_{\mathbf{D}} + \mathbf{P}_{\mathbf{OC}} \cdot \boldsymbol{t}_{\mathbf{BI}}^{\mathsf{T}} \tag{2.17}$$

where $\boldsymbol{e}_{\mathbf{D}}$ derives from E_{D}^{i} and the relationships among $\boldsymbol{t}_{\mathbf{BI}}$, $\boldsymbol{t}_{\mathbf{I}}$ and $\boldsymbol{t}_{\mathbf{AI}}$ are as in (2.18):

$$\boldsymbol{t}_{\mathbf{BI}} + \boldsymbol{t}_{\mathbf{I}} + \boldsymbol{t}_{\mathbf{AI}} = \mathbf{1} \tag{2.18}$$

2.2.4 Analysis Procedure

The proposed well-being analysis is carried out as follows:

1. Read system information and data from demand side; calculate ORR of each generating unit.

2. Calculate and form a COPT for the original system with ORR; obtain P_{H}, P_{M} and P_{R} with required well-being criteria.

3. Derive $\mathbf{P}_{\mathbf{OC}}$, $\mathbf{T}_{\mathbf{A}}$ and $\boldsymbol{e}_{\mathbf{D}}$ from t_{HA}^{i}, t_{HD}^{i}, and E_{D}^{i}.

4. Given time of the day and the corresponding load level, obtain $\boldsymbol{t}_{\mathbf{BI}}$, $\boldsymbol{t}_{\mathbf{I}}$ and $\boldsymbol{t}_{\mathbf{AI}}$.

5. Calculate p_{I} following the method provided in Subsection 2.2.2; obtain a COPT for the scenario of interruptible EV charging.

6. Calculate p_{V2G} following the method provided in Subsection 2.2.3; obtain a COPT for the V2G enabled scenario.

7. Calculate P_{EH}, P_{EM} and P_{ER} for both the above scenarios respectively.

8. Stop if all periods of interest and corresponding load levels are investigated; Go to Step 4 otherwise.

2.3 Numerical Study

The concepts developed in the previous sections are applied to the RBTS [28]. The generating unit model is shown in Figure 2.4. Units are scheduled following the

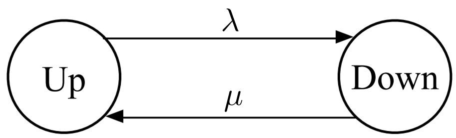

FIGURE 2.4: Two-state model

second loading order given in [28]. The generating system and load data are included in Appendix C.

Multiple criteria are required. In addition to an acceptable risk level of 0.001, a healthy state probability of 0.99 is required. The load on Monday of the 11th week is used. In addition to conventional units in the system, there are 5,000 identical EVs in the RBTS. Together with EV charging, the aggregate load varies from 38.6% to 66.5% of the 180 MW peak load. Energy capacity of EV is 25 kWh. and are both 5 kW. The equivalent rapid start unit for V2G is described by the four-state model shown in Figure 2.5. Its transition rates are given in Table 2.1. The system lead time is assumed to be 1 hour. Lead time is unit start time plus notification time. While the charging and discharging of EVs can be called on in a very short time, it is a common practice in conventional interruptible service programs to notify customers before the interruption [1]. We first assume the lead time of EV charging is 10 minutes, i.e. EV charging can be called in for both interruption and V2G in 10 minutes.

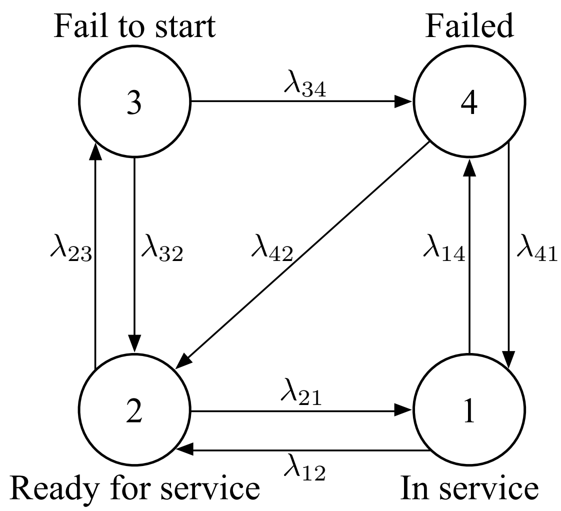

FIGURE 2.5: Four-state model for rapid start units

Table 2.1: Transition rates (f/hour) of the equivalent rapid start unit [18]

$\lambda_{11} = 0$	$\lambda_{12} = 0.005$	$\lambda_{13} = 0$	$\lambda_{14} = 0.03$
$\lambda_{21} = 0.0033$	$\lambda_{22} = 0$	$\lambda_{23} = 0.0008$	$\lambda_{24} = 0$
$\lambda_{31} = 0$	$\lambda_{32} = 0$	$\lambda_{33} = 0$	$\lambda_{34} = 0.025$
$\lambda_{41} = 0.015$	$\lambda_{42} = 0.025$	$\lambda_{43} = 0$	$\lambda_{44} = 0$

2.3.1 Daily Charging Requirements Simulation

As stated in Subsection 2.2.3, information such as EV travel and charging requirements should be obtained before the well-being analysis. Since no ready-made data of a population of EVs is available with regard to daily travel and charging, in this chapter, a simulation method is developed to generate the basic information required, i.e. t^i_{HA}, t^i_{HD} and E^i_{D}, from which other information such as $\mathbf{P_{OC}}$, $\mathbf{T_A}$ and $\mathbf{e_D}$ can be derived.

Dallinger *et al* [38] simulated EV daily driving by using the statistical distributions of driving behaviors [15], [69] such as start and end times of daily travel and daily mileage. Given the same distributions, available charging periods and SOC

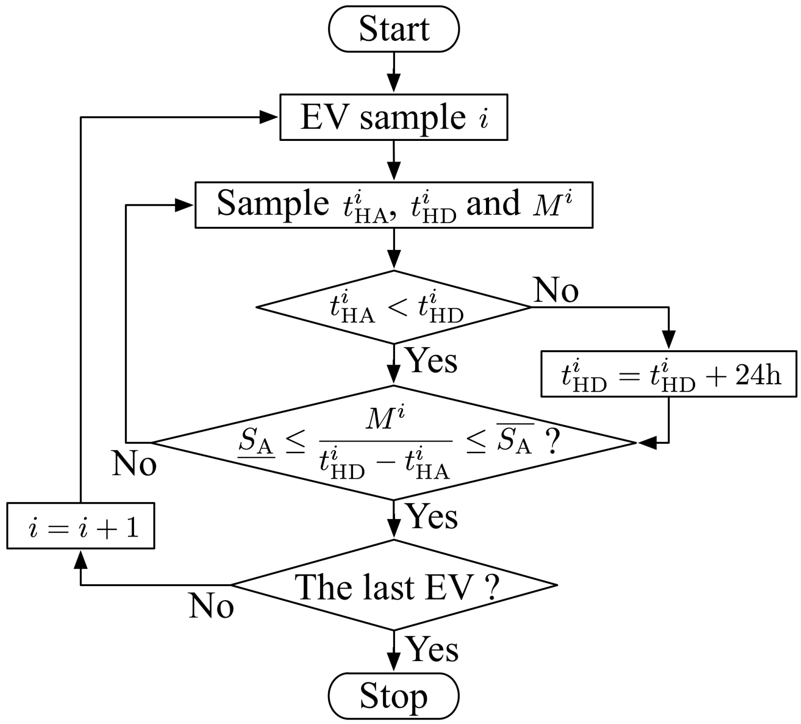

FIGURE 2.6: Sampling daily travel times and mileages of EVs

requirements can be obtained from sampling. The procedure is given in Figure 2.6. Rather than simply sampling, which would result in infeasible combinations of samples, this procedure checks the feasibility of samples and filters out the infeasible ones. Home arrival time should be prior to the departure time and average daily speed should be within a practical range (Figure 2.6). The upper and lower limits of daily average speed in this chapter are 60 miles/h and 5 miles/h, respectively. Following the sampling procedure, the available charging period is from t^i_{HA} to t^i_{HD} and the SOC requirement of charging is obtained by (2.19), assuming daily travel and charging requirements remain fixed for each EV:

$$E^i_{\mathrm{D}} = R_{\mathrm{A}} \cdot M^i \tag{2.19}$$

where R_{A} is assumed to be 0.23 kWh/mile in this chapter.

2.3.2 Numerical Results

With information obtained from the above, capacities available for EV charging interruption and V2G for the 24 load levels of the day are calculated as given in Figure 2.7, given that outages respectively take place at the top of each hour of the calendar day.

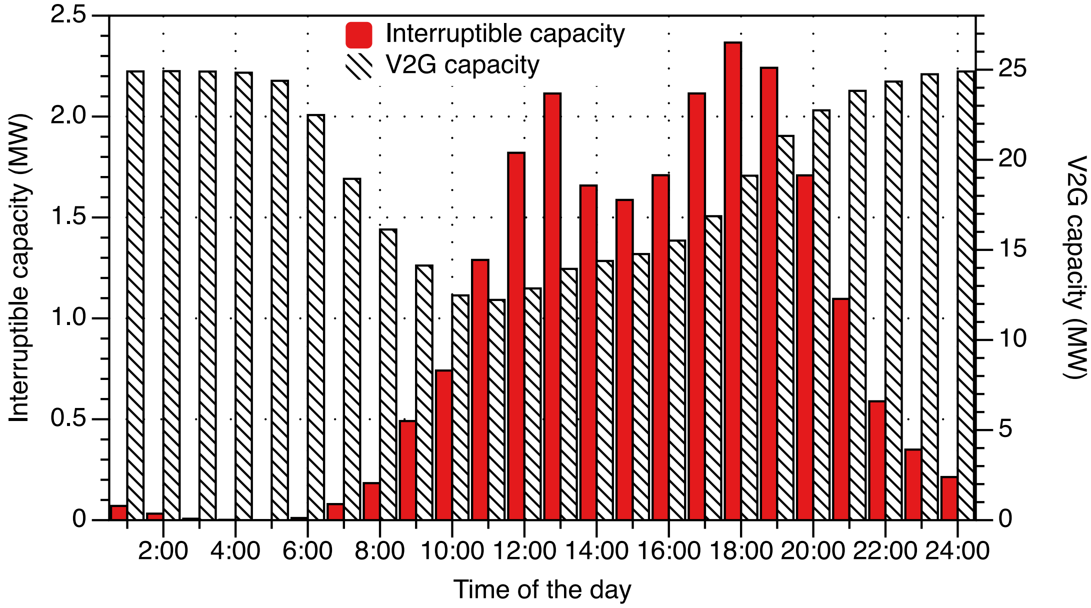

FIGURE 2.7: Capacities available for load interruption and V2G

According to (2.8), the charging of EVs can be regarded as interruptible load only when original charging load is nonzero (2.10) and the expected energy loss due to the interruption can be compensated afterwards (2.11). So interruptible capacities during the home arrival period (around 11:00 to 20:00 [38]) of the EVs are greater than any other periods of the day.

The situation is quite different for V2G. In accordance with (2.13) to (2.17), there are mainly four factors affecting the V2G capacity is subjected: population of grid-connected EVs, SOC available for discharging, maximum charging compensation after outage and maximum discharging rate. For example, the V2G capacity reaches its minimum at 11:00. This is attributed to two factors: the population of grid-connected EVs is small and SOC of EVs available for discharging is low at this time. On the other hand, when most EVs are at home with enough SOC (e.g. during 1:00 to 5:00), V2G capacity reaches its maximum, which is limited mainly by the maximum discharging rate (5kW $\times$ 5,000 EVs = 25 MW). In this example, the capacity for V2G is generally much greater than the interruptible capacity.

Table 2.2 shows the results of well-being analysis without and with interruptible EV charging. In this case, the system well-being remains the same during the day except for the 12th hour. For that hour, probabilities at the bottom of the cells represent ones with consideration of the interruptible load. The risk reduction (D_{r}) is 0.00000191, which accounts for 67.0% decrease of the original risk level (0.00000285). On the contrary, the probability of the system being in a healthy state at that hour is slightly higher and the marginal state is barely improved. It can be seen from (2.3) and (2.4) that except for the negligible second term $P_{\mathrm{R}} \cdot D_{\mathrm{r}}$ in (2.3), probabilities of healthy and marginal states are improved by D_{r}, which is far less than 1. That means the probabilities of healthy and marginal states after including interruptible load or rapid start units depend mainly on their values when the system has no emergency aid.

Since there is a big concern about the system risk level increasing in the presence of EV penetration, the system well-being without EV penetration is given in Table 2.3 for comparison. Given the definition of penetration level of EV charging as in (2.20), the 5,000 EVs represent a 13.9% penetration into the system:

$$L_{\mathrm{EV}} = \frac{m \cdot p_{\mathrm{O}}}{p_{\mathrm{syst}}} \times 100\% \tag{2.20}$$

It is worth noting that at the current penetration level (13.9%) the risk level during the day increases only at the 12th hour, from 0.00000188 to 0.00000285 (51.6% increasing). Rather than compensation, the system well-being is even improved at

Table 2.2: Generating system well-being without and with consideration of the interruptible capacity provides by EVs with multiple criteria

hr	Load level (MW)	no.of unit*	Interruptible capacity (MW)	Probability of		
				Health*	Margin*	Risk*
1	76	4	0.07	0.99842553	0.00157367	0.00000080
2	74	4	0.03	0.99842553	0.00157367	0.00000080
3	72	4	0.01	0.99842553	0.00157367	0.00000080
4	69	4	0.00	0.99842553	0.00157367	0.00000080
5	71	4	0.00	0.99842553	0.00157367	0.00000080
6	78	4	0.01	0.99842553	0.00157367	0.00000080
7	86	5	0.08	0.99828853	0.00171053	0.00000094
8	102	5	0.18	0.99774168	0.00225645	0.00000188
9	114	5	0.49	0.99774168	0.00225645	0.00000188
10	119	5	0.74	0.99774168	0.00225645	0.00000188
11	121	6	1.29	0.99717219	0.00282496	0.00000285
12	120	6	1.82	0.99717219 0.00282497	0.99717410 0.00000285	0.00282496 0.00000094
13	113	5	2.11	0.99774168	0.00225645	0.00000188
14	112	5	1.66	0.99774168	0.00225645	0.00000188
15	109	5	1.59	0.99774168	0.00225645	0.00000188
16	107	5	1.71	0.99774168	0.00225645	0.00000188
17	110	5	2.11	0.99774168	0.00225645	0.00000188
18	113	5	2.37	0.99774168	0.00225645	0.00000188
19	117	5	2.24	0.99774168	0.00225645	0.00000188
20	119	5	1.71	0.99774168	0.00225645	0.00000188
21	116	5	1.10	0.99774168	0.00225645	0.00000188
22	108	5	0.59	0.99774168	0.00225645	0.00000188
23	96	5	0.35	0.99828853	0.00171053	0.00000094
24	84	5	0.21	0.99828853	0.00171053	0.00000094

*Same for both scenarios if only one value is provided

that hour (risk reducing to 0.00000094) when interruptible capacity is included due to an additional unit being started.

Table 2.4 shows the system well-being when V2G is considered in addition to interruption of EV charging. Compared to Table 2.2, it can be seen that the risk during the day is largely reduced and the number of committed units for load levels of the 7th, 11th, 12th, 23rd and 24th hours decreases when both interruptible load

Table 2.3: Generating system well-being with multiple criteria without EV charging

hr	Load level (MW)	no.of unit	Probability of		
			Health	Margin	Risk
1	75	4	0.99842553	0.00157367	0.00000080
2	74	4	0.99842553	0.00157367	0.00000080
3	72	4	0.99842553	0.00157367	0.00000080
4	69	4	0.99842553	0.00157367	0.00000080
5	71	4	0.99842553	0.00157367	0.00000080
6	78	4	0.99842553	0.00157367	0.00000080
7	86	5	0.99828853	0.00171053	0.00000094
8	102	5	0.99774168	0.00225645	0.00000188
9	114	5	0.99774168	0.00225645	0.00000188
10	118	5	0.99774168	0.00225645	0.00000188
11	120	6	0.99717219	0.00282496	0.00000285
12	118	5	0.99774168	0.00225645	0.00000188
13	111	5	0.99774168	0.00225645	0.00000188
14	110	5	0.99774168	0.00225645	0.00000188
15	108	5	0.99774168	0.00225645	0.00000188
16	105	5	0.99774168	0.00225645	0.00000188
17	108	5	0.99774168	0.00225645	0.00000188
18	110	5	0.99774168	0.00225645	0.00000188
19	115	5	0.99774168	0.00225645	0.00000188
20	117	5	0.99774168	0.00225645	0.00000188
21	115	5	0.99774168	0.00225645	0.00000188
22	108	5	0.99774168	0.00225645	0.00000188
23	96	5	0.99828853	0.00171053	0.00000094
24	84	5	0.99828853	0.00171053	0.00000094

and V2G are considered. Similarly, probabilities of healthy and marginal state do not improve significantly in the presence of V2G.

2.4 Sensitivity Study

Section 2.2 shows that given the same system and the same EV travel behaviors, improvement in well-being of the generating system is dependent on the energy capacity of EVs, charging and discharging power limits, EV population in the system and the lead time of EV charging. This section investigates impacts of these factors.

Table 2.4: Generating system well-being considering V2G capacities of EVs with multiple criteria

hr	Load level (MW)	no.of unit	V2G capacity (MW)	Probability of		
				Health	Margin	Risk
1	76	4	24.90	0.99897295	0.00102700	0.00000005
2	74	4	24.92	0.99897295	0.00102700	0.00000005
3	72	4	24.90	0.99897295	0.00102700	0.00000005
4	69	4	24.83	0.99897295	0.00102700	0.00000005
5	71	4	24.38	0.99897295	0.00102700	0.00000005
6	78	4	22.48	0.99897295	0.00102700	0.00000005
7	86	4	18.94	0.99842597	0.00157367	0.00000035
8	102	5	16.13	0.99828927	0.00171053	0.00000020
9	114	5	14.13	0.99774242	0.00225645	0.00000113
10	119	5	12.47	0.99774242	0.00225645	0.00000113
11	121	5	12.22	0.99774242	0.00225645	0.00000113
12	120	5	12.86	0.99774242	0.00225645	0.00000113
13	113	5	13.94	0.99828853	0.00171053	0.00000094
14	112	5	14.38	0.99828853	0.00171053	0.00000094
15	109	5	14.77	0.99828927	0.00171053	0.00000020
16	107	5	15.51	0.99828927	0.00171053	0.00000020
17	110	5	16.87	0.99828927	0.00171053	0.00000020
18	113	5	19.11	0.99828927	0.00171053	0.00000020
19	117	5	21.32	0.99828927	0.00171053	0.00000020
20	119	5	22.74	0.99828927	0.00171053	0.00000020
21	116	5	23.82	0.99828927	0.00171053	0.00000020
22	108	5	24.34	0.99828927	0.00171053	0.00000020
23	96	4	24.75	0.99842597	0.00157367	0.00000035
24	84	4	24.90	0.99897295	0.00102700	0.00000005

As indicated by (2.1) and (2.6), the reduction of UCR is equal to the increase of sum of probabilities of healthy and marginal states. The daily risk reduction is introduced in this section to represent improvement of daily operating well-being of the system. Here we define the daily risk reduction as the sum of the magnitudes by which the probabilities of risk states corresponding to the 24 load levels of the day are reduced (i.e. sum of the 24 values of D_{r}, according to (2.5)) by interruptible EV charging and V2G capacities.

2.4.1 Effects of Energy Capacity of EV and Power Limits

Increasing energy capacity from 20 kWh to 50 kWh and the charging/discharging limits (assuming p_{O} equals p_{R}) from 1.4 kW (110 V / 12 A) to 10 kW (240 V / 40 A), the effects of the variance of energy capacity and charging/discharging limits on daily risk reduction of the system are shown in Figure 2.8.

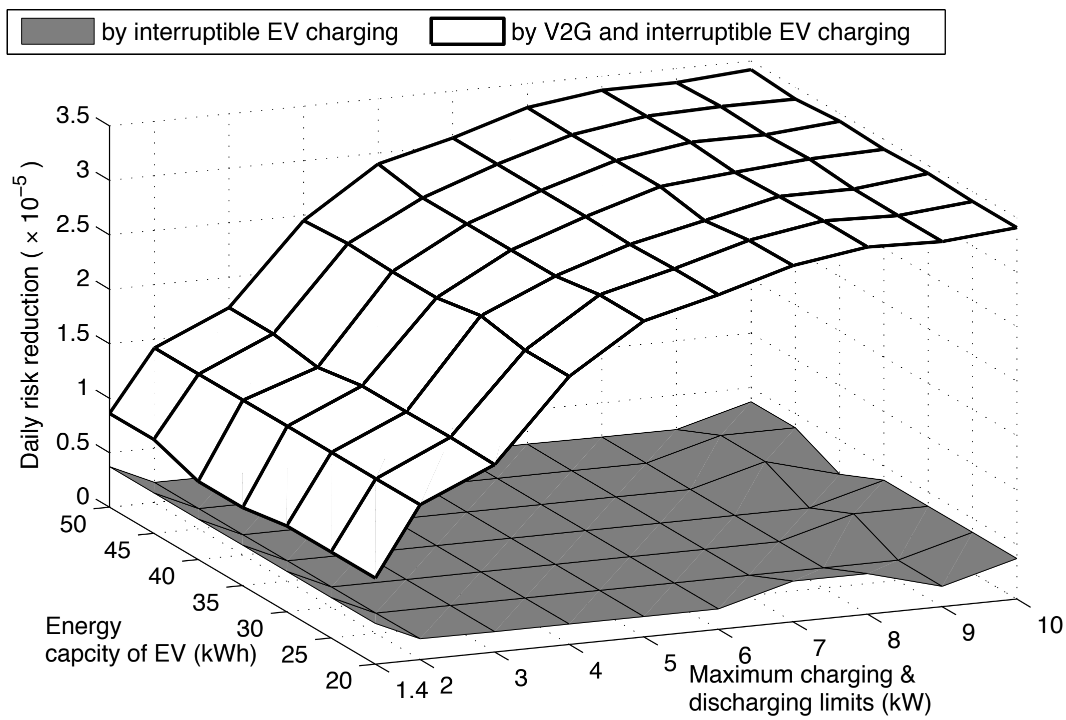

FIGURE 2.8: Effects of EV energy capacity and charging/discharging limits on total risk reduction

For the V2G enabled scenario, generally, daily risk reduction continues to increase with increase in maximum charging/discharging limits. However, the magnitude of reduction decreases with the increase. The reason is that by the nature of COPT, the possibility of at risk state can never equal zero as long as generating units with non-zero ORR are involved. So the decrease of the UCR becomes harder when it is getting closer to zero. On the other hand, the increase of energy capacity hardly improves the system well-being.

It is noted that the trend of daily risk reduction is not absolutely monotonic. For example, when the energy capacity of EV is set to 20 kWh, the daily risk reduction decreases at 9 kW charging rate before it increases again at 10 kW. The reason can be found by investigating the detailed results. The numbers of units committed during the day in the V2G enabled scenario are given in Table 2.5 with energy capacity of EV set to 20 kWh. It can be seen from the table that with charging/discharging limits raised from 8 kW to 9 kW the numbers of units at the 6th, 16th to 20th and 24th hours are reduced. This heightens the risk at those hours, which cancels the additional well-being improvement resulting from the rise of charging/discharging limits. When the limits are raised from 9 kW to 10 kW, the unit commitment is only changed at the 4th hour. The consequent risk increase is still outpaced by the risk reduction. Thus a further well-being improvement can be spotted at 10 kW.

Table 2.5: Number of units with energy capacity of EV set to 20 kWh

Hour		1	2	3	4	5	6	7	8	9	10	11	12	13	14	15	16	17	18	19	20	21	22	23	24
Charging/discharging limits (kW)	8	3	3	3	3	3	4	4	4	5	5	5	5	5	5	5	5	5	5	5	5	4	4	4	4
	9	3	3	3	3	3	3	4	4	5	5	5	5	5	5	5	4	4	4	4	4	4	4	4	3
	10	3	3	3	2	3	3	4	4	5	5	5	5	5	5	5	4	4	4	4	4	4	4	4	3

In the scenario where only interruptible EV charging is involved, given the acceptable risk and probability of healthy state, neither the maximum charging/discharging limits nor energy capacity can affect the UCR much. This is because interruptible capacity is dependent on the daily charging requirement, which is determined by driving behaviors of EVs. As the driving behaviors remain unchanged, system well-being improved by interruptible EV charging stays small compared to the V2G enabled scenario.

2.4.2 *Effects of EV Penetration Level*

With the maximum charging rate limited to 5 kW, the daily risk reduction achievable by varying the EV population from 1,000 to 10,000, that is, by increasing penetration from 2.8% to 28.8%, is given in Figure 2.9.

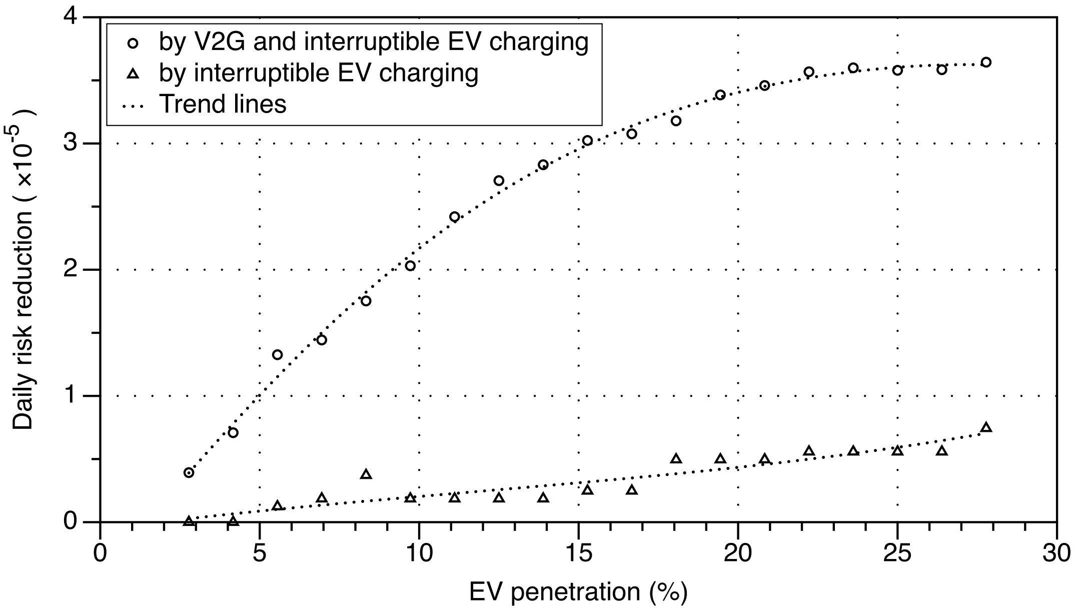

FIGURE 2.9: Effects of EV penetration on total risk reduction

Daily risk reduction is generally increased with increasing EV population in both scenarios. In V2G enabled scenario, the system well-being improves with increase of the penetration by a continuously reducing magnitude until some penetration level is reached, which is 25% in this case. When only interruptible EV charging is included, the risk reduction is not as sensitive to changes in EV penetration as in a V2G enabled scenario. This is because, as found in Section 2.3, inclusion of interruptible EV charging has a limited impact on system well-being since the unit commitment is changed only for limited hours during the day. In comparison, a more consistently increasing trend can be spotted in a V2G enabled scenario since the inclusion of V2G capacity triggers more unit commitment schedules being changed during the day. It is also noted that in some instances daily risk reduction declines with the increased penetration level, especially in the scenario of interruptible EV charging. The reason is that, as mentioned in Subsection 2.3.1, information from demand side is stochastically generated. With EV population size changed, travel and charging requirements for the population have to be updated as well. Consequently, according to the evaluation methods provided in Section 2.2, increases in interruptible and V2G capacities along with EV population for each hour during the day cannot be always expected.

To investigate the increase of system risk level caused by EV charging, the total risk increase during the day is plotted against EV penetration level, as shown in Figure 2.10. Without the help from EVs, the daily risk is dependent only on the system load and the unit commitment during the day. The system load gradually builds up with the increase of EV penetration. However, the unit commitment is not changed as long as the reliability criteria are guaranteed. By the discrete nature of UCR from a COPT, the resultant risk index is not changed when the load is within a certain range, for the same COPT. This is why the risk increases in a step-like manner.

No doubt the system health will deteriorate with the rise of EV population. However, compared to Figure 2.9, it can be seen that from the perspective of system reliability, activating EVs' responsiveness can achieve not only migration of the harm EV charging does to the system but also a further improvement of the system well-being, especially when V2G is considered.

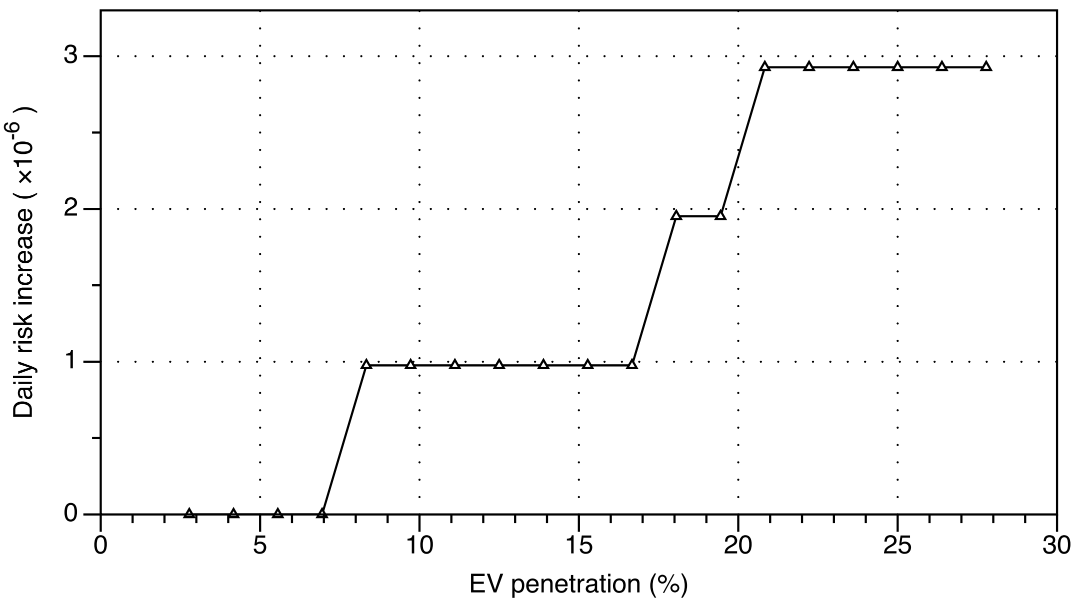

FIGURE 2.10: Daily risk increases under various EV penetration levels

2.4.3 Effects of EV Charging Lead Time

Apart from the above factors, in the presence of given interruptible capacities and V2G capacities, the system well-being is a function not only of the system lead time, but also of the lead time of EV charging itself. The lead time includes a notification time and a time delay that EV charging facility requires to respond to the notification. As EV batteries can respond very quickly and there may be agreements between EV users and the grid on duration of the notification time, the lead time could vary over a wide range. Figure 2.11 shows the results in terms of daily risk reduction with various EV charging lead times, from 30s to 15 minutes, while the remaining parameters of the system are the same.

It can be seen that for both interruptible EV charging and V2G enabled scenarios the shorter the EV charging lead time is the more the system well-being can be improved.

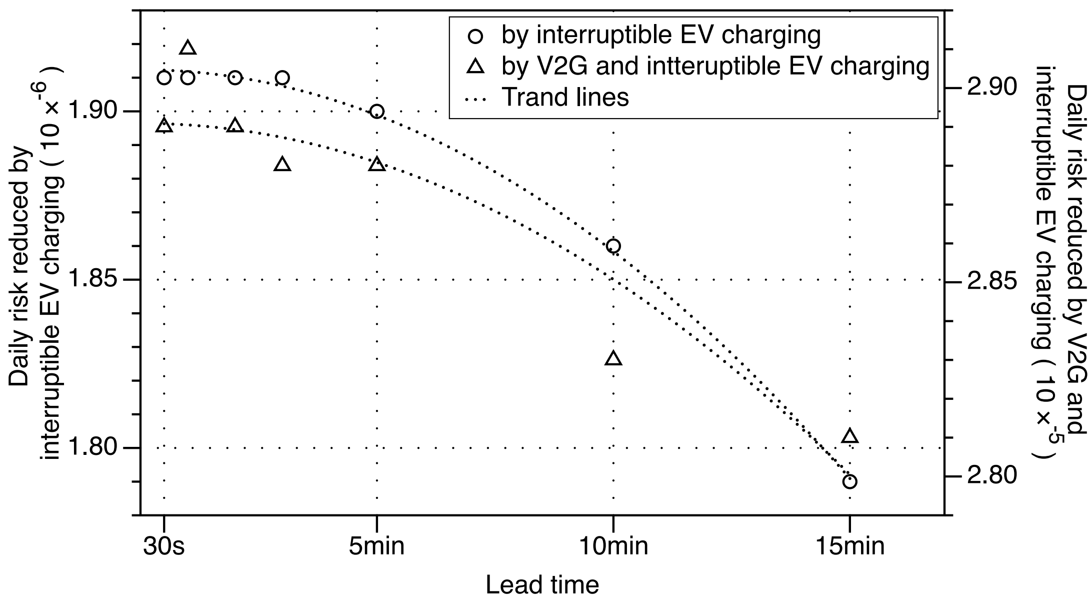

FIGURE 2.11: Effects of EV charging lead time

2.5 Summary

One of the major achievements of this chapter is the methodology to incorporate EVs' contribution into the generating system operating health analysis. Variables used are given in the form of matrices. By doing this, the calculation for a large population of EVs is clearly facilitated. Besides, matrix handling is more efficient for numerical analysis softwares such as Matlab than simple loop control statements.

One of the significant insights that can be drew from the numerical study provided is that EVs' providing interruptible charging and V2G capacities not only migrate the potential health deterioration of the generating system due to EVs' penetration but could also further improve the system reliability.

3

Uncertainties of EV Charging and Effects on Well-Being Analysis of Generating Systems

The chapter is organized as follows. The well-being analysis of generating systems and EVs' inclusion are reviewed in Section 3.1, where the motivation and the need for this study are also given. The basic methodologies for assessing capacity contribution of EVs and other basics are briefly reviewed in Section 3.2. Uncertainties of EV charging are identified and formulated in Section 3.3. In Section 3.4 methods are proposed to incorporate the uncertainties in well-being assessment. Numerical results are given in Section 3.5, followed by the sensitivity study in Section 3.6. In Section 3.7 the load forecast uncertainty is considered.

3.1 Well-Being Analysis of Generating Systems Incorporating EV Charging

3.1.1 Reduction of Unit Commitment Risk

To allow the inclusion of rapid start and hot reserve units, interruptible load and postponable outages in the assessment of unit commitment risk [7], a modified PJM approach was proposed by Billinton *et al.* [18], [16]. When additional generation such as rapid start units and/or demand response programs such as interruptible load are included, it is important to take into consideration the type of the additional units and/or demand response programs since they have different delay time associated with their load carrying capability [21]. The effect on the reliability of generating systems, i.e. the reduction of the unit commitment risk, can be illustrated by area risk curve concept [18, 21]. The probability of finding an operating unit on outage at time t is

$$P(\text{down}) = \frac{\lambda}{\lambda+\mu} - \frac{\lambda}{\lambda+\mu}\, e^{-(\lambda+\mu)\cdot t} \tag{3.1}$$

Usually no repairs can be accomplished during the short period t, i.e. $\mu = 0$, then (3.1) becomes

$$P(\text{down}) = 1 - e^{-\lambda t} \tag{3.2}$$

The risk (or density) function $f(R)$ is

$$f(R) = \frac{dP(\text{down})}{dt} = \lambda e^{-\lambda t} \tag{3.3}$$

and probability of the unit failing during the time period between 0 to T is given by

$$P(0,T) = \int_0^T f(R)\, dt = \int_0^T \lambda e^{-\lambda t}\, dt \tag{3.4}$$

Consider a hypothetical system where a certain amount of interruptible load can be called on in T_1 and some rapid start units can be placed in service after a T_2 delay, while the lead time of conventional generation is T_3. If a decision is made at $t = 0$ to call on interruptible load and start rapid start units, the risk function $f(R_1)$ will decrease to a new value ($f(R_2)$) after the lead time of interruptible load (T_1) and become $f(R_3)$ after the lead time of T_2 when rapid start unit is available, as pictorially illustrated by Fig. 3.1. The risk level for the entire lead time T_3 without and with interruptible load and rapid start units are given by (3.5) and (3.6), respectively.

$$P(0, T_3) = \int_0^{T_3} f(R_1)\, dt \tag{3.5}$$

$$\begin{aligned} &P'(0, T_3) = \\ &\int_0^{T_1} f(R_1)\, dt + \int_{T_1}^{T_2} f(R_2)\, dt + \int_{T_2}^{T_3} f(R_3)\, dt \end{aligned} \tag{3.6}$$

Then it is clear that the reduction of risk level achieved by demand response and additional generation is the difference between the two, i.e. the shaded area in Fig. 3.1.

The computation of the risk level contribution is detailed in [21] and [18].

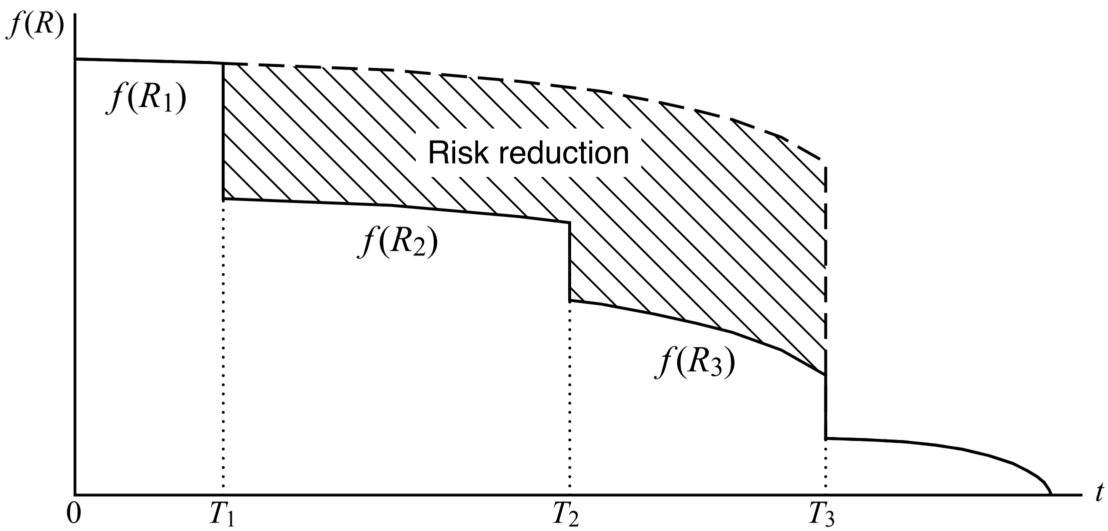

FIGURE 3.1: Concept of area risk curve

3.1.2 Incorporating EV Charging Into Well-Being Analysis

To address the difficulty of interpreting the numerical risk index and inadequacy of information provided by a single index, Billinton *et al.* [19] developed the well-being analysis framework, where a system is identified as being healthy, marginal or at risk. A system is regarded as being healthy if the generation is adequate to supply the existing total load demand. A system is in a marginal state if it does not have enough operating reserve to satisfy the deterministic criterion. In the state of risk, the system load is equal to or greater than the operating capacity. The method for well-being analysis of generating systems considering standby units, interruptible load and postponable outages was provided in [16]. It should be noted that the risk level, i.e. the probability of being in state of risk, and its reduction serve as the base for calculating the other well-being indices considering additional resources [16].

It can be seen from Fig. 3.1 that the reduction of the total risk depends upon how much difference $f(R_2)$ and $f(R_3)$ can make, compared to $f(R_1)$. The values of new risk functions are heavily dependent upon the capacities of the additional generation and load interruption. For conventional generation, demand response programs and unconventional resources such as wind turbine generators and solar panels, it is not a problem to obtain the capacities since rated output values or capacities available for spinning reserve are known. It is, however, not the case for EVs' grid service provision. Firstly, given the distributed nature, each EV has different "parameters" such as energy capacity and charging requirements. Secondly, as a result of the daily travel, the capacity EVs could provide, either as interruptible load or additional generation, varies during the day. Keeping this in mind, a quantitative framework for analyzing the system well-being with the involvement of EVs charging was proposed in [94], where a method for evaluating EVs' capacity contributions as interruptible load and V2G was provided.

Nevertheless, the risk reduction is not just solely determined by the "rated" capacities of additional generation. Suitable models are required for the standby units (or other resources) that realistically account for the fact that they may or may not come into service successfully after their respective lead times [18]. When additional resources are considered into reliability study, their probabilistic nature has to be considered and relevant models typifying their distinctive operating characteristics are required. The primary energy fluctuations as well as the failure and repair characteristics associated with unconventional energy sources such as solar power plants and wind turbine generators were included in reliability assessment of generating systems [80]. Different wind speed models were presented and their effects on generating capacity adequacy were compared [20]. The effects of distributed generation (DG) were examined in [9] and [4], where different models for wind/solar DG were used. To make the evaluation process more accurate, the correlation between multiple wind speeds from different sites was modeled into generating system reliability evaluation in [73].

Table 3.1: Consideration of uncertainties for modeling generating units and demand response programs

	Conventional	Unconventional
Generating units	– Hardware failure / malfunction e.g. Thermal / hydro [18]	– Hardware concerns – Intermittent and/or distributed nature – Forecast error e.g. Solar / wind [80, 20, 9, 4, 73]
Demand-side programs	– 100% available e.g. Interruptible load [16]	– Hardware concerns – Distributed nature – Forecast error – Human behaviors – Grid realization e.g. EV charging

Table 3.1 summarizes the typical uncertainties considered for modeling units and services from generating and demand sides of power systems. Different from other unconventional energy resources, little is known about the probabilistic nature associated with EVs' grid services provision given multiple aspects involved (i.e. the entry of "unconventional, demand-side programs" in Table 3.1). Traditionally, programs such as interruptible load are treated as 100% available after the lead time. Thus the

new risk level can be calculated without updating the capacity outage probability table [16]. That is not the case for EVs' provision of interruptible load. As stated above, the evaluation of EVs' capacity contribution is based on not only the types of vehicle but also their daily travel and charging schedules, which can be easily affected by human activities as well as hardware failures. Besides, model used to represent these uncertainties is not expected to be exactly the same for different points of time in the day. To make the assessment process more accurate, uncertainties of EVs' grid contribution and their causes have to be investigated, as depicted by the upper right block in Fig. 1.6.

3.2 Capacity Evaluation

The interruptible capacity is the aggregate capacity contributed from EVs that can be interrupted during the outage, while the V2G capacity is the capacity to be injected back to the system if V2G is allowed. The basic premise for their evaluation is that daily travel and charging requirements of each EV ought not to be compromised, that is, the capacity, either to be interrupted or fed back, can be fully compensated after system lead time and before EV's departure [94]. For the ease of illustration the methods for evaluating the interruptible and V2G capacities are reviewed here.

3.2.1 Interruptible Capacity

The interruptible capacity (p_{I}) is determined by the amount of charging energy that can be interrupted (E_{I}) and duration of interruption (T_{I}):

$$P_{\mathrm{I}} = \frac{E_{\mathrm{I}}}{T_{\mathrm{I}}} \tag{3.7}$$

where E_{I} is subject to two variables: the maximum energy loss due to the interruption and maximum energy provided by supplementary charging, as given by (3.8); T_{I} is given by (3.9):

$$E_{\mathrm{I}} = \min\left(\sum_{i}^{m} e_{\mathrm{IC},i}\,, \sum_{i}^{m} e_{\mathrm{SC},i}\right) \tag{3.8}$$

$$T_{\mathrm{I}} = \mathbf{1} \cdot \boldsymbol{t}_{\mathbf{I}}^{\mathsf{T}} \tag{3.9}$$

where $e_{\mathrm{IC},i}$ is equal to the energy supposed to be charged originally during the period of interruption, as given by (3.10); $e_{\mathrm{SC},i}$ is defined as the amount of energy that can be delivered to an EV, in addition to its original charging arrangement, after the interruption, as defined by (3.11); $\boldsymbol{t}_{\mathbf{I}}$ represents the period during which EV charging is to be interrupted.

$$\boldsymbol{e}_{\mathbf{IC}} = \mathbf{P}_{\mathbf{OC}} \cdot \boldsymbol{t}_{\mathbf{I}}^{\mathsf{T}} \tag{3.10}$$

$$\boldsymbol{e}_{\mathbf{SC}} = \left(p_{\mathrm{O}}\mathbf{T}_{\mathbf{A}} - \mathbf{P}_{\mathbf{OC}}\right) \boldsymbol{t}_{\mathbf{AI}}^{\mathsf{T}} \tag{3.11}$$

where two $m \times 2n$ matrices $\mathbf{P}_{\mathbf{OC}}$ and $\mathbf{T}_{\mathbf{A}}$ are used to represent the charging of every EV during each time interval. The reason for $2n$ is that typically a period of daily charging is cut by two calendar days (e.g. home parking period) and in order to facilitating the evaluation and fitting it into daily generating schedules—which are usually based on calendar days—the idea of extended study period [94] is applied. Details of the matrix manipulation are given in Subsection 2.2.2 and 2.2.3.

3.2.2 Capacity for V2G

The basic idea of evaluating the V2G capacity is similar to evaluating the interruptible capacity. The idea of equivalent interruptible capacity for V2G is used to implement the calculation. V2G capacity (p_{V2G}) is obtained by subtracting the actual interruptible capacity from the V2G-equivalent interruptible capacity:

$$p_{\mathrm{V2G}} = \frac{E_{\mathrm{V2G}}}{T_{\mathrm{I}}} \tag{3.12}$$

$$E_{\mathrm{V2G}} = E_{\mathrm{EI}} - E_{\mathrm{I}} \tag{3.13}$$

where T_I is the same as in (3.9); the calculation of E_EI is similar to E_I, except for the V2G-equivalent maximum energy loss ($\boldsymbol{e}_\mathbf{EIC}$):

$$E_\mathrm{EI} = \min\left(\sum_i^m e_{\mathrm{EIC},i}\,,\,\sum_i^m e_{\mathrm{SC},i}\right) \tag{3.14}$$

where the V2G equivalence ($e_{\mathrm{EIC},i}$) is obtained by (3.15):

$$\boldsymbol{e}_\mathbf{EIC} = \mathbf{P}_\mathbf{OC} \cdot {\boldsymbol{t}_\mathbf{I}}^\mathsf{T} + \boldsymbol{e}_\mathbf{R} \tag{3.15}$$

where the amount of reverse energy ($\boldsymbol{e}_\mathbf{R}$) is subject to SOC at the time when interruption takes place and the capacity limits of the reverse power:

$$\boldsymbol{e}_\mathbf{R} = \min\left(\mathbf{e}_\mathbf{EV}\,,\,p_\mathrm{R}\mathbf{T}_\mathbf{A} \cdot {\boldsymbol{t}_\mathbf{I}}^\mathsf{T}\right) \tag{3.16}$$

where the SOC ($\boldsymbol{e}_\mathbf{EV}$) is dependent on energy consumed for daily travel and energy charged by the original charging arrangement:

$$\boldsymbol{e}_\mathbf{EV} = \boldsymbol{e}_\mathbf{F} - \boldsymbol{e}_\mathbf{D} + \mathbf{P}_\mathbf{OC} \cdot {\boldsymbol{t}_\mathbf{BI}}^\mathsf{T} \tag{3.17}$$

where $\boldsymbol{e}_\mathbf{D}$ derives from E_D^i and the relationships among $\boldsymbol{t}_\mathbf{BI}$, $\boldsymbol{t}_\mathbf{I}$ and $\boldsymbol{t}_\mathbf{AI}$ are as in (3.18):

$$\boldsymbol{t}_\mathbf{BI} + \boldsymbol{t}_\mathbf{I} + \boldsymbol{t}_\mathbf{AI} = \mathbf{1} \tag{3.18}$$

For details of capacity evaluation and the extended study period, the reader is referred to Subsection 2.2.2 and 2.2.3.

3.3 Uncertainties of EV Charging

To enable EVs' grid services, the grid operator needs first to be informed of the estimated capacity contribution from the aggregators, i.e. interruptible and V2G capacities (p_I and p_V2G) of each aggregated EV population. As potential failures of conventional generating units derate their actual capacities for the nominal or scheduled ones, and as the consideration of primary energy fluctuations is indispensable to unconventional units such as solar panels and wind turbine generators, the probabilistic nature of EV charging ought to be considered along with the "rated" capacity contribution. As an emerging grid resource, EVs' commitment to power systems is subject to not only hardware failures and repairs but also multiple other elements.

It can be found from the above section that for a given interruption period $\boldsymbol{t_\mathrm{I}}$ and charging/discharging limits p_O and p_R, the original charging plans $\mathbf{P_{OC}}$ and available periods for EV charging $\mathbf{T_A}$ serve as fundamental variables for capacity evaluation. The two variables are determined by EVs' travel schedules and charging requirements. As a result, this information needs to be collected beforehand. Unlike other resources or services in power systems, EVs are "operated" by populations of human beings and it is only fair to expect that this information can be affected by forecast uncertainties as well as human errors. In this chapter, elements could compromise EVs' grid commitment are collected. At the individual level, there are five elements make the capacity contribution uncertain: punctuality, rounding of time, forecast error of daily energy consumption, charging component failure and EV absence, as depicted in Fig. 3.2. Among these, punctuality and rounding of time are alternative and charging component failure and EV absence have the same impact—charging failure—no capacity is available from the EVs involved. At the aggregated level, the failure of an aggregator implies it will have no contribution to the grid.

3.3.1 Punctuality

If errors exist in travel schedule, i.e. time of arrival and departure, ($\mathbf{P_{OC}}$) and ($\mathbf{T_A}$) would vary. For vehicle arrival and departure, general relationships between actual and expected time are given in (3.19) and (3.20), assuming the charging begins right

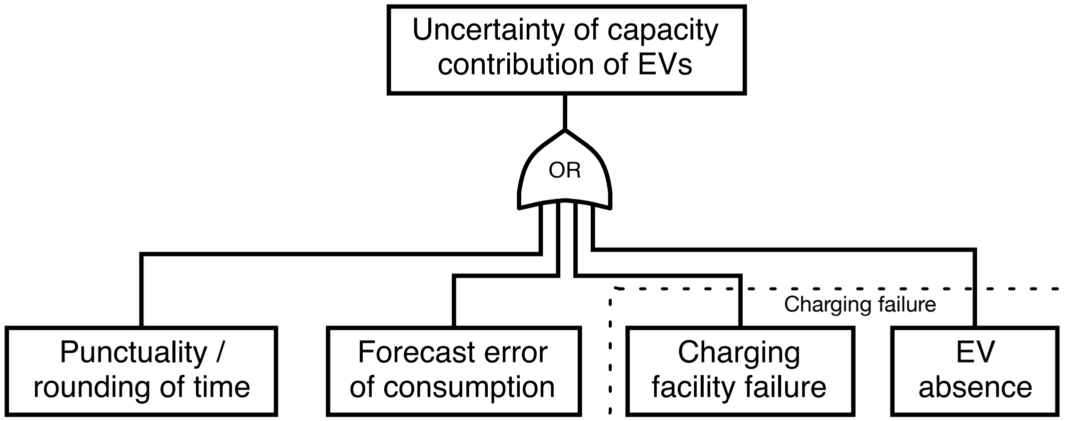

FIGURE 3.2: Fault tree of EV charging at the individual level

after the daily travel:

$$t^i_{\mathrm{ATA}} = t^i_{\mathrm{ETA}} + t^i_{\mathrm{Err,A}} \tag{3.19}$$

$$t^i_{\mathrm{ATD}} = t^i_{\mathrm{ETD}} + t^i_{\mathrm{Err,D}} \tag{3.20}$$

where negative values of errors $t^i_{\mathrm{Err,A}}$ and $t^i_{\mathrm{Err,D}}$ indicate earliness while positive denotes lateness.

One of the causes of the errors is punctuality. Companies and factories normally have regulated working hours. If EV charging takes place during working hours, the expected time of arrival and departure is used directly to evaluate the capacity contribution. However, it is common people being late or early for appointments.

A typical distribution describing the effect of punctuality is given in Fig. 3.3. Punctuality varies with personalities, genders and types of appointments, etc. [10], [54], [42]. Historically, punctuality was first described by "J-curve" and "double J-curve" in [5]. After examining the J-curve hypothesis, Dudycha [41] drew the conclusion that punctuality distributions may best be described by normal curves.

3.3.2 Rounding of Time

If the expected time of arrival and departure is scheduled and reported by individual EV users, e.g. when EV charging takes place while parked at home, then the rounding

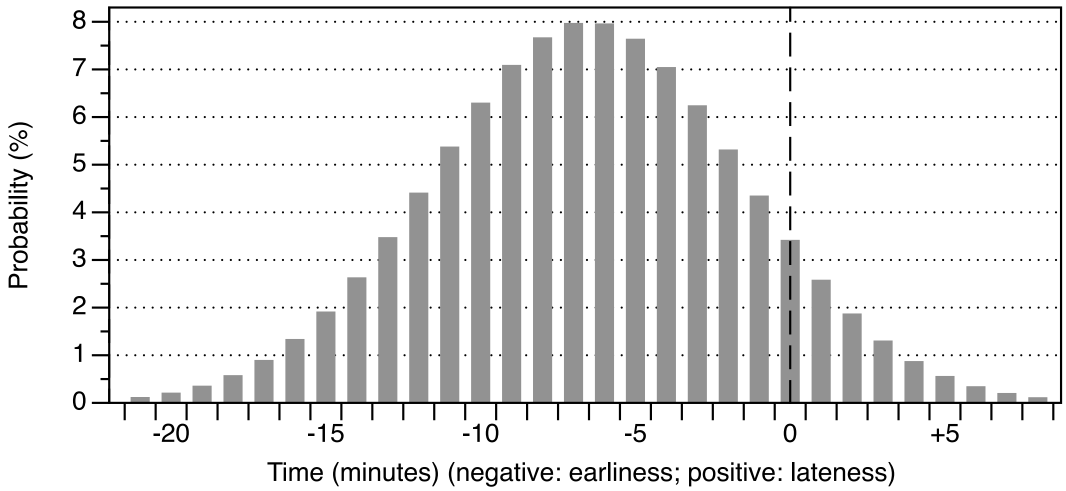

FIGURE 3.3: A typical distribution of punctuality [41]

of time is the reason for uncertainty. People tend to have tentative schedule with approximate time [75]. It is found that most travel surveys have reported times in multiples of 5 minutes [75], [34], [83]. For example 82.87% of the reported times of daily departure in National Household Travel Survey (NHTS [86]) are given as multiples of 5 minutes. Rietveld *et al.* [75] demonstrated that for both scheduled and unscheduled activities the variance of rounded travel times is much larger than that of unrounded ones. In this chapter, the reported time in travel schedules is considered to be accurate if it is not multiples of 5 minutes:

$$t^i_{\mathrm{ATA}} = t^i_{\mathrm{ETA}} \quad \text{if } t^i_{\mathrm{ETA}} \bmod 5 \neq 0 \tag{3.21}$$

$$t^i_{\mathrm{ATD}} = t^i_{\mathrm{ETD}} \quad \text{if } t^i_{\mathrm{ETD}} \bmod 5 \neq 0 \tag{3.22}$$

while (3.19) and (3.20) are applied to the other occasions. A typical distribution of time rounding is given as in Fig. 3.4.

Punctuality and rounding of time are two alternatives that explain the error of expected time of arrival and departure. In case of regulated time, punctuality should be applied. For self-scheduled driving plans, the rounding effect is to be considered.

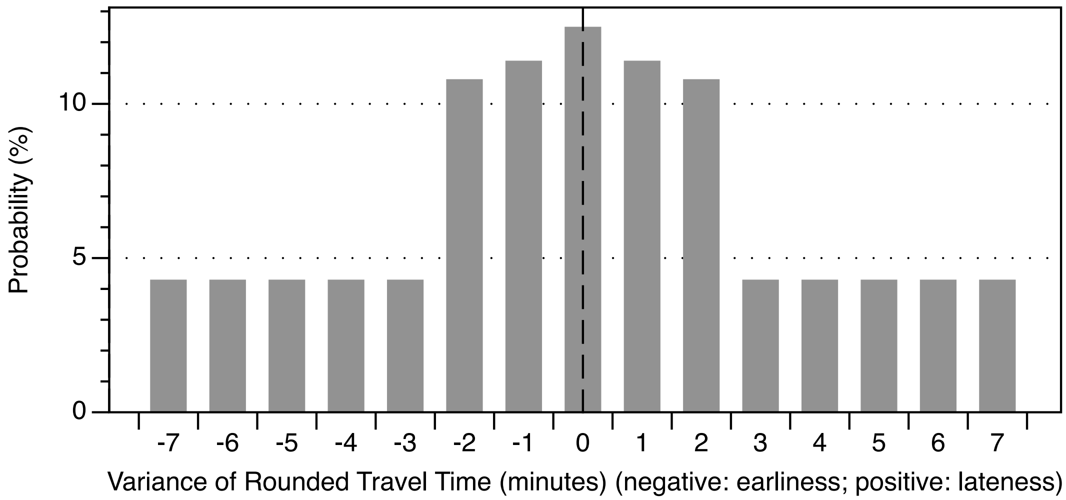

FIGURE 3.4: A typical distribution of variance of rounded travel time [75]

3.3.3 Forecast Error of Energy Consumption

The charging arrangement can also be affected by errors in the forecast of energy consumption. In the future, there could be two ways to predict the daily energy consumption of EV. One is that individual EV users plan and report their daily mileages in advance. Then daily energy consumption can be predicted with an estimated consumption rate. But if smart meters are fully integrated in the future grids, historical data of daily consumption can be fetched easily, based on which the prediction can be made. In this chapter, given the availability of existing study and data, the former way is assumed. The forecast uncertainty comprises two parts: misreporting of daily travel distances and error of the estimated consumption rate. Forecast and actual values of the daily consumption are given by (3.23) and (3.24), respectively:

$$E^i_{\mathrm{FD}} = M^i_{\mathrm{S}} \cdot R_{\mathrm{FA}} \tag{3.23}$$

$$E^i_{\mathrm{AD}} = (M^i_{\mathrm{S}} + M^i_{\mathrm{Err}}) \cdot R^i_{\mathrm{AA}} \tag{3.24}$$

where in (3.23) consumption rate R_{FA} is a fixed value while in (3.24) either R^i_{AA} or M^i_{Err} follows a certain distribution. Walsh *et al.* [87] examined the electricity consumption of typical EVs and found it is affected by driver type, driving style, route and battery type, etc. Based on their observations, we use a Gaussian distribution to represent the possible variance of the actual value of average consumption rate (Fig. 3.5).

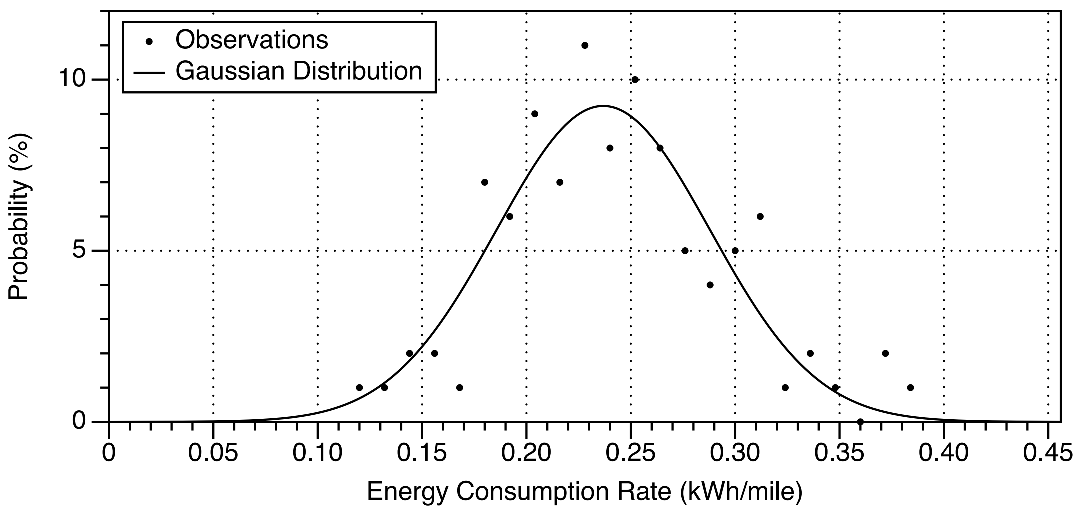

FIGURE 3.5: Distribution of average energy consumption rate during EV driving

Stopher *et al.* [83] assessed the accuracy of reported daily travel distance, which was found to be consistently overestimated on average, as shown in Fig. 3.6.

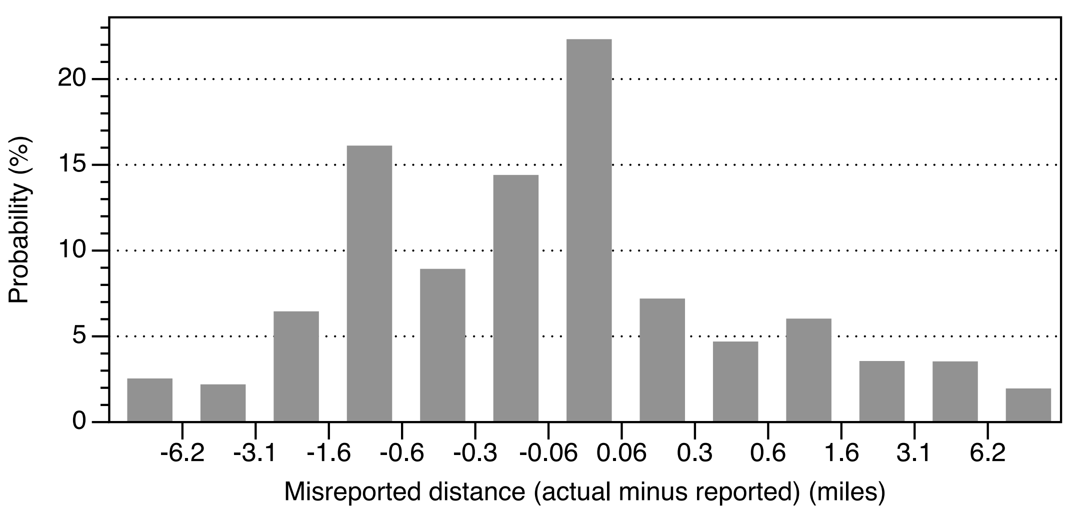

FIGURE 3.6: A typical distribution of misreporting of trip distance [83]

3.3.4 Charging Component Failure and EV Absence

Unlike punctuality and rounding of time, which shift or/and alter the charging schedule, charging component failure and EV absence nullify scheduled contribution of EV for a certain period of time. The charging component failure depicts the failure of charging facilities, e.g. inverters, rectifiers and switches, etc. EV absence denotes the uncertainties from EV itself. For instance, an EV may fail to get home on schedule due to some internal failure. Obviously, human activities contribute to the absence as well. An EV could depart without prior notice due to some emergency, or the EV is off duty as a result of a traffic collision. At this point, it is difficult to distinguish the cause of each instance of those "off-grid" EVs, i.e. whether it is hardware failure or human activity. A two-state model is used to generally represent the probability of EV being absent for scheduled grid services (Fig. 3.7).

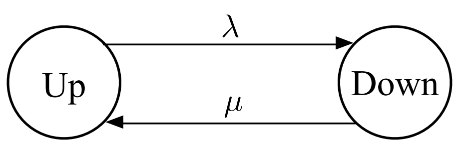

FIGURE 3.7: Two state model charging component and aggregator

3.3.5 Aggregator Failure And Grid Realization

The aggregator could be either existing utilities that will offer new financial contracts specifically for the charging load, or new for-profit entities that will participate in the wholesale market [93]. One single aggregator can be sufficient for handling the charging and grid services of EVs, if the system is small and the penetration level of EVs is not significant. At the instance when the EV penetration is high in the system or it covers a large geographical area, multiple aggregators coexisting in the system are likely to be the case. Especially, multiple aggregators are more expected in a deregulated market. The possible grid realization for EV charging and EVs' grid services are given in Fig. 3.8.

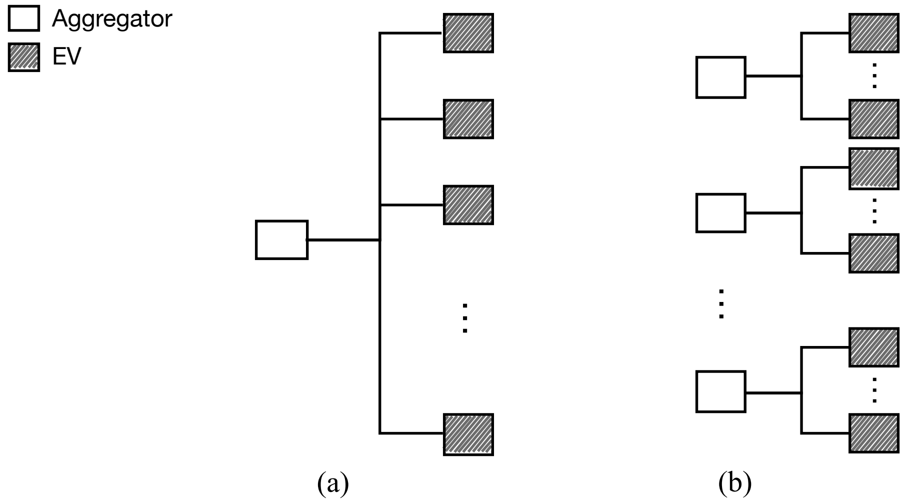

FIGURE 3.8: Grid realizations: (a) Single aggregator; (b) Multiple aggregators

The aggregator can be modeled by the two-state representation shown in Fig. 3.7. It is aggregators' responsibility to both handle the charging and gather available capacities from EVs for any grid services. When an aggregator fails, neither the interruptible EV charging nor the V2G can be contributed from EVs under that aggregator.

3.4 Well-Being Assessment Considering Uncertainties of EV Charging

When capacity contribution of EV charging and its uncertainties are involved, it is essential to examine the operating well-being at different times of the day. It is because the usage of EVs strongly depends on the time of the day and so does their capacity contribution. Generating capacity and system load vary during the day as well. In this chapter, the generating system well-being is studied on an hourly basis. It is assumed that V2G is enabled so both interruptible and V2G capacities (i.e. p_{I} and p_{V2G}) can be called on in case of outages.

Generally, with necessary information provided and their uncertainties considered (the top two blocks in Fig. 1.6), two consecutive procedures remain to fully assess the system well-being (the following two blocks in Fig. 1.6): parameter evaluation (Steps 1 to 7) and well-being analysis (Steps 8 and 9). In parameter evaluation, a Monte Carlo simulation is required to take account of all the uncertainties. Then the availability of statistics of the capacities, based on which a multi-state model is derived for each aggregator at each hour, can be obtained. Multiple criteria are required for the unit commitment. For construction of the COPT and computation of reliability indices from the multi-state model, the reader may refer to [18]. The basic calculation of well-being indices associated with interruptible load and stand by units is also illustrated in [18] and [16].

1. Read system information including travel schedules and charging requirements of EVs; obtain scheduled and forecast data such as t^i_{ETA}, t^i_{ETD} and E^i_{FD}.

2. Set the next hour and obtain $\boldsymbol{t}_{\mathbf{BI}}$, $\boldsymbol{t}_{\mathbf{I}}$ and $\boldsymbol{t}_{\mathbf{AI}}$.

3. Apply uncertainties of EV charging on the individual level. According to Section 3.3.1 to 3.3.4, sample $t^i_{\mathrm{Err,A}}$, $t^i_{\mathrm{Err,D}}$ and R^i_{AA}; calculate t^i_{ATA}, t^i_{ATD} and E^i_{AD}; determine $\mathbf{P_{OC}}$, $\mathbf{T_A}$ and $\boldsymbol{e}_{\mathbf{D}}$.

4. Calculate p_{I} and p_{V2G} for EVs under each aggregator following the methods provided in Section 3.2; accumulate the corresponding frequencies.

5. Repeat Steps 3 and 4 until acceptable availability of statistics of p_{I} and p_{V2G} or the stopping rule is reached.

6. Obtain models to represent those capacities; proceed if all hours are investigated. Go to Step 2 otherwise.

7. Reset the hour count and proceed if all grid realizations (Section 3.3.5) are considered. Change the grid realization and go to Step 2 otherwise.

8. Perform unit commitment at each lead time with multiple criteria, form COPTs and calculate well-being indices for all hours.

9. Stop if all realizations are considered. Change the grid realization and go to Step 8 otherwise.

3.5 Numerical Study

In this chapter the study case in [94] is used, where 5,000 EVs are included in the generating system of RBTS [28]. The load on Monday of the 11th week is used. Multiple criteria are required. The acceptable risk level and healthy state probability are 0.001 and 0.99, respectively. Energy capacity of each EV is 25 kWh. The lead time for both charging interruption and V2G is 10 minutes. For ease of illustration it is assumed that system lead time is 1 hour. The charging load of EV constitutes 13.9% penetration. The information from demand side in our previous study such as time of arrival and departure and daily energy consumption is used here as the scheduled values (t^i_{ETA}, t^i_{ETD}, and E^i_{FD}). The expected time of arrival and departure is regarded as self-scheduled. So the rounding effect (Fig. 3.4) applies. Actual rate of energy consumption (R^i_{AA}) follows the distribution given in Fig. 3.5, while the forecast one (R^i_{FA}) is the mean value, i.e. 0.23 kWh/mile. Misreported distance (M^i_{Err}) is sampled following the distribution in Fig. 3.6. The transition rates λ and μ for EV absence are 5×10^{-4} and 1×10^{-2} /hour, respectively. Each aggregator has a failure rate of 1 /year and a repair rate of 99 /year. For the multi-aggregator realization, two aggregators are first assumed with 2,500 EVs each.

Results of the Monte Carlo simulation for the single-aggregator realization are plotted in Fig. 3.9. Box-and-whisker representation is used to show the distribution for each hour (not including occasions of 0 MW capacity), where the whiskers are from the minimum to the maximum. Evaluated capacities without taking into account the uncertainties are also provided in the figure for comparison.

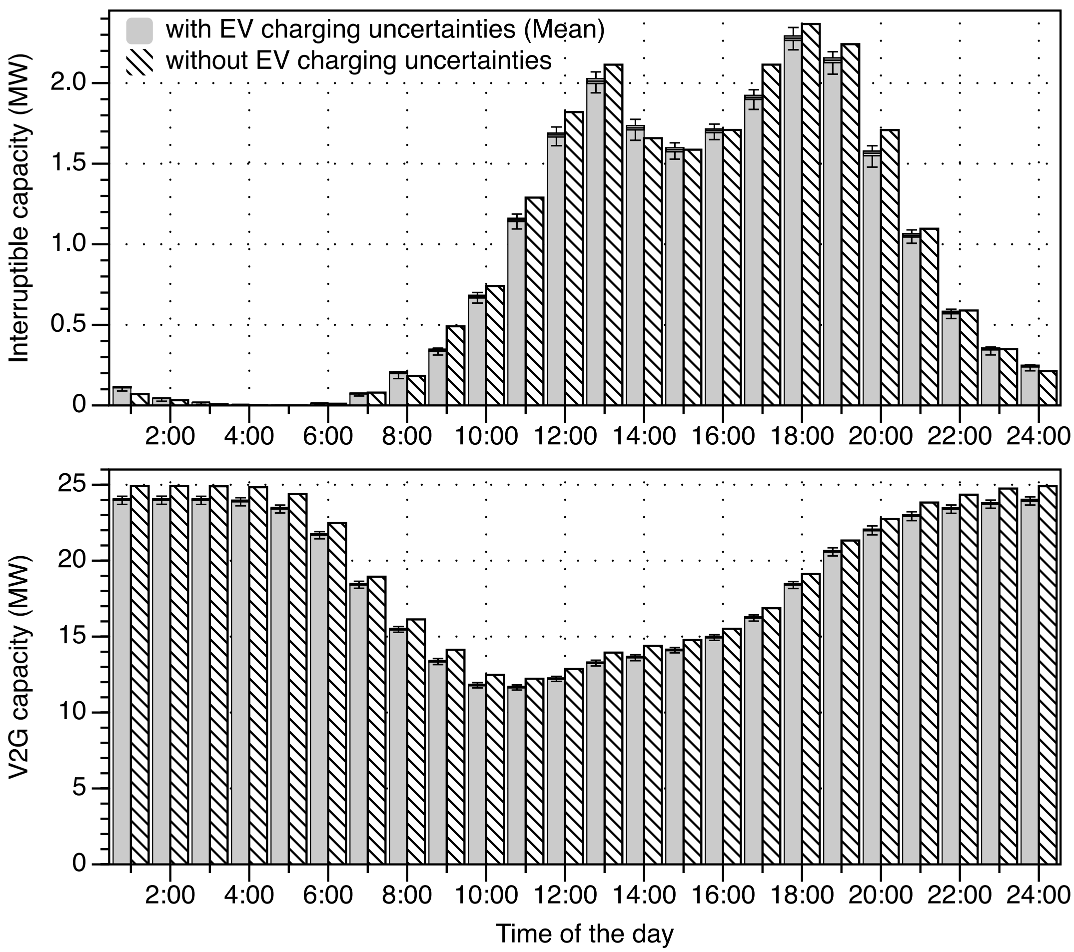

FIGURE 3.9: Interruptible and V2G capacities with and without the consideration of EV charging uncertainties

With consideration of uncertainties of EV charging, both interruptible and V2G capacities become uncertain during the day. Compared to the results without considering uncertainties, the expected values of interruptible capacities for some hours of the day increase, e.g. the 1st, 2nd, 8th and 24th hour, because of shifting of time of arrival and departure. As can be seen from Section 3.3.1 and 3.3.2 and Section 3.2, errors of arrival and departure time lead to changes in the charging plans ($\mathbf{P_{OC}}$) as well as periods available for charging ($\boldsymbol{T}_{\mathbf{A}}$). Charging processes of some EVs may start earlier while some may start later. This moves some of the capacities from one hour to another. This effect is quite unique to EV charging as a grid resource. For almost all the other conventional and unconventional units in power systems, the uncertainties bring down nominal or scheduled capacities. In contrast, the effect of punctuality and time rounding could rather increase the "rated" value of capacity contribution. For most of the day, however, the capacities decrease. It is because errors other than earliness and lateness generally make the capacity contribution less, for example, overestimation of daily mileage (Fig. 3.6) and charging failure. This is more evident when it comes to V2G (Fig. 3.9). From the results of our previous study, the V2G capacity is sensitive to EV population (i.e. EV penetration). With the charging failure introduced (Section 3.3.4), V2G capacity decreases with the drop of the EV population available for grid services.

Without considering the aggregator failure, which results in 0 MW capacity for both charging interruption and V2G, the possible values of the total capacity for each hour generally vary within a 1 MW range (Fig. 3.9). A two-state model can be obtained for each hour, as given in Table 3.2. Each state consists of one interruptible capacity and one V2G capacity. If the aggregator fails, then no capacities can be delivered (State 2), otherwise the mean values in Fig. 3.9 are used in the model (State 1).

Well-being indices can be calculated with the model. Since the sum of the three well-being indices is fixed [19], the decrease of risk level equals the total increase in probabilities of healthy and marginal state. Table 3.3 shows the risk levels with

Table 3.2: Two-state representations for capacity contribution of EVs with single-aggregator realization

hr	State 1		State 2	
	Capacity* (MW)	Probability	Capacity* (MW)	Probability
1	0.11 / 24.02	0.98872796	0 / 0	0.01127204
2	0.04 / 24.02	0.98765330		0.01234670
3	0.02 / 24.01	0.99042423		0.00957577
4	0.01 / 23.92	0.99006761		0.00993239
5	0.00 / 23.45	0.98973639		0.01026361
6	0.01 / 21.72	0.99036113		0.00963887
7	0.07 / 18.44	0.99074071		0.00925929
8	0.20 / 15.48	0.99054715		0.00945285
9	0.34 / 13.37	0.99161877		0.00838123
10	0.67 / 11.80	0.98912146		0.01087854
11	1.15 / 11.67	0.98985399		0.01014601
12	1.68 / 12.23	0.99029920		0.00970080
13	2.01 / 13.27	0.98886578		0.01113422
14	1.72 / 13.64	0.98843819		0.01156181
15	1.59 / 14.12	0.98955355		0.01044645
16	1.70 / 14.96	0.98888677		0.01111323
17	1.91 / 16.25	0.99316424		0.00683576
18	2.28 / 18.43	0.99139953		0.00860047
19	2.14 / 20.61	0.98928309		0.01071691
20	1.56 / 22.02	0.98966274		0.01033726
21	1.06 / 22.97	0.99191925		0.00808075
22	0.58 / 23.44	0.99169255		0.00830745
23	0.35 / 23.77	0.99246578		0.00753422
24	0.24 / 23.98	0.99295541		0.00704459

*Interruptible capacity / V2G capacity

and without the consideration of aggregator failure. Corresponding probabilities of healthy and marginal state are provided in Table 3.4. System risks without any help from the EVs are also given in Table III for comparison.

Risk levels are reduced remarkably during the day when charging interruption and V2G are included. The amount of reduction depends on the load level (the second column in Table 3.3) and capacities provided by EVs (Fig. 3.9). From the comparison between the third and fourth columns in Table 3.3, the possible failure

Table 3.3: Probability of risk during the day with a single aggregator

hr	Load level (MW)	Probability of risk ($\times 10^{-6}$)		
		With aggregator failure	Without aggregator failure	Without V2G and charging interruption
1	76	0.009177	0.000194	0.797189
2	74	0.010034	0.000194	0.797189
3	72	0.007826	0.000194	0.797189
4	69	0.008110	0.000194	0.797189
5	71	0.008374	0.000194	0.797189
6	78	0.007876	0.000194	0.797189
7	86	0.241311	0.234799	0.938069
8	102	0.018651	0.000935	1.875047
9	114	0.946181	0.938330	1.875047
10	119	0.948520	0.938330	1.875047
11	121	0.957734	0.938330	2.850841
12	120	0.947420	0.938330	2.850841
13	113	0.948760	0.938330	1.875047
14	112	0.948903	0.938069	1.875047
15	109	0.020513	0.000935	1.875047
16	107	0.021763	0.000935	1.875047
17	110	0.013746	0.000935	1.875047
18	113	0.017053	0.000935	1.875047
19	117	0.021020	0.000935	1.875047
20	119	0.020308	0.000935	1.875047
21	116	0.016079	0.000935	1.875047
22	108	0.016504	0.000935	1.875047
23	96	0.240098	0.234799	0.938069
24	84	0.006956	0.000350	0.938069

of the aggregator does introduce additional risks. But the amounts increased are limited. Given the availability of the aggregator ($\mu/(\lambda+\mu) = 0.99$), the contribution these EVs make during the day is far from being overshadowed by aggregator failure.

3.5.2 Two-aggregator Realization

Similar two-state models can be obtained for EVs under each of the two aggregators. A four-state model is then created from the two models to represent the entire EV

Table 3.4: Probability of health and margin with a single aggregator

hr	With aggregator failure		Without aggregator failure	
	Probability of		Probability of	
	Health	Margin	Health	Margin
1	0.99896683	0.00103317	0.99897300	0.00102700
2	0.99896624	0.00103375	0.99897300	0.00102700
3	0.99896775	0.00103224	0.99897300	0.00102700
4	0.99896756	0.00103243	0.99897300	0.00102700
5	0.99896738	0.00103261	0.99897300	0.00102700
6	0.99896772	0.00103227	0.99897300	0.00102700
7	0.99842482	0.00157494	0.99842609	0.00157367
8	0.99828429	0.00171569	0.99828947	0.00171053
9	0.99774260	0.00225645	0.99774261	0.00225645
10	0.99774260	0.00225645	0.99774261	0.00225645
11	0.99773682	0.00226222	0.99774261	0.00225645
12	0.99773709	0.00226197	0.99774261	0.00225645
13	0.99774260	0.00225645	0.99774261	0.00225645
14	0.99828221	0.00171684	0.99828853	0.00171053
15	0.99828375	0.00171623	0.99828947	0.00171053
16	0.99828338	0.00171660	0.99828947	0.00171053
17	0.99828573	0.00171426	0.99828947	0.00171053
18	0.99828476	0.00171522	0.99828947	0.00171053
19	0.99828360	0.00171638	0.99828947	0.00171053
20	0.99828381	0.00171617	0.99828947	0.00171053
21	0.99828504	0.00171494	0.99828947	0.00171053
22	0.99828492	0.00171506	0.99828947	0.00171053
23	0.99842506	0.00157470	0.99842609	0.00157367
24	0.99842535	0.00157464	0.99842633	0.00157367

population. The model for a typical hour is given in Table 3.5.

It can be seen from Tables 3.2 and 3.5 that with two aggregators, two "derated" states (State 2 and 3) are added to the model, leaving the decreased probabilities of "all-in" state (State 1) and "all-out" state (State 4). The unit commitment risk during the day is provided in Table 3.6.

The daily risk reduction can be used to represent the improvement of daily operating well-being of the system and is defined as the sum of risk reduction of all hours

Table 3.5: A typical four-state representations for capacity contribution of EVs with two-aggregator realization

hr	State 1		State 2	
	Capacity* (MW)	Probability	Capacity* (MW)	Probability
14	1.72 / 13.64	0.98157305	0.86 / 6.82	0.00894292
	State 3		State 4	
	Capacity* (MW)	Probability	Capacity* (MW)	Probability
	0.86 / 6.82	0.00939841	0 / 0	0.00008563

* Interruptible capacity / V2G capacity.

(the fifth column minus the third column in Table 3.3). From Table 3.6, the daily risk reduction for the two-aggregator realization is 3.127674×10^{-5}, increased slightly from the single aggregator (3.127172×10^{-5}). This can be ascribed to the dissipated state probabilities. With two aggregators, the chance of total failure (i.e. State 2 in Table 3.2 and State 4 in Table 3.5) is lower. The healthy and marginal states are barely changed, given their much higher probabilities.

3.6 Sensitivity Study

The aggregator is regarded as essential to EVs' grid service participation. To find the effect of the number of aggregators on the operating well-being, the number of aggregators is varied from 1 to 5. EV population is divided equally among aggregators. The consequent daily risk reduction is plotted in Fig. 3.10.

It can be found in the figure that increasing the number of aggregators does not necessarily further improve the system well-being. On the contrary, in this case the daily well-being improvement shrinks when more than two aggregators coexist in the system. The reason is that with more aggregators, probabilities of the multi-state model are dissipated dramatically with more "derated" states, e.g. the model for three aggregators has 8 states and 16 for four aggregators.

Table 3.6: Results of well-being analysis with two aggregators

hr	Probability of		
	Health	Margin	Risk ($\times 10^{-6}$)
1	0.99896413	0.00103587	0.004035
2	0.99896220	0.00103779	0.004878
3	0.99896297	0.00103703	0.004542
4	0.99897295	0.00102704	0.004256
5	0.99897293	0.00102707	0.005352
6	0.99896211	0.00103789	0.004920
7	0.99842607	0.00157369	0.246247
8	0.99828941	0.00171058	0.018282
9	0.99774259	0.00225645	0.957891
10	0.99774259	0.00225645	0.957323
11	0.99774255	0.00225650	0.955734
12	0.99774253	0.00225652	0.958300
13	0.99774261	0.00225645	0.938426
14	0.99827847	0.00172059	0.938154
15	0.99827868	0.00172130	0.019527
16	0.99827907	0.00172091	0.018852
17	0.99827860	0.00172138	0.019658
18	0.99827999	0.00171999	0.017255
19	0.99827769	0.00172229	0.021244
20	0.99827865	0.00172133	0.019572
21	0.99828018	0.00171981	0.016934
22	0.99828939	0.00171059	0.021040
23	0.99842376	0.00157601	0.230874
24	0.99842630	0.00157368	0.014595

Given the importance of the aggregator in realizing EVs' grid services. Increasing its availability from 0.97 to 0.997, the daily risk reduction for the system with two aggregators is plotted in Fig. 3.11. The almost linear relationship shows that increased availability of aggregators has a positive influence on the daily operating well-being.

At this stage the transition rates associated with charging component failure and EV absence are unknown. The resultant unavailability affects both the interruptible and V2G capacities, hence the well-being indices. Well-being analysis is performed

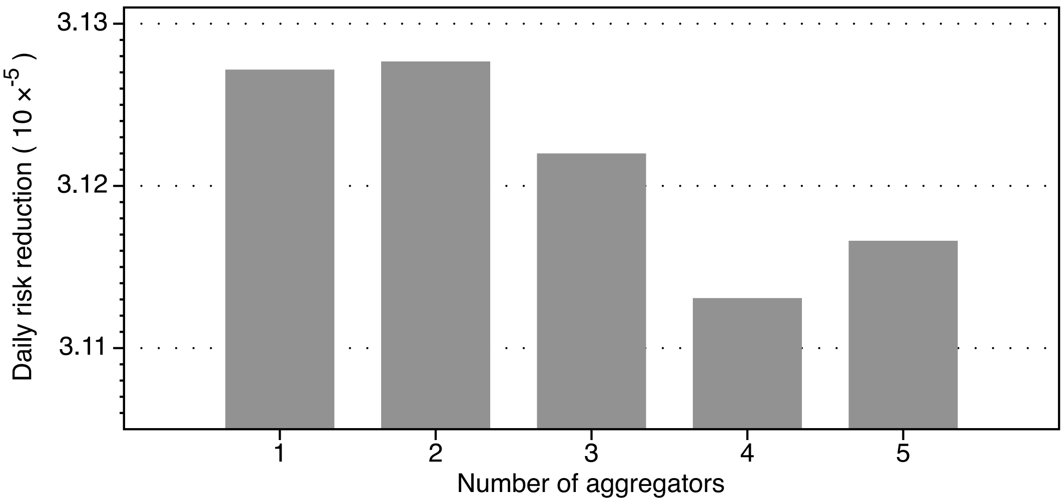

FIGURE 3.10: The effect of the number of the aggregators

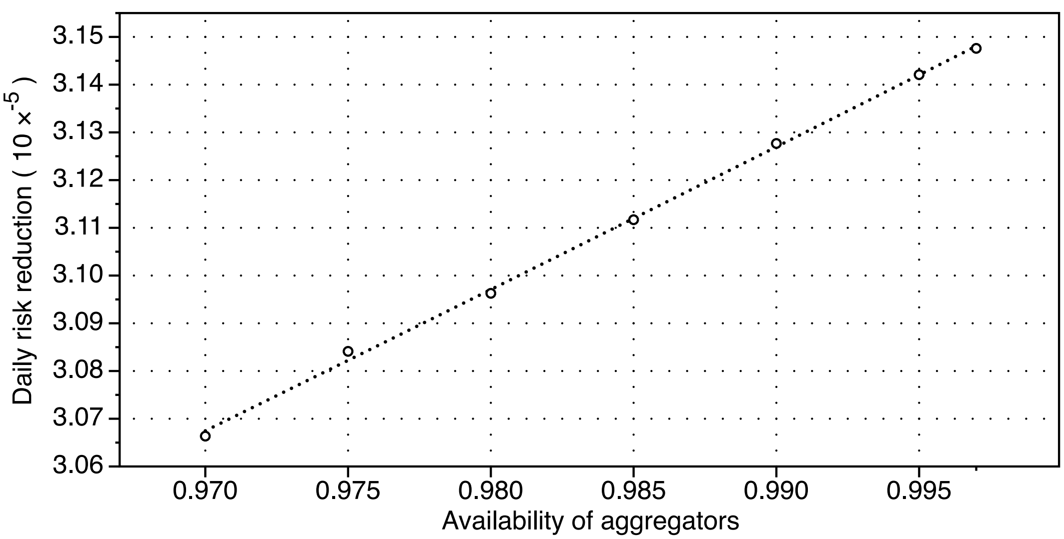

FIGURE 3.11: The effect of availability of aggregators

with a wide range of variation of the availability associated with charging failure (Fig. 3.12).

Though the increase in the availability does affect the system well-being positively, the effects are not uniform. With a low value of the availability, e.g. 0.6—0.8, the final improvement of system well-being is sensitive to the absence of EVs. From Fig. 3.12, upon the availability being raised to 0.85 and above, further enhancement of daily risk reduction dwindles. Except for the result of the random sampling of the

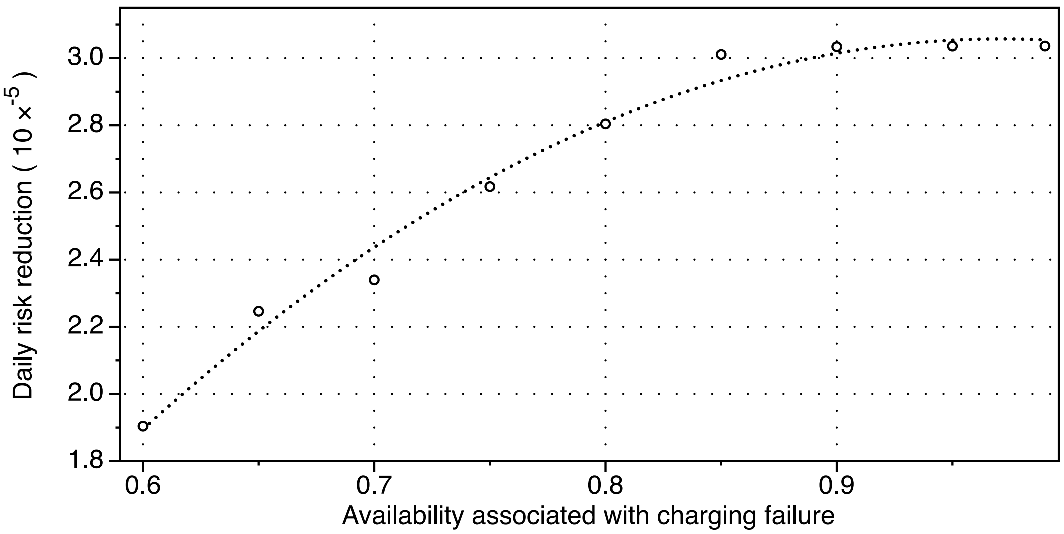

FIGURE 3.12: The effect of charging component failure and EV absence

information from the demand side, the major reason is that by the nature of COPT, the decrease of the risk level becomes harder when it is getting closer to zero since the possibility of at risk state can never equal zero.

3.7 Consideration of Load Forecast Uncertainty

In real world, uncertainty of forecast load other than EV charging is also common. It is necessary to consider load forecast uncertainty in the well-being analysis. A classic seven-step approximation model with a standard deviation of 2% [18] is included in the evaluation. Table 3.7 gives the system well-being indices with two aggregators considering the load forecast uncertainty.

The deterioration of the system well-being due to the load forecast uncertainty is unveiled by comparing the results from Tables 3.6 and 3.7. As expected, for most of the hours during the day the probabilities of healthy and marginal states are decreased while the risk levels are increased. On a daily basis, the average risk level is raised from 0.266578×10^{-6} up to 0.282759×10^{-6}. The daily risk reduction is decreased to 3.104031×10^{-5} accordingly, from 3.127674×10^{-5} when load forecast

Table 3.7: Results of well-being analysis with two aggregators considering load forecast uncertainty

hr	Probability of		
	Health	Margin	Risk ($\times 10^{-6}$)
1	0.99896418	0.00103581	0.004035
2	0.99896292	0.00103707	0.004878
3	0.99896605	0.00103394	0.004541
4	0.99897233	0.00102767	0.004248
5	0.99896928	0.00103072	0.005353
6	0.99895889	0.00104110	0.004989
7	0.99842588	0.00157387	0.245168
8	0.99828935	0.00171063	0.018277
9	0.99790776	0.00209128	0.951800
10	0.99774250	0.00225654	0.962861
11	0.99774180	0.00225718	1.016153
12	0.99774247	0.00225657	0.963835
13	0.99790789	0.00209118	0.938667
14	0.99811301	0.00188611	0.877754
15	0.99824326	0.00175644	0.303514
16	0.99828226	0.00171772	0.024366
17	0.99827867	0.00172125	0.081198
18	0.99827740	0.00172258	0.022879
19	0.99824189	0.00175809	0.028116
20	0.99824277	0.00175720	0.026366
21	0.99827701	0.00172297	0.017036
22	0.99825681	0.00174315	0.036151
23	0.99842377	0.00157600	0.231202
24	0.99859221	0.00140778	0.012838

uncertainty is not considered.

Varying the population to see how much the increased risk level can be compensated by efforts of EV charging, Fig. 3.13 shows the average risk levels of the day with and without the consideration of load forecast uncertainty.

As can be seen from the figure, in this case the increased amount of the risk level can be eliminated by even the slightest penetration, say, 500 EVs. The risk level continues to shrink with increased EV population. From Table 3.8, it can be found

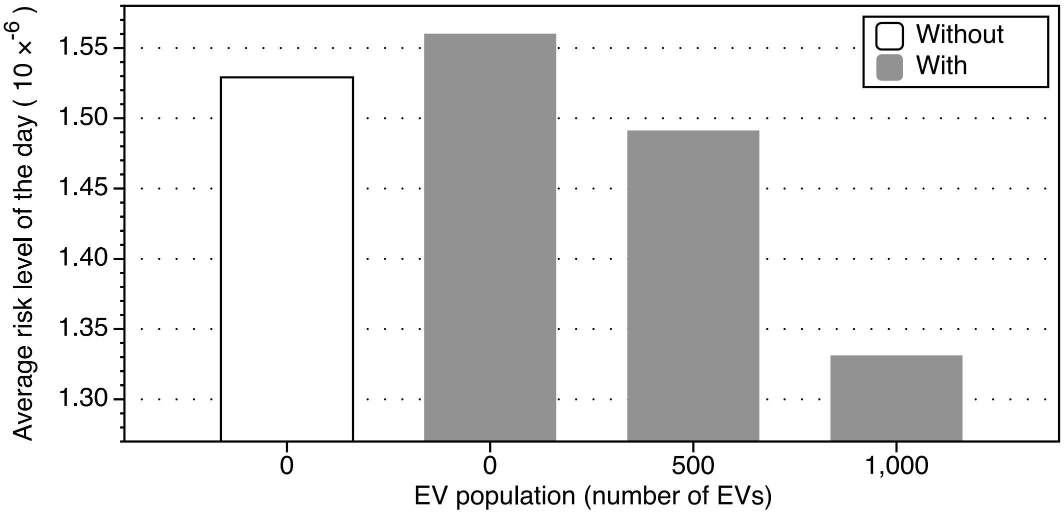

FIGURE 3.13: Average risk level without and with the consideration of load forecast uncertainty two aggregators

that for each scenario with different number of aggregators, 500 EVs (i.e. 1.4% penetration level [94]) are enough to absorb the risk rise caused by load forecast uncertainty.

Table 3.8: Average risk level without and with the consideration of load forecast uncertainty with different numbers of aggregators

Aggregators	without	with load forecast uncertainty		
	0 EVs	0 EVs	500 EVs	1000 EVs
1	1.529130	1.560159	1.491172	1.330259
2	1.529130	1.560159	1.491321	1.331263
3	1.529130	1.560159	1.491715	1.333000
4	1.529130	1.560159	1.491875	1.332937
5	1.529130	15.60159	1.492030	1.333651

3.8 Summary

Based on the work in Chapter 2, this chapter achieves to provide a complete framework for the well-being analysis including EV charging by taking the consideration of the probabilistic nature of EV charging.

The distinction of EVs providing services in the power grid is rooted in the multi-purposefulness of EVs. The simple fact is that customers buy automobiles for driving, and it only makes sense when errors from individual human beings, as EV drivers, are expected. This chapter systematically integrates sources of EV charging uncertainties. At the individual level, punctuality, rounding of time, forecast error of energy consumption, charging component failure and EV absence can make the schedules of EV charging uncertain. At the upper level, the failure of the aggregator can nullify the contribution from EVs under its control.

4

Reliability Evaluation of Distribution Systems Including V2G and V2H

Methods given in Section 4.1 and 4.2 are for evaluating EVs' capacity contribution in islanding mode of operation with topologies of centralized and dispersed charging, respectively. Section 4.3 focuses on the grid connected mode of operation, i.e. the scenarios of interregional V2G. A procedure for reliability evaluation including EVs' contribution is proposed in Section 4.4. In Section 4.5, an example from textbook [29] is used for illustration and comparison.

4.1 Local V2G for Centralized Charging

4.1.1 Information Required and Other Basics

The fundamental premise is that daily activities of EVs ought not to be affected by potential V2H and/or V2G during the period of interruption. Basic requirements for EVs' daily charging comprising of daily travel time and state-of-charge (SOC) should be met before drawing energy from them. This thesis assumes EV charging takes place at home or local parking lots. The time period between arrival of an EV and its departure is thus the available charging period, during which replenishing

SOC of EVs is required.

Given multiple numbers of EVs and time slots are involved during the day, variables are represented in the form of matrices to effectively gather information and facilitate the evaluation. Intuitively, each row is assigned to each EV while columns represent time slots. With data required from demand side, such as home arrival and departure time and energy depleted during daily driving of every EV, basic variables for the evaluation such as $\mathbf{T_A}$, $\boldsymbol{t}_\mathbf{I}$, $\mathbf{P_{OC}}$, and $\boldsymbol{e}_\mathbf{D}$ can be obtained.

4.1.2 Evaluation Methodology

Fig. 4.1 shows a local circuit is disconnected from the lateral. When centralized EV charging is applied at a load point, the only way for EVs to supply power to local households is through the local grid.

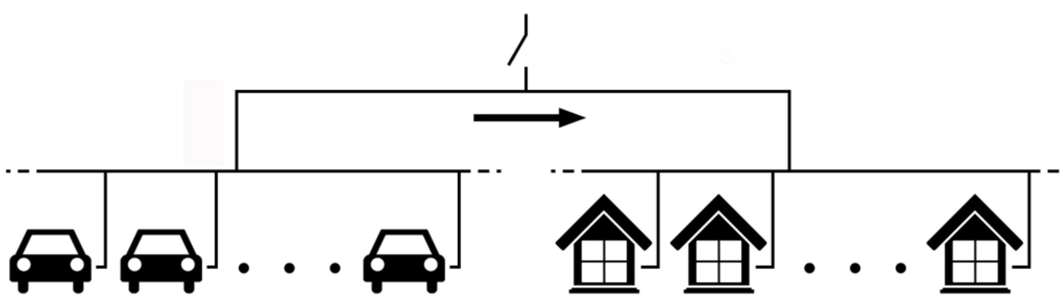

FIGURE 4.1: Local V2G for topology of centralized EV charging

The amount of local demand that can be backed up during the period of interruption is given as (4.1), assuming numbers of EVs and households are identical and each household owns one EV:

$$E_\mathrm{B} = \min\left(\eta\sum_{i}^{m} e_{\mathrm{R},i}\ , \sum_{i}^{m} e_{\mathrm{lim},i}\right) \tag{4.1}$$

where reversible energy $e_{\mathrm{R},i}$ is determined by (4.2) and capacity limit $e_{\mathrm{lim},i}$ is given as (4.6). Given the centralized EV charging, a summation of $e_{\mathrm{R},i}$ over all EVs is used, with which battery efficiency η is also considered.

Apparently the reversible energy ($\boldsymbol{e}_{\mathbf{R}}$) is from battery packs of EVs and thus subject to their SOC when an interruption happens ($\boldsymbol{e}_{\mathbf{EV}}$), i.e. the first term in (4.2), which is given by (4.3). Since V2G should not compromise charging requirements of EVs, supply is not allowed if the same quantity cannot be replenished by the supplementary charging ($\boldsymbol{e}_{\mathbf{SC}}$), i.e. the second term in (4.2), as defined by (4.4). Lastly the power reversed should not exceed its capacity limit (p_{R}) and is only possible when the EV is connected at home or parking lots ($\mathbf{T}_{\mathbf{A}}$), i.e. the last term in (4.2):

$$\boldsymbol{e}_{\mathbf{R}} = \min\left(\boldsymbol{e}_{\mathbf{EV}}\,,\, \boldsymbol{e}_{\mathbf{SC}}\,,\, \frac{p_{\mathrm{R}}}{\eta}\mathbf{T}_{\mathbf{A}} \cdot {\boldsymbol{t}_{\mathbf{I}}}^{\mathsf{T}}\right) \tag{4.2}$$

The SOC ($\boldsymbol{e}_{\mathbf{EV}}$) is determined by energy capacities of EVs, the amount of energy depleted during daily travel and energy charged by the original charging arrangement prior to the interruption:

$$\boldsymbol{e}_{\mathbf{EV}} = \boldsymbol{e}_{\mathbf{F}} - \boldsymbol{e}_{\mathbf{D}} + \mathbf{P}_{\mathbf{OC}} \cdot {\boldsymbol{t}_{\mathbf{BI}}}^{\mathsf{T}} \tag{4.3}$$

Energy provided by the supplementary charging ($\boldsymbol{e}_{\mathbf{SC}}$) is defined as the amount of energy that can be delivered to EVs, in addition to their original charging arrangement, after the interruption, as given by (4.4):

$$\boldsymbol{e}_{\mathbf{SC}} = (p_{\mathrm{O}}\mathbf{T}_{\mathbf{A}} - \mathbf{P}_{\mathbf{OC}}) \cdot {\boldsymbol{t}_{\mathbf{AI}}}^{\mathsf{T}} \tag{4.4}$$

The relationship among $\boldsymbol{t}_{\mathbf{BI}}$, $\boldsymbol{t}_{\mathbf{I}}$ and $\boldsymbol{t}_{\mathbf{AI}}$ is as in (4.5):

$$\boldsymbol{t}_{\mathbf{BI}} + \boldsymbol{t}_{\mathbf{I}} + \boldsymbol{t}_{\mathbf{AI}} = \mathbf{1} \tag{4.5}$$

On the other side of the local network, energy supplied by EVs should be no more than the demand of households. The upper limits $\boldsymbol{e}_{\mathbf{lim}}$ here are defined as the total consumption of each household during the interruption $\boldsymbol{t}_{\mathbf{I}}$:

$$\boldsymbol{e}_{\mathbf{lim}} = \mathbf{P}_{\mathbf{H'}} \cdot {\boldsymbol{t}_{\mathbf{I}}}^{\mathsf{T}} \tag{4.6}$$

where, instead of using consumption levels of household $\mathbf{P_H}$ directly, a modified matrix $\mathbf{P_{H'}}$ is applied. As multiple supply (i.e. EVs) and demand (i.e. households) are involved in each islanded section, $\mathbf{P_{H'}}$ ensures power balance (4.7) is maintained at each time j:

$$\sum_{i}^{m} \mathrm{P}_{\mathrm{H}',ij} \leqslant p_{\mathrm{R}} \sum_{i}^{m} \mathrm{T}_{\mathrm{A},ij} \tag{4.7}$$

The ceiling of the total power consumption recovered by EVs at each time is the maximum reverse power possible, which takes into consideration both capacity p_{R} and availability $\mathbf{T_A}$. For example, during an outage no power can be consumed when all EVs are on the roads. Consumption levels beyond the ceiling, therefore, have to be trimmed. It does not matter from which household i the power consumption is trimmed, since it is the summation of all EVs being considered in the evaluation, (4.1).

In the process of calculating the matrices such as $\boldsymbol{e}_{\mathbf{SC}}$, $\boldsymbol{e}_{\mathbf{EV}}$ and $\boldsymbol{e}_{\mathbf{lim}}$, inconveniences are that an EV's home-charging period often starts near the end of the day and is separated by two calendar days; available periods and arrangements for EV charging also vary. The idea of an extended charging period and equivalent periods of charging interruption is adopted to guarantee a single and continuous charging period for each EV, by which the calculation of these variables is facilitated. For details of the matrix representation and the equivalence of calculation, the reader is referred to [94].

4.2 V2H and Local V2G for Dispersed EV Charging

4.2.1 V2H Only

Fig. 4.2 shows a local grid with dispersed EV charging where only V2H is deployed, following a supply failure.

Total demand that can be met in this case is calculated by the summation of all

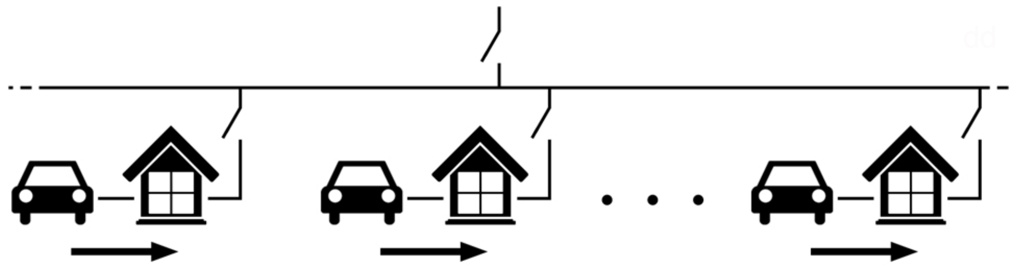

FIGURE 4.2: V2H for topology of dispersed EV charging

EVs:

$$E_{\mathrm{B}} = E_{\mathrm{B}}^{\mathrm{V2H}} = \sum_{i}^{m} e_{\mathrm{V2H},i} \tag{4.8}$$

where $e_{\mathrm{V2H},i}$ is from (4.9). The V2H capacity of each EV is determined by its reversible energy and capped by the limit of each household:

$$\boldsymbol{e}_{\mathbf{V2H}} = \min(\eta \boldsymbol{e}_{\mathbf{R}}\, , \boldsymbol{e}_{\mathbf{lim}}) \tag{4.9}$$

where $\boldsymbol{e}_{\mathbf{R}}$ is the same as given in (4.2) and $\boldsymbol{e}_{\mathbf{lim}}$ is given as (4.10). Different from (4.1), reversible energy from an EV is subject to the upper limit of its own household before the summation in (4.8) since every household is an isolated point of consumption.

The upper limits $\boldsymbol{e}_{\mathbf{lim}}$ in this case is derived from either the consumption level $\mathbf{P}_{\mathbf{H}}$ or EV's ability to supply power ($p_{\mathrm{R}}\mathbf{T}_{\mathbf{A}}$) during the period of interruption:

$$\boldsymbol{e}_{\mathbf{lim}} = \min(\mathbf{P}_{\mathbf{H}}\, , p_{\mathrm{R}}\mathbf{T}_{\mathbf{A}}) \cdot \boldsymbol{t}_{\mathbf{I}}^{\top} \tag{4.10}$$

4.2.2 V2H + Local V2G

More demand can be served if local V2G is allowed, in addition to V2H. The schematic is given in Fig. 4.3.

The demand backed up comprises of two portions:

$$E_{\mathrm{B}} = E_{\mathrm{B}}^{\mathrm{V2H}} + E_{\mathrm{B}}^{\mathrm{LV2G}} \tag{4.11}$$

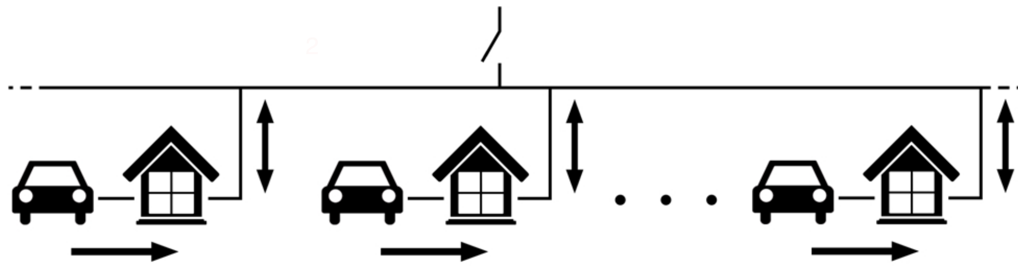

FIGURE 4.3: V2H + local V2G for topology of dispersed EV charging

where $E_{\mathrm{B}}^{\mathrm{V2H}}$ is given in (4.8) and the local V2G portion $E_{\mathrm{B}}^{\mathrm{LV2G}}$ is determined by (4.12):

$$E_{\mathrm{B}}^{\mathrm{LV2G}} = \min\left(\sum_{i}^{m}(\eta e_{\mathrm{R},i} - e_{\mathrm{V2H},i}), \sum_{i}^{m} e_{\mathrm{lim},i}\right) \tag{4.12}$$

The basic concept of the calculation is similar to the previous ones—the reversible amount capped by its upper limit. However, both terms need to be revised in the instance of V2H + local V2G. The local V2G is possible only if the reversible energy of an EV is greater than the V2H amount, i.e. the first term in (4.12), where $e_{\mathrm{R},i}$ and $e_{\mathrm{V2H},i}$ are from (4.9). Judging by (4.9), it can be found that for each i, $(\eta e_{\mathrm{R},i} - e_{\mathrm{V2H},i})$ is nonnegative. The upper limit $e_{\mathrm{lim},i}$ here is redefined correspondingly:

$$\boldsymbol{e}_{\mathbf{lim}} = \mathbf{P}_{\mathbf{H}'} \cdot \boldsymbol{t}_{\mathbf{I}}^{\mathsf{T}} - \boldsymbol{e}_{\mathbf{V2H}} \tag{4.13}$$

the calculation of which is similar to (4.6) except that the V2H portion should be taken out.

4.3 Interregional V2G

4.3.1 Energy and Power Available for Interregional V2G

Fig. 4.4 shows the interregional V2G applied in a local grid with both charging topologies. Note that local V2G (Fig. 4.1) and V2H + local V2G (Fig. 4.3) are the foundation of interregional V2G.

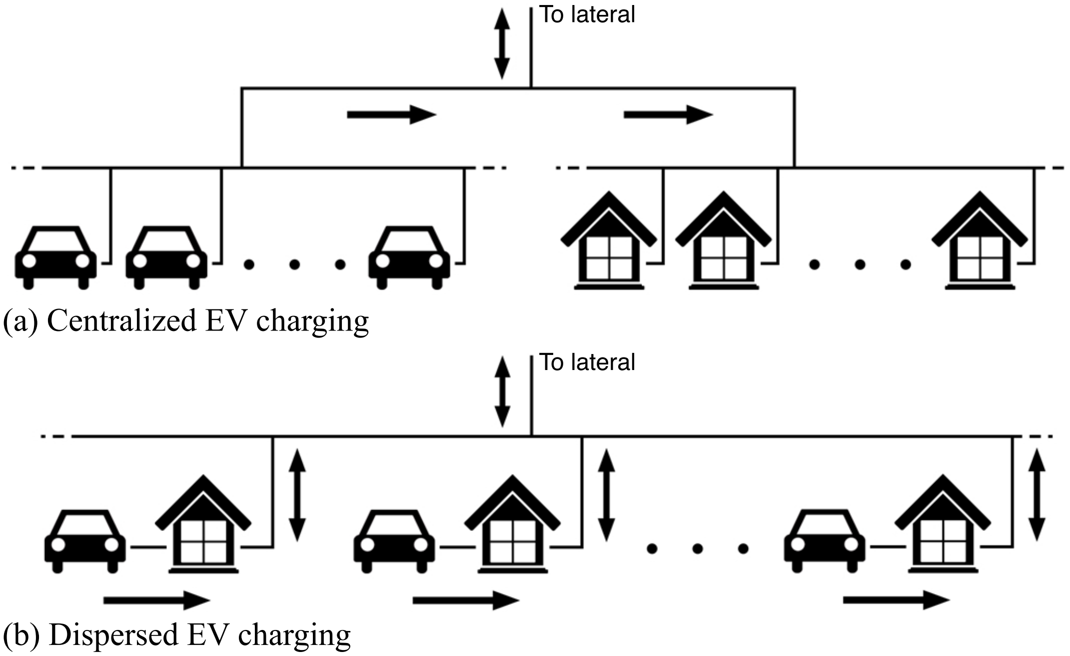

FIGURE 4.4: Interregional V2G for topologies of centralized and dispersed EV charging

Interregional V2G can be deployed on the condition that (a) local circuits remain connected to laterals after the outage, as shown in Fig. 4.4; (b) extra energy can be spared at some load points in addition to local V2G; and (c) energy is further required at some load points in spite of inclusion of local V2G. Thus for a node x we have:

$$\overline{E_{\mathrm{ex}}^{x}} = \eta \sum_{i}^{m} e_{\mathrm{R},i} - E_{\mathrm{B}} \tag{4.14}$$

$$\left|\overline{s_{\mathrm{ex},j}^{x}}\right| = \max\left(p_{\mathrm{R}} \sum_{i}^{m} \mathrm{T}_{\mathrm{A},ij} - \sum_{i}^{m} \mathrm{P}_{\mathrm{H},ij}\,, 0\right) \tag{4.15}$$

$$\overline{E_{\mathrm{im}}^{x}} = \sum_{i}^{m} \left(\mathbf{P_H} \cdot \boldsymbol{t}_{\mathbf{I}}^{\mathsf{T}}\right) - E_{\mathrm{B}} \tag{4.16}$$

where, for each network topology E_{B} used in (4.14) and (4.16) should refer to the corresponding calculation, that is, (4.1) or (4.11). In order to export and import energy, the requirements are $\overline{E^x_{\text{ex}}} \geqslant 0$, $\overline{s^x_{\text{ex},j}} \geqslant 0$, and $\overline{E^x_{\text{im}}} \geqslant 0$. The power capacity $\overline{s^x_{\text{ex},j}}$ in (4.15) denotes apparent power.

4.3.2 Problem Formulation

Typically, there could be multiple nodes involved in interregional V2G and power loss along the line should not be neglected. Thus, the problem becomes an optimization problem where the objective is to minimize the residual amount of energy not supplied at all nodes:

$$\textit{Maximize:} \qquad \sum_{x}^{k} \left(\overline{E^x_{\text{im}}} - E^x_{\text{im}}\right) \tag{4.17}$$

where $\overline{E^x_{\text{im}}}$ is fixed for each node x and a given interruption period $\boldsymbol{t_{\mathrm{I}}}$, (4.16). (4.17) is equivalent to:

$$\textit{Maximize:} \qquad \sum_{x}^{k} E^x_{\text{im}} = \sum_{x}^{k}\sum_{j}^{n} \left|s^x_{\text{im},j}\right| \tag{4.18}$$

That is, to maximize the total energy imported during the period of outage throughout all nodes. This thesis assumes the power electronics are able to provide any desired angle. In accordance with (4.14)—(4.16), energy and power imported to / exported from each node should be within the given limits, (4.19)—(4.21):

$$\textit{s.t.:} \qquad \sum_{j}^{n} \left|s^x_{\text{im},j}\right| \leqslant \overline{E^x_{\text{im}}} \tag{4.19}$$

$$\sum_{j}^{n} \left|s^x_{\text{ex},j}\right| \leqslant \overline{E^x_{\text{ex}}} \tag{4.20}$$

$$\left|s^x_{\text{ex},j}\right| \leqslant \left|\overline{s^x_{\text{ex},j}}\right| \tag{4.21}$$

where,

$$\left|s^x_{\text{im},j}\right| = \sqrt{\left(p^x_{\text{im},j}\right)^2 + \left(q^x_{\text{im},j}\right)^2} \tag{4.22}$$

$$\left|s^x_{\text{ex},j}\right| = \sqrt{\left(p^x_{\text{ex},j}\right)^2 + \left(q^x_{\text{ex},j}\right)^2} \tag{4.23}$$

Meanwhile, other constraints such as power balance and limits during each time and voltage boundaries should be satisfied at each node x as well ((4.24))—(4.28)):

$$\sum_{x}^{k} \left(p^x_{\text{im},j} - p^x_{\text{ex},j}\right) = 0 \tag{4.24}$$

$$\sum_{x}^{k} \left(q^x_{\text{im},j} - q^x_{\text{ex},j}\right) = 0 \tag{4.25}$$

$$\underline{p^x} < p^x_{\text{im},j} - p^x_{\text{ex},j} < \overline{p^x} \tag{4.26}$$

$$\underline{q^x} < q^x_{\text{im},j} - q^x_{\text{ex},j} < \overline{q^x} \tag{4.27}$$

$$\underline{\theta^x} < \theta^x < \overline{\theta^x} \tag{4.28}$$

$$\underline{v^x} < v^x < \overline{v^x} \tag{4.29}$$

4.3.3 Solution

While maximizing the total imports over the whole period, the power flow for each time slot $j = 1, 2, \cdots, n$ should be within constraints (4.19)—(4.28). This nonlinear optimization problem is similar to the one in [35], where the goal is to minimize power losses over the network during the period of EV charging. In that study, the quadratic programming technique serves as an efficient solution while the iterative backward-forward sweep method is used to calculate the power flow. The quadratic optimization and power flow computation are carried out alternately until convergence. Bearing the same notion, the interior-point method is employed in this chapter to optimize the objective while in each attempt optimal power flow (OPF) is conducted to maximize the power import at each time [40].

4.4 Assessment Procedures

From the above sections, for a given system and a population of EVs the household demand covered by EVs depends on EV charging schedules, household consumption levels and the time and duration of an event of outage, which vary with the time of day and the season. A Monte Carlo method is used for reliability evaluation. This thesis assumes the daily travel and charging requirements of EVs remain fixed during the year. A random sampling process is carried out prior to the assessment to generate the travel information and charging requirements of a population of EVs [94]. The travel patterns used can be found in [38]. The optimization is based on MATLAB.

1. Read system information, lengths and outage rates of mains and laterals, travel information and charging requirements of EVs;
2. Form matrices $\mathbf{T_A}$, $\boldsymbol{e}_\mathbf{F}$, $\boldsymbol{e}_\mathbf{D}$ and $\mathbf{P_{OC}}$;
3. Adopt the charging topology, i.e. centralized or dispersed, to each load point;
4. Adopt scenarios for each load point: local V2G or interregional V2G for centralized EV charging; and V2H, local V2G or interregional V2G for dispersed EV charging;
5. Sample the events of main and lateral failures; note the time and duration of each event and energy not supplied triggered by it;
6. Obtain $\boldsymbol{t}_\mathbf{BI}$, $\boldsymbol{t}_\mathbf{I}$ and $\boldsymbol{t}_\mathbf{AI}$ in accordance with the outage; calculate using (4.2)—(4.5).
7. Calculate $\boldsymbol{e}_\mathbf{lim}$ and then E_B using methods provided in the above sections depending on the scenario applied; calculate constraints (4.14)—(4.16) and solve problems (4.18)—(4.28) if interregional V2G is applied;

8. Note the residual energy not supplied; calculate expected energy not supplied (EENS) with and without EV charging;

9. Repeat Steps 5—8 until acceptable values of EENS or the stopping rule are reached;

10. Repeat Steps 4—9 until all scenarios for the charging topology are evaluated;

11. Stop if both charging topologies are considered; go to Step 3 otherwise.

4.5 Numerical Study

A textbook example [29] is used for illustration and validation. The results with and without EV charging are compared. The network is shown in Fig. 1.7, where 2500, 1000 and 500 households are assumed at load points A, B and C, respectively. Each household owns an EV. Load data are from [53] (included in Appendix C). The annual peak consumption of a household is assumed between 10 to 15 kW, following a uniform distribution. Energy capacity of each EV is 25 kWh. p_{O} and p_{R} are both 10 kW. The basic information of EV daily travel and charging requirements are from Section 2.3. The impedance is $0.1+j0.5$ p.u. per mile and the system bases are 10 MVA and 10kV. Acceptable voltages are from 0.9 to 1.1 of the base value.

4.5.1 Local V2G

As stated in Section 4.1 and 4.2, load demand recovered (E_{B}) depends on variables such as $\mathbf{T_A}$, $\boldsymbol{t}_{\mathbf{I}}$ and $\mathbf{P_H}$ which vary with time of the day. Given a typical failure of a primary main feeder (3 hour repair time [29]) taking place at a given hour of a typical day, the value of E_{B} varies as the hour varies. Fig. 4.5 shows the results of load point B (1,000 EVs) in the scenario of local V2G with centralized EV charging.

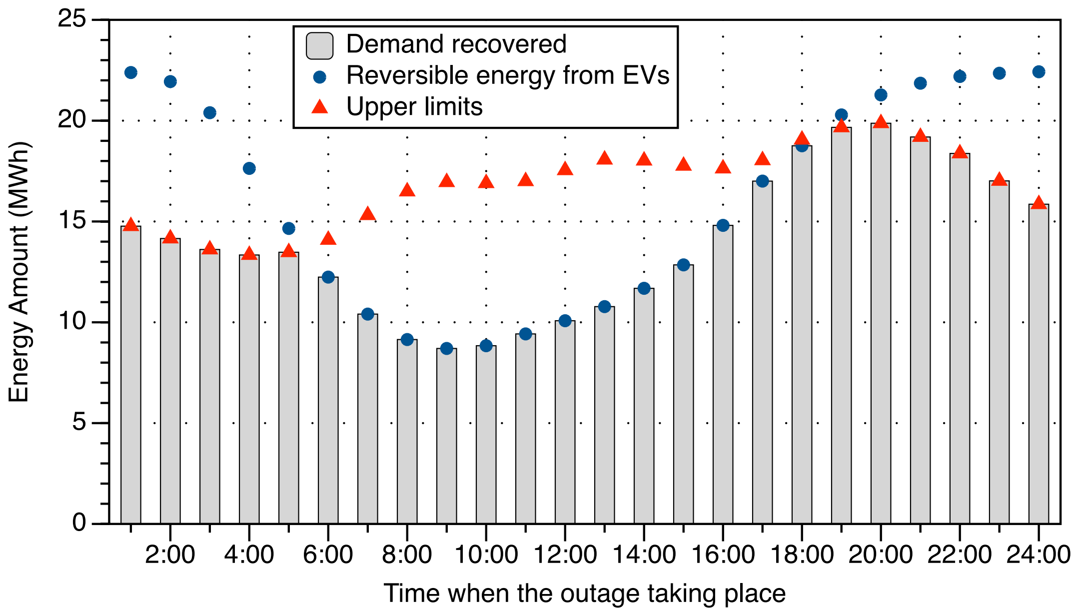

FIGURE 4.5: Demand recovered at region B by local V2G with centralized EV charging

It can be seen from Fig. 4.5 that energy reversible for local V2G varies widely during the day. It reaches its maximum when the outage starts at 24:00 and 1:00 since most of the automobiles remain connected and have enough SOC to spare ($\boldsymbol{e}_{\mathbf{EV}}$) and enough time to refill the EVs ($\boldsymbol{e}_{\mathbf{SC}}$), whereas the minimum occurs at 9:00 as the majority of EVs are on the road (4.2). On the other hand, the load demand that eventually gets recovered is restrained by its upper limits, i.e. the second term in (4.1), which is the total of household consumption and EV availability, (4.6) and (4.7). This suggests that in this case, there are additional amounts of energy available if outages take place during the period between 6:00 and 18:00.

Table 4.1 gives the results of reliability evaluation for the scenario. The first row shows values of EENS when EVs are not included. For the topology of centralized charging, EENS at load point A, B and C are reduced by 22.53, 11.04 and 5.26 MWh per year by local V2G, i.e. 75.6%, 69.8% and 67.1% of each region, respectively. The reduction is generally proportional to the number of EVs in each region.

Table 4.1: Results of reliability evaluation for local V2G (in four cases)

EENS (MWh/year)	Region			Total
	A	B	C	
Without EVs	29.80	15.81	7.84	53.45
Base case	7.27	4.77	2.58	14.62
Increasing power limits	3.69	3.65	2.17	9.51
Increasing energy capacity	6.03	3.54	1.86	11.43
Increasing both above	1.08	1.01	0.61	2.69

In recent years, more EVs with higher energy storage capacities and power capabilities have appeared as the development of the EV industry has quickened its pace. For example, the dual charger [2] is able to offer twice the normal charging power. It is necessary to study the effects of energy capacities ($\boldsymbol{e}_{\mathbf{F}}$) and charging and discharging limits (p_{O} and p_{R}). In addition to the base case, three cases are considered in Table 4.1: (a) increasing the charging / discharging power limits from 10 kW to 20 kW; (b) increasing the energy storage capacity of each EV from 25 kWh to 50 kWh; and (c) increasing both the power limits and energy storage capacity.

As can be seen from Table 4.1, while the reliability improves with either the upgraded charging specs or energy capacity, the residual EENS descends to 3.6%, 6.4% and 7.8% of original value for load points A, B and C, respectively, and 5.0% (2.69 MWh) for the whole system when both charging specs and energy capacity are lifted.

4.5.2 V2H and V2H + local V2G

Substituting dispersed EV charging for the local network topology, portions of energy recovered by V2H and local V2G are given in Fig. 4.6. In the scenario of V2H, energy

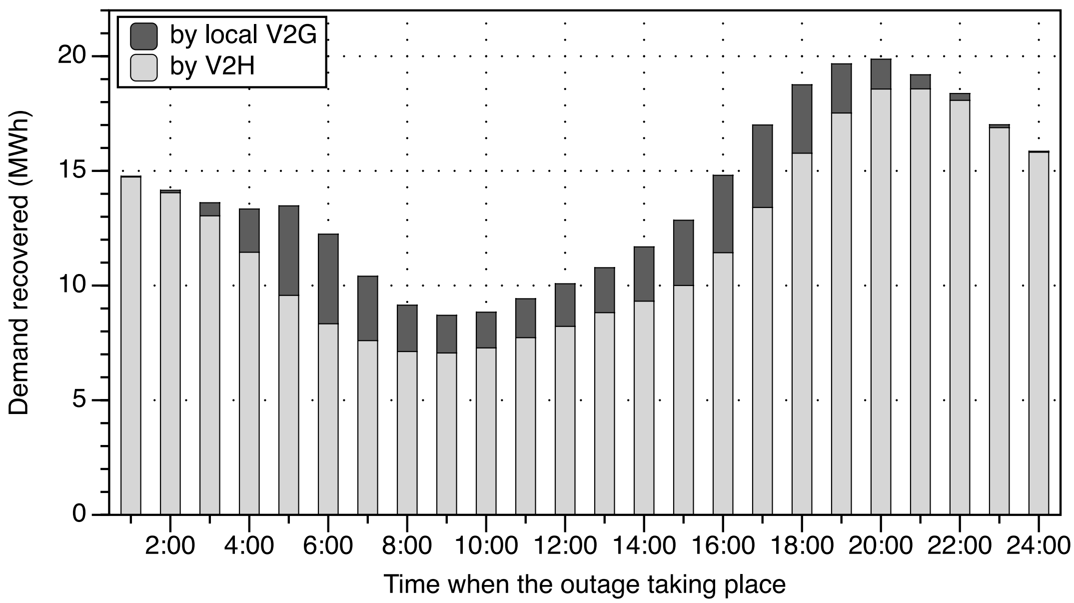

FIGURE 4.6: Demand recovered at region B by V2H and local V2G with dispersed EV charging

not supplied of each household is independently picked up by its own EV. This leaves further backups to be desired when local V2G is enabled, as can be seen in Fig. 4.6. Taking the average of the 24 instances, the local V2G can pick up an additional 1.82 MWh household demand on daily basis. That is 15.04% of the capability provided by V2H (12.10 MWh on average).

Table 4.2 lists the average capacity for local V2G in each case. From (4.10) and (4.13), the levels of household consumption ($\mathbf{P_H}$ and $\mathbf{P_{H'}}$) is critical for determining capacities for V2H and local V2G. In Table 4.2, an additional case where the peak load of each household increases to 15˜20 kW is considered (the last row in the table).

As can be seen from the table, the higher the household consumption is, the less difference the local V2G would make. This is because power supply from each EV is primarily consumed by the household it is directly connected to. On the other hand, with increased charging / discharging limits or energy capacities of EVs the extra ability for local exchange would also be enhanced. The additional capability

Table 4.2: Sensitivity studies of power limits, energy capacity and load levels for local V2G at region B with dispersed EV charging

	Local V2G (MWh)	V2H (MWh)	% of V2H (%)
Base case	1.82	12.10	15.04
Increasing power limits	2.17	12.43	17.43
Increasing energy capacity	2.97	12.16	24.42
Increasing both above	4.51	12.48	36.13
Increasing load levels	0.50	15.19	3.27

Table 4.3: Results of reliability evaluation for V2H and V2H + local V2G

EENS (MWh/year)	V2H			Total	V2H + local V2G			Total
	A	B	C		A	B	C	
Base case	9.02	5.45	2.88	17.35	7.23	4.80	2.59	14.62
Increasing power limits	8.41	5.11	2.71	16.22	3.67	3.61	2.15	9.43
Increasing energy capacity	8.36	4.76	2.49	15.61	6.09	3.57	1.87	11.52
Increasing both above	7.60	4.27	2.23	14.10	1.08	1.02	0.62	2.72

provided by local V2G surges when both the energy and power limits are raised (the penultimate row in Table 4.2). This suggests that the capacity of local V2G can also benefit from the upgraded battery and charging / discharging specs of EVs.

Table 4.3 shows the results of evaluation of V2H and V2H + local V2G. When only V2H is applied in the topology of dispersed EV charging, the reliability improvement is relatively hampered, compared to V2H + local V2G. Increasing the energy capacity and charging / discharging limits, the reliability improvement becomes more obvious for V2H + local V2G than for V2H. With each household served by its own EV only, the reduction in energy not supplied is capped by the consumption of each household.

Table 4.4: Results of reliability evaluation for interregional V2G

EENS (MWh/year)	Centralized charging		Dispersed charging	
	Total	Reduction	Total	Reduction
Base case	14.30	0.32	14.29	0.33
Increasing power limits	9.11	0.40	9.06	0.36
Increasing energy capacity	11.08	0.36	11.81	0.35
Increasing both above	2.15	0.54	2.16	0.55

Compared to Table 4.1, the reliability improvement for V2H + local V2G is at the same level as local V2G with centralized EV charging.

4.5.3 Interregional V2G

Table 4.4 shows EENS of the whole system and its further improvement when interregional V2G is applied. For both charging topologies the inclusion of energy exchange among regions achieves enhancement of the system reliability. From the perspective of the whole system, the evaluation results show little difference between the two topologies. It can be explained by the fact that, viewing from the grid side, the topology applied locally matters little as long as there are extra capacities and the power constraint (4.7) is fulfilled. The EENS reduction increases when either power limits or energy capacities of EVs are increased. A limited amount of EENS remains when both are increased.

Fig. 4.7 compares the system reliability under all possible scenarios for each charging topology. The most prominent reliability enhancement is achieved by the scenario of local V2G for centralized EV charging and by V2H for dispersed EV charging. The V2H + local V2G goes on reducing the EENS by a perceptible amount specially in the case of both increased energy capacity and charging / discharging limits. The

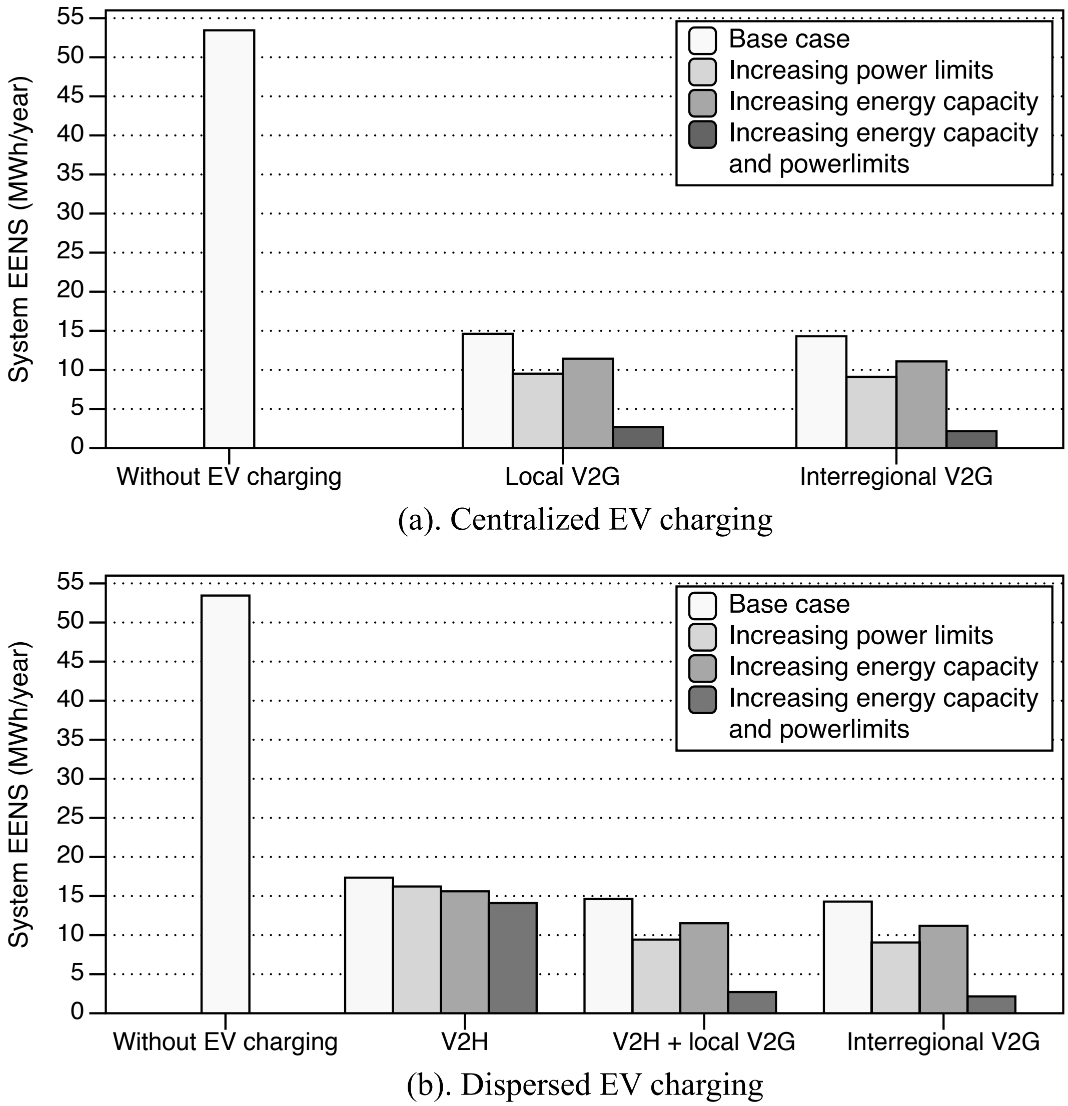

FIGURE 4.7: Comparison of different scenarios for centralized and dispersed EV charging topologies

further improvement made by interregional V2G is relatively limited in each case. There are three major reasons: (a) For the typical radial system, events of failure take place more frequently at lateral sections, which merely isolates a single region. For example, in this given case [29], the failures of laterals account for 71.4% of the total number of failures; (b) Further requirements (4.14)—(4.16) and (4.19)—(4.21) are imposed on the imports and exports of energy among regions. Interregional V2G only works when simultaneously there is extra supply at one node and demand at another. Besides, the network introduces additional loss for power exchange other than the efficiency loss during charging and discharging (η); (c) The scenario of local V2G for centralized EV charging and scenarios of V2H and V2H + local V2G for dispersed EV charging are more basic and eliminate large portions of energy not supplied.

Tables 4.1, 4.3 and 4.4 and Fig. 4.7 show that increasing the charging / discharging limits unilaterally favors the whole system reliability more than alternatively increasing the energy capacity of EV instead. An exception is in the scenario of V2H for dispersed EV charging. As can be seen from Fig. 4.7 (b) not much difference is made even when both energy capacity and charging / discharging limits are increased, since the contribution of each EV is capped by the demand of each household during the outage period, (4.9) and (4.10).

4.6 Summary

It is the distribution system in the power grid that EVs are directly connected to. Two charging topologies—centralized and dispersed charging and two modes of operation following an incident—islanding and grid-connected modes—are considered in this chapter. Thus multiple scenarios need to be considered such as local V2G, V2H, V2H + local V2G and interregional V2G. Case study shows that charging topologies and operating modes impose additional ceilings for EVs' providing household backup energy. Among those scenarios, interregional V2G is favored as it minimize energy not supplied with wider connection in a given system.

5

Conclusion and Discussion

5.1 Conclusion

In Chapter 2, this thesis extends the generating system operating health analysis by taking EV charging into consideration. To the best of the authors knowledge, this thesis is the first work that proposes the idea of EV charging being treated as interruptible load and serving as emergency units to improve system well-being. Numerical results show that V2G is more effective for well-being improvement than the interruptible EV charging. In the V2G enabled scenario, EVs are able to provide more capacities to help the system.

Results of the sensitivity study show that the daily risk reduced by V2G is more sensitive to the charging/discharging limits and the EV population than to the energy capacity of EV. In general, the growth of EV population marginally improves the system well-being, especially in V2G enabled scenarios, while the reduction of the lead time has a positive influence on the generating system.

The procedure illustrated in this thesis provides a quantitative framework for analyzing generating system well-being when EV charging is involved. The method for evaluating the capacity for interruptible load and V2G can be used in studies where flexible EV charging is allowed.

In Chapter 3, this thesis first identifies the major uncertainties that can affect EV charging. They are punctuality, rounding of time, forecast error of energy consumption, charging component failure and EV absence, and aggregator failure and grid realization. Methodologies are developed to consider these elements in well-being analysis. As expected, results show the uncertainties identified directly affect EVs' contribution to the system well-being.

Other main conclusions reached in this thesis are: i). Different from traditional interruptible load programs, the capacity provided by EVs is not 100% interruptible, because of EV charging uncertainties. ii). In contrast to conventional and other unconventional units/services of which actual capacities provided would not be greater than rated or scheduled ones, the interruptible capacities contributed from EVs can exceed the scheduled values at some hours during the day due to the effect of the punctuality and time rounding. iii). At the aggregated level, the realization of EVs' grid services plays an important role. Increasing the number of aggregators does not necessarily further improve the system well-being, though the increase of aggregator's reliability has a positive influence on EVs' role in system reliability enhancement. iv). EVs are able to eliminate the deterioration of system well-being caused by load forecast uncertainty with a penetration level of EVs as low as 1.4% in the given system.

In Chapter 4, this thesis examines V2H and V2G as leverage for improvement of distribution system reliability. Methods are proposed to evaluate the capacity contribution of EV for possible scenarios with each of the two potential charging topologies applied on the local circuit level.

Results show that with participation of EV charging, the reliability of a distribution system improves even with basic involvement of EVs, that is, the local V2G for centralized EV charging and V2H for dispersed EV charging. Instead of individual houses drawing energy only from their own EVs, sharing the energy from all local EVs is very important for dispersed EV charging and to gain additional reliability. The system can benefit more as EV industry evolves.

5.2 Discussion

To be part of the grid services, it is very important that basic information of new units and services is provided beforehand and a proper model is established so that the potential roles they play can be scheduled and their effects can be evaluated by grid operators. Nevertheless, as an energy resource that is distributed on the demand side yet is supposed to serve with priority in the transportation sector, one of the big questions is that how firmly individuals (EV owners in this case) can abide by rules and standards imposed by their grid participation while not compromising driving duties. To the best of our knowledge, this thesis is the first to answer the questions that how reliable is the scheduled information of EVs, and how it can be modeled. Due to the lack of data at present, some assumptions in our studies are made and thus sensitivity studies are conducted with considering various scenarios. These assumptions and difficulties can be obviated once actual data is available. Besides, with more and more demand response programs emerging, it is expected that more relevant uncertain elements would be brought to light and be considered in future studies. On the other hand, these uncertainties need to be considered in many of the scheduling problems (e.g. on unit commitment, power flow and reliability assessment) as long as EVs are supposed to be lucrative in power systems.

Though as a basic computational algorithm, the sequential Monte Carlo method adopted in this Chapter 4 proves to be a sufficient tool for the assessment providing reliable results. To have the same accuracy as of the results in [29], the running time for each case spans from several minutes to 10 minutes (Matlab 2011b for OS X, 2011 iMac with 2.5GHz Intel Core i5). During the process, the calculation of $\mathbf{T_A}$ and the iteration are the two procedures cost most of the execution time. Though the program runs much faster with the matrix formation, it still costs much effort due to the large sizes of the matrices. In this paper, is 1440 (i.e. 1440 minutes during calendar day), so, for instance, is a 2500×1440 matrix for region A. On the other hand, the optimal power flow does not take much processing time since, as explained in Section 4.5.3, the occurrence of interregional V2G is limited. The other reason is that the network of a typical distribution system is relatively simple and fewer nodes can be involved in interregional V2G following an outage. To further improve the efficiency and the speed of convergence, advanced sampling methods [52, 99] can be used in future works. The other method to significantly reduce the running time is making full use of the hardware such as parallel processing, since multi-core processors dominate modern computers.

Appendix A

Probabilistic Criteria and Indices

The following indices are frequently used in power system reliability evaluation.

1. Loss of load probability (LOLP).

2. Loss of load expectation (LOLE).

3. Loss of energy expectation (LOEE)/expected energy not supplied (EENS).

4. Frequency and duration (F&D) indices.

5. Energy index of reliability (EIR).

6. Energy index of unreliability (EIU).

A.1 Loss of Load Probability (LOLP)

LOLP is defined as the probability that the load will exceed the available generation. As the most basic probability index in power system reliability evaluation, it defines the likelihood of encountering trouble (loss of load) but not the severity, e.g. for the same value of LOLP, the degree of interruption may be less than 1 MW or greater than 100 MW. Therefore it cannot recognize the degree of capacity or energy shortage.

Because of the less physical significance and difficulty to interpret of LOLP, it has been superseded by one of the following expected values in most planning applications.

A.2 Loss of Load Expectation (LOLE)

LOLE is generally defined as the average number of days (or hours) on which the daily peak load is expected to exceed the available capacity. It therefore indicates the expected duration for which a load loss or deficiency may occur. This concept implies a physical significance not forthcoming from the LOLP, although the two values are directly related.

The individual daily peak loads can be used in conjunction with the capacity outage probability table to obtain the expected number of days in the specified period in which the daily peak load will exceed the available capacity. The index in this case is designated as the loss of load expectation (LOLE).

$$\text{LOLE} = \sum_{i}^{n} P_i(C_i - L_i) \quad \text{days/period} \tag{A.1}$$

where C_i = available capacity on day i.

L_i = forecast peak load on day i.

$P_i(C_i - L_i)$ = probability of loss of load on day i. This value is obtained directly from the capacity outage cumulative probability table.

The same LOLE index can also be obtained using the daily peak load variation curve. Figure A.1 shows a typical system load—capacity relationship where the load model is shown as a continuous curve for a period of 365 days, O_k is the magnitude of the kth outage in the system capacity outage probability table, and t_k is the number

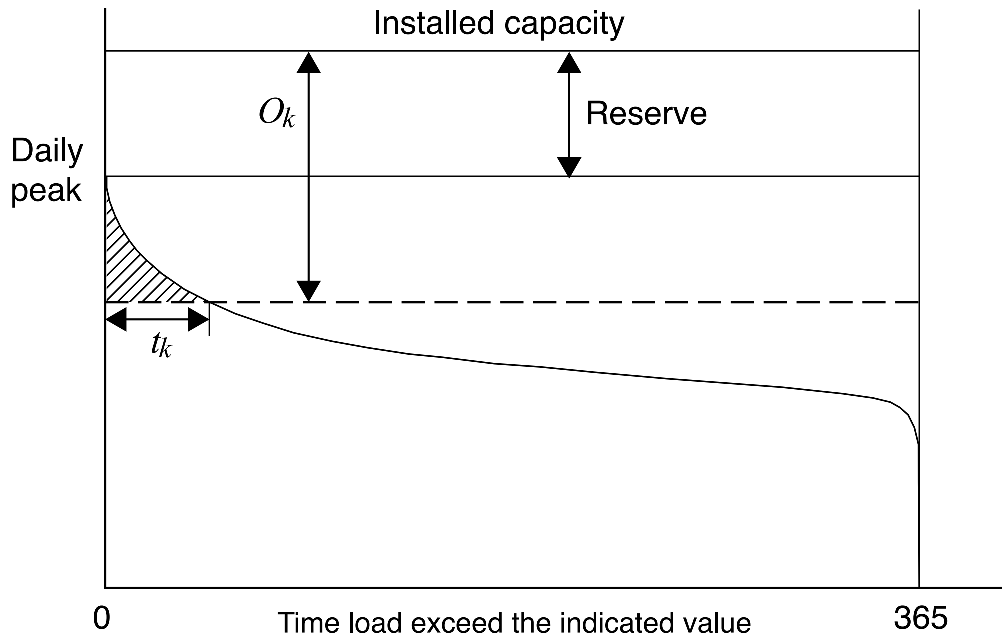

FIGURE A.1: Relationship between load, capacity and reserve

of time units in the study interval that an outage magnitude of O_k would result in a loss of load.

A particular capacity outage will contribute to the system LOLE by an amount equal to the product of the probability of existence of the particular outage and the number of time units in the study interval that loss of load would occur if such a capacity outage were to exist. It can be seen from the figure that any capacity in excess of the reserve will result in varying numbers of time units during which loss of load could occur. Expressed mathematically, the contribution to the system LOLE made by capacity outage O_k is $p_k t_k$ time units where p_k is the individual probability of the capacity outage O_k. The total LOLE for the study interval is

$$\text{LOLE} = \sum_{k=1}^{n} P_k t_k \quad \text{time units} \tag{A.2}$$

The p_k values are the individual probabilities associated with the capacity outage states. The equation can be modifies to use the cumulative sate probabilities. In this case

$$\text{LOLE} = \sum_{k=1}^{n} (t_k - t_{k-1}) P_k \tag{A.3}$$

where P_k = cumulative outage probability for capacity state O_k.

If the load characteristic in Figure A.1 is the load duration curve, the value of LOLE is in hours. If a daily peak load variation curve is used, the LOLE is in days for the period of study.

LOLE is now the most widely used probabilistic index in deciding future generation capacity. Yet it has the same weaknesses that exist in the LOLP.

A.3 Loss of Energy Expectation (LOEE)

LOEE is defined as the expected energy not supplied (EENS) due to those occasions when the load exceeds the available generation. It therefore reflects risk more truly and is likely to gain popularity as power systems become more energy-limited due to reduced prime energy and increased environmental controls. LOEE is illustrated by (A.4).

Any outage of generating capacity exceeding the reserve will result in a curtailment of system load energy. Let:

P_k = probability of a capacity outage equal to O_k.

E_k = energy curtailed by a capacity outage equal to O_k.

This energy curtailment is given by the shaded area in Figure A.2. The probable energy curtailed is $E_k P_k$. The sum of these products is the total expected energy curtailment or LOEE/EENS:

$$\text{LOEE} = \sum_{k=1}^{n} E_k P_k \tag{A.4}$$

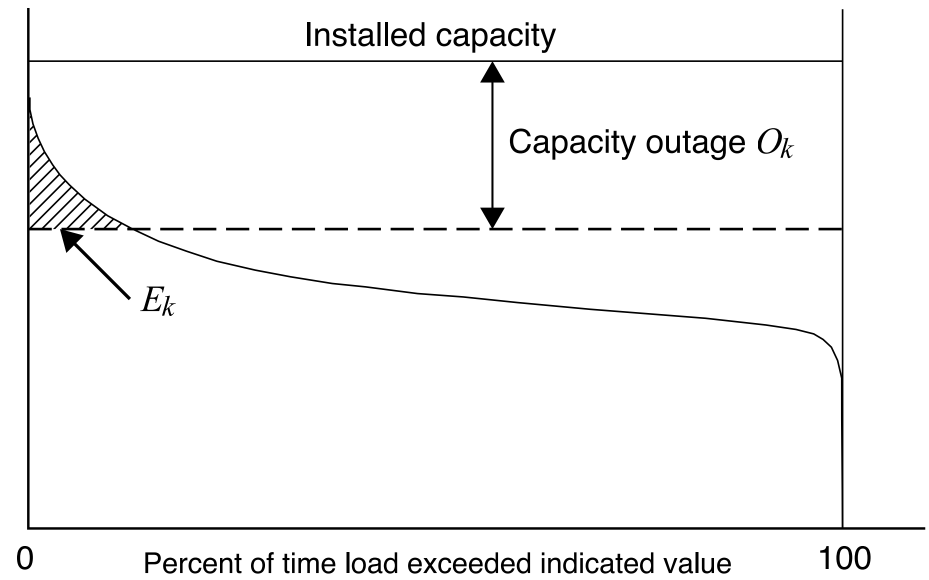

FIGURE A.2: Energy curtailment due to a given capacity outage condition

LOEE/EENS is presently less used than LOLE but is a more appealing index since it encompasses severity of the deficiencies as well as their likelihood.

A.4 Frequency and Duration (F&D) Indices

The F&D criterion is an extension of LOLE and identifies expected frequencies of encountering deficiencies and their expected durations. It contains additional physical characteristics but, although widely documented, is not used in practice. This is due mainly to the need for additional data and greatly increased complexity of the analysis without having any significant effect on the planning decisions.

A.5 Energy Index of Reliability (EIR) and Energy Index of Unreliability (EIU)

Both EIR and EIU are directly related to LOEE which is normalized by dividing by the total energy demanded. This basically ensures that large and small systems can be compared on an equal basis and chronological changes in a system can be tracked.

LOEE/EENS can be normalized by utilizing the total energy under the load duration curve designated as E.

$$\mathrm{LOEE}_{\text{p.u.}} = \sum_{k=1}^{n} \frac{E_k P_k}{E} \tag{A.5}$$

The per unit LOEE value represents the ratio between the probable load energy curtailed due to deficiencies in available generating capacity and the total load energy required to serve the system demand. The energy index of reliability, EIR, is then

$$\mathrm{EIR} = 1 - \mathrm{LOEE}_{\text{p.u.}} \tag{A.6}$$

and the energy index of unreliability, EIU, is

$$\begin{aligned} \mathrm{EIU} &= 1 - \mathrm{EIR} \\ &= \mathrm{LOEE}_{\text{p.u.}} \end{aligned} \tag{A.7}$$

Appendix B

Additional Indices

In order to reflect the severity or significance of a system outage, additional reliability indices can be and frequently evaluated. The additional indices that are most commonly used are defined as followings.

B.1 Customer-oriented Indices

B.1.1 System Average Interruption Frequency Index, SAIFI

$$\text{SAIFI} = \frac{\text{total number of customer interruptions}}{\text{total number of customers served}} = \frac{\sum \lambda_i N_i}{\sum N_i} \tag{B.1}$$

where λ_i is the failure rate and N_i is the number of customers of load point i.

B.1.2 Customer Average Interruption Frequency Index, CAIFI

$$\text{CAIFI} = \frac{\text{total number of customer interruptions}}{\text{total number of customers affected}} \tag{B.2}$$

This index differs from SAIFI only in the value of the denominator. It is particularly useful when a given calendar year is compared with other calendar years since, in any given calendar year, not all customers will be affected and many will experience complete continuity of supply. The value of CAIFI therefore is very useful in recognizing chronological trends in the reliability of a particular distribution system.

In the application of this index, the customers affected should be counted only once, regardless of the number of interruptions they may have experienced in year.

B.1.3 System Average Interruption Duration Index, SAIDI

$$\text{SAIDI} = \frac{\text{sum of customer interruption durations}}{\text{total number of customers}} = \frac{\sum U_i N_i}{\sum N_i} \tag{B.3}$$

where U_i is the annual outage time and N_i is the number of customers of load point i.

B.1.4 Customer Average Interruption Duration Index, CAIDI

$$\text{CAIDI} = \frac{\text{sum of customer interruption durations}}{\text{total number of customer interruptions}} = \frac{\sum U_i N_i}{\sum \lambda_i N_i} \tag{B.4}$$

where λ_i is the failure rate, U_i is the annual outage time and N_i is the number of customers of load point i.

B.1.5 Average Service Availability (Unavailability) Index, ASAI (ASUI)

$$\begin{aligned} \text{ASAI} &= \frac{\text{customer hours of available service}}{\text{customer hours demanded}} \\ &= \frac{\sum N_i \times 8760 - \sum U_i N_i}{\sum N_i \times 8760} \end{aligned} \tag{B.5}$$

$$\begin{aligned} \text{ASUI} &= 1 - \text{ASAI} \\ &= \frac{\text{customer hours of unavailable service}}{\text{customer hours demanded}} \\ &= \frac{\sum U_i N_i}{\sum N_i \times 8760} \end{aligned} \tag{B.6}$$

where 8760 is the number of hours in a calendar year.

B.2 Load- and Energy-oriented Indices

One of the important parameters required in the evaluation of load- and energy-oriented indices is the average load at each load-point busbar.

The average load L_a is given by

$$L_\mathrm{a} = L_\mathrm{p} f \tag{B.7}$$

where L_p = peak load demand

f = load factor

$$L_\mathrm{a} = \frac{\text{total energy demanded in period of interest}}{\text{period of interest}} = \frac{E_d}{t} \tag{B.8}$$

where E_d is the total area under the load-duration curve and t is normally one calendar year, as shown in Figure B.1.

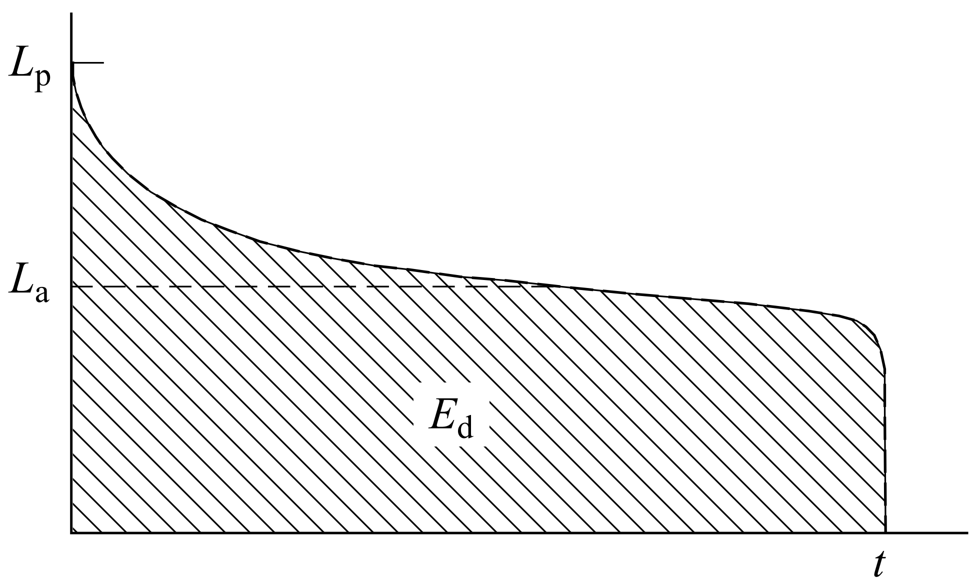

FIGURE B.1: Illustration of L_p, L_a, E_d and t

B.2.1 Energy Not supplied Index, ENS

$$\text{ENS} = \text{total energy not supplied by the system} = \sum L_{a_i} U_i \tag{B.9}$$

where L_{a_i} is the average load connected to load point i.

B.2.2 Average Energy Not Supplied, AENS or Average System Curtailment Index, ASCI

$$\text{AENS} = \frac{\text{total energy not supplied}}{\text{total number of customers served}} = \frac{\sum L_{a_i} U_i}{\sum N_i} \tag{B.10}$$

B.2.3 Average Customer Curtailment Index, ACCI

$$\text{ACCI} = \frac{\text{total energy not supplied}}{\text{total number of customers affected}} \tag{B.11}$$

This index differs from AENS in the same way that CAIFI differs from SAIFI. It is therefore a useful index for monitoring the changes of average energy not supplied between one calendar year and another.

Appendix C

RBTS Data

C.1 Generating System

The generating unit ratings and reliability data for the RBTS are shown in Table C.1

Table C.1: Generating unit reliability data

Unit size (MW)	Type	No. of units	Forced outage rate	MTTF (hr)	Failure rate per year	MTTR (hr)	Repair rate per year	Scheduled mainte-nance week/year
5	hydro	2	0.010	4380	2.0	45	198.0	2
10	thermal	1	0.020	2190	4.0	45	196.0	2
20	hydro	4	0.015	3650	2.4	55	157.6	2
20	thermal	1	0.025	1752	5.0	45	195.0	2
40	hydro	1	0.020	2920	3.0	60	147.0	2
40	thermal	2	0.030	1460	6.0	45	194.0	2

C.2 Load Model

The data on weekly peak loads in percent of the annual peak load, daily peak load in percent of the weekly peak, and hourly peak load in percent of the daily peak are the same as that given in the IEEE-RTS [53]. The total number of data points required to define the daily peak load curve is 364. In the case of the hourly peak load curve or the load duration curve, 8736 points are required.

Table C.2: Weekly peak load in percent of annual peak

Week	Peak load	Week	Peak load	Week	Peak load	Week	Peak load
1	86.2	14	75.0	27	75.5	40	72.4
2	90.0	15	72.1	28	81.6	41	74.3
3	87.8	16	80.0	29	80.1	42	74.4
4	83.4	17	75.4	30	88.0	43	80.0
5	88.0	18	83.7	31	72.2	44	88.1
6	84.1	19	87.0	32	77.6	45	88.5
7	83.2	20	88.0	33	80.0	46	90.9
8	80.6	21	85.6	34	72.9	47	94.0
9	74.0	22	81.1	35	72.6	48	89.0
10	73.7	23	90.0	36	70.5	49	94.2
11	71.5	24	88.7	37	78.0	50	97.0
12	72.7	25	89.6	38	69.5	51	100.0
13	70.4	26	86.1	39	72.4	52	95.2

Table C.3: Daily load in percent of weekly peak

Day	Peak load
Monday	93
Tuesday	100
Wednesday	98
Thursday	96
Friday	94
Saturday	77
Sunday	75

Table C.4: Hourly peak load in percent of daily peak

	Winter weeks 1–8 & 44–52		Summer weeks 18–30		Spring/fall weeks 9–17 & 31–43	
Hour	Weekday	Weekend	Weekday	Weekend	Weekday	Weekend
12-1 am	67	78	64	74	63	75
1-2	63	72	60	70	62	73
2-3	60	68	58	66	60	69
3-4	59	66	56	65	58	66
4-5	59	64	56	64	59	65
5-6	60	65	58	62	65	65
6-7	74	66	64	62	72	68
7-8	86	70	76	66	85	74
8-9	95	80	87	81	95	83
9-10	96	88	95	86	99	89
10-11	96	90	99	91	100	92
11-noon	95	91	100	93	99	94
noon-1pm	95	90	99	93	93	91
1-2	95	88	100	92	92	90
2-3	93	87	100	91	90	90
3-4	94	87	97	91	88	86
4-5	99	91	96	92	90	85
5-6	100	100	96	94	92	88
6-7	100	99	93	95	96	92
7-8	96	97	92	95	98	100
8-9	91	94	92	100	96	97
9-10	83	92	93	93	90	95
10-11	73	87	87	88	80	90
11-12	63	81	72	80	70	85

Bibliography

[1] "Interruptible power rates and their role in utility distributed resources programs," Electric Power Research Institute, Palo Alto, CA, Tech. Rep. Tech. Rep. 1007717, Feb. 2003.

[2] (2014) Tesla motors. [Online]. Available: http://www.teslamotors.com/

[3] A. Abiri-Jahromi, M. Fotuhi-Firuzabad, and E. Abbasi, "Optimal scheduling of spinning reserve based on well-being model," *IEEE Trans. Power Syst.*, vol. 22, no. 4, pp. 2048–2057, Nov. 2007.

[4] M. Al-Muhaini and G. T. Heydt, "Evaluating future power distribution system reliability including distributed generation," *IEEE Trans. Power Syst.*, vol. 28, no. 4, pp. 2264–2272, Oct. 2013.

[5] F. H. Allport, "The J-curve hypothesis of conforming behavior," *J. Soc. Psychol.*, vol. 5, no. 2, pp. 141–183, May 1934.

[6] S.-L. Andersson, A. K. Elofsson, M. D. Galus, L. Goransson, S. Karlsson, F. Johnsson, and G. Andersson, "Plug-in hybrid electric vehicles as regulating power providers: Case studies of sweden and germany," *Energy Policy*, vol. 38, no. 6, pp. 2751–2762, Jun. 2010.

[7] L. T. Anstine, R. E. Burke, J. E. Casey, R. Holgate, R. S. John, and H. G. Stewart, "Application of probability methods to the determination of spinning reserve requirements for the Pennsylvania-New Jersey-Maryland interconnection," *IEEE Trans. Power App. Syst.*, vol. 82, no. 68, pp. 726–735, Oct. 1963.

[8] Y. M. Atwa, E. F. El-Saadany, and A.-C. Guise, "Supply adequacy assessment of distribution system including wind-based dg during different modes of operation," *IEEE Trans. Power Syst.*, vol. 25, no. 1, pp. 78–86, Feb. 2010.

[9] Y. M. Atwa, E. F. El-Saadany, M. M. A. Salama, R. Seethapathy, M. Assam, and S. Conti, "Adequacy evaluation of distribution system including wind/solar

dg during different modes of operation," *IEEE Trans. Power Syst.*, vol. 26, no. 4, pp. 1945–1952, Nov. 2011.

[10] M. D. Back, S. C. Schmukle, and B. Egloff, "Who is late and who is early? Big five personality factors and punctuality in attending psychological experiments," *J. Res. in Pers.*, vol. 40, no. 5, pp. 841–848, Oct. 2006.

[11] I.-S. Bae and J.-O. Kim, "Reliability evaluation of distributed generation based on operation mode," *IEEE Trans. Power Syst.*, vol. 22, no. 2, pp. 785–790, May. 2007.

[12] ——, "Reliability evaluation of customers in a microgrid," *IEEE Trans. Power Syst.*, vol. 23, no. 3, pp. 1416–1422, Aug. 2008.

[13] Bagen and R. Billinton, "Incorporating well-being considerations in generating systems using energy storage," *IEEE Trans. Energy Convers.*, vol. 20, no. 1, pp. 225–230, Mar. 2005.

[14] Z. Bie, P. Zhang, G. Li, B. Hua, M. Meehan, and X. Wang, "Reliability evaluation of active distribution systems including microgrids," *IEEE Trans. Power Syst.*, vol. 27, no. 4, pp. 2342–2350, Nov. 2012.

[15] D. Biere, D. Dallinger, and M. Wietschel, "Ökonomische Analyse der Erstnutzer von Elektrofahrzeugen," *Zeitschrift für Energiewirtschaft*, vol. 33, no. 2, pp. 173–181, 2009.

[16] R. Billinton and M. Fotuhi-Firuzabad, "Generating system operating health analysis considering stand-by units, interruptible load and postponable outages," *IEEE Trans. Power Syst.*, vol. 9, no. 3.

[17] R. Billinton and D. Lakhanpal, "Impacts of demand-side management on reliability cost/reliability worth analysis," *Proc. Inst. Elect. Eng., Gen., Transm., Distrib.*, vol. 143, no. 3, pp. 225–231, May 1996.

[18] R. Billinton and R. N. Allan, *Reliability evaluation of power systems*, 2nd ed. New York, NY: Plenum Press, 1996.

[19] R. Billinton and M. Fotuhi-Firuzabad, "A basic framework for generating system operating health analysis," *IEEE Trans. Power Syst.*, vol. 9, no. 3, pp. 1610–1617, Aug. 1994.

[20] R. Billinton and D. Huang, "Incorporating wind power in generating capacity reliability evaluation using different models," *IEEE Trans. Power Syst.*, vol. 26, no. 4, pp. 2509–2517, Nov. 2011.

[21] R. Billinton and A. V. Jain, "The effect of rapid start and hot reserve units in spinning reserve studies," *IEEE Trans. Power App. Syst.*, vol. PAS-91, no. 2, pp. 511–516, Mar. 1972.

[22] R. Billinton and B. Karki, "Well-being analysis of wind integrated power systems," *IEEE Trans. Power Syst.*, vol. 26, no. 4, pp. 2101–2108, Nov. 2011.

[23] R. Billinton, B. Karki, R. Karki, and G. Ramakrishna, "Unit commitment risk analysis of wind integrated power systems," *IEEE Trans. Power Syst.*, vol. 24, no. 2, pp. 930–939, May 2009.

[24] R. Billinton and R. Karki, "Maintaining supply reliability of small isolated power systems using renewable energy," in *Proc. Inst. Elect. Eng., Gen., Transm., Distrib.*, vol. 148, no. 6, Nov. 2001, pp. 530–534.

[25] ——, "Application of Monte Carlo simulation to generating system well-being analysis," *IEEE Trans. Power Syst.*, vol. 14, no. 3, pp. 1172–1177, Aug. 1999.

[26] ——, "Capacity reserve assessment using system well-being analysis," *IEEE Trans. Power Syst.*, vol. 14, no. 2, pp. 433–438, May 1999.

[27] R. Billinton and E. Khan, "A security based approach to composite power system reliability evaluation," *IEEE Trans. Power Syst.*, vol. 7, no. 1, pp. 65–72, Feb. 1992.

[28] R. Billinton, S. Kumar, N. Chowdhury, K. Chu, K. Debnath, L. Goel, E. Khan, P. Kos, G. Nourbakhsh, and J. Oteng-Adjei, "A reliability test system for educational purposes-basic data," *IEEE Trans. Power Syst.*, vol. 4, no. 3, pp. 1238–1244, Aug. 1989.

[29] R. Billinton and W. Li, *Reliability Assessment of Electrical Power Systems Using Monte Carlo Methods*, 1st ed. New York, NY: Plenum Press, 1994.

[30] A. N. Brooks, "Vehicle-to-grid demonstration project: Grid regulation ancillary service with a battery electric vehicle," Prepared for the California Air Resources Board and the California Environmental Protection Agency, Tech. Rep. Final report, Contract number 01-313, Dec. 2002.

[31] A. Brooks, E. Lu, D. Reicher, C. Spirakis, and B. Weihl, "Demand dispatch," *IEEE Power Energy Mag.*, vol. 8, no. 3, pp. 20–29, May 2010.

[32] J. Choi, J. Park, M. Shahidehpour, and R. Billinton, "Assessment of co2 reduction by renewable energy generators," in *Innovative Smart Grid Technologies (ISGT), 2010*, Jan. 2010, pp. 1–5.

[33] S. Civanlar and J. J. Grainger, "Volt/Var control on distribution systems with lateral branches using shunt capacitors and voltage regulators part III: The numerical results," *IEEE Trans. Power App. Syst.*, vol. PAS-104, no. 11, pp. 3291–3297, Nov. 1985.

[34] M. Clarke, M. Dix, and P. Jones, "Error and uncertainty in travel surveys," *Transportation*, vol. 10, no. 2, pp. 105–126, Jun. 1981.

[35] K. Clement-Nyns, E. Haesen, and J. Driesen, "The impact of charging plug-in hybrid electric vehicles on a residential distribution grid," *IEEE Trans. Power Syst.*, vol. 25, no. 1, pp. 371–380, Feb. 2010.

[36] S. Conti, S. A. Rizzo, E. F. El-Saadany, M. Essam, and Y. M. Atwa, "Reliability assessment of distribution systems considering telecontrolled switches and microgrids," *IEEE Trans. Power Syst.*, vol. 29, no. 2, pp. 598–607, Mar. 2014.

[37] I. Cvetkovic, T. Thacker, D. Dong, G. Francis, V. Podosinov, D. Boroyevich, F. Wang, R. Burgos, G. Skutt, and J. Lesko, "Future home uninterruptible renewable energy system with vehicle-to-grid technology," in *Energy Conversion Congress and Exposition, 2009. ECCE 2009. IEEE*, Sep. 2009, pp. 2675–2681.

[38] D. Dallinger, D. Krampe, and M. Wietschel, "Vehicle-to-grid regulation reserves based on a dynamic simulation of mobility behavior," *IEEE Trans. Smart Grid*, vol. 2, no. 2, pp. 302–313, Jun. 2011.

[39] S. Deilami, A. Masoum, P. Moses, and M. A. S. Masoum, "Real-time coordination of plug-in electric vehicle charging in smart grids to minimize power losses and improve voltage profile," *IEEE Trans. Smart Grid*, vol. 2, no. 3, pp. 456–467, Sep. 2011.

[40] H. W. Dommel and W. F. Tinney, "Optimal power flow solutions," *IEEE Trans. Power App. Syst.*, no. 10, pp. 1866–1876, Oct. 1968.

[41] G. J. Dudycha, "An examination of the J-curve hypothesis based on punctuality distributions," *Sociometry*, vol. 1, no. 1/2, pp. 144–154, Jul.-Oct. 1937.

[42] ——, *An objective study of punctuality in relation to personality and achievement*. Columbia university, 1936, vol. 29, no. 204.

[43] M. Duvall, E. Knipping, and M. Alexander. (2007) Environmental assessment of plug-in hybrid electric vehicles. EPRI. [Online]. Available: http://www.epri.com/abstracts/Pages/ProductAbstract.aspx?ProductId=000000000001015325

[44] M. Fotuhi-Firuzabad and R. Billinton, "Impact of load management on composite system reliability evaluation short-term operating benefits," *IEEE Trans. Power Syst.*, vol. 15, no. 2, pp. 858–864, May 2000.

[45] M. D. Galus, S. Koch, and G. Andersson, "Provision of load frequency control by PHEVs, controllable loads, and a cogeneration unit," *IEEE Trans. Ind. Electron.*, vol. 58, no. 10, pp. 4568–4582, Oct. 2011.

[46] D. L. Geier and G. M. Samaniego, "Evaluation of load management as an electric system resource," *IEEE Trans. Power Syst.*, vol. 1, no. 3, pp. 40–45, Aug. 1986.

[47] C. Guille and G. Gross, "A conceptual framework for the vehicle-to-grid (V2G) implementation," *Energy Policy*, vol. 37, no. 11, pp. 4379–4390, Nov. 2009.

[48] S. Han, S. Han, and K. Sezaki, "Development of an optimal vehicle-to-grid aggregator for frequency regulation," *IEEE Trans. Smart Grid*, vol. 1, no. 1, pp. 65–72, Jun. 2010.

[49] E. Hirst, "Reliability benefits of price-responsive demand," vol. 22, no. 11, pp. 16–21, Nov. 2002.

[50] D. Huang and R. Billinton, "Effects of wind power on bulk system adequacy evaluation using the well-being analysis framework," *IEEE Trans. Power Syst.*, vol. 24, no. 3, pp. 1232–1240, Aug. 2009.

[51] ——, "Effects of load sector demand side management applications in generating capacity adequacy assessment," *IEEE Trans. Power Syst.*, vol. 27, no. 1, pp. 335–343, Feb 2012.

[52] H. Huang, C. Y. Chung, K. W. Chan, and H. Chen, "Quasi-Monte Carlo based probabilistic small signal stability analysis for power systems with plug-in electric vehicle and wind power integration," *IEEE Trans. Power Syst.*, vol. 28, no. 3, pp. 3335–3343, Aug. 2013.

[53] IEEE Task Force, "IEEE reliability test system," *IEEE Trans. Power App. Syst.*, vol. PAS-98, no. 6, pp. 2047–2054, Nov./Dec. 1979.

[54] D. T. D. James and J. Fleck, "The relationship of personality to punctuality for a variety of types of appointment," *Pers. and Indiv. Differ.*, vol. 7, no. 1, pp. 95–102, Jan. 1986.

[55] F. Katiraei, M. R. Iravani, and P. Lehn, "Micro-grid autonomous operation during and subsequent to islanding process," *IEEE Trans. Power Del.*, vol. 20, no. 1, pp. 248–257, Jan. 2005.

[56] W. Kempton and J. Tomić, "Vehicle-to-grid power fundamentals: Calculating capacity and net revenue," *J. Power Sources*, vol. 144, no. 1, pp. 268–279, Jun. 2005.

[57] W. Kempton, J. Tomi, S. Letendre, A. Brooks, and T. Lipman. (2001) Vehicle-to-grid power: Battery, hybrid, and fuel cell vehicles as resources for distributed electric power in California. [Online]. Available: http://escholarship.org/uc/item/5cc9g0jp

[58] W. Kempton, U. Victor, K. Huber, K. Komara, S. Letendre, S. Baker, D. Brunner, and N. Pearre. (2009) A test of vehicle-to-grid (V2G) for energy storage and frequency regulation in the PJM system. [Online]. Available: http://www.magicconsortium.org/_Media/test-v2g-in-pjm-jan09.pdf

[59] D. K. Khatod, V. Pant, and J. Sharma, "Analytical approach for well-being assessment of small autonomous power systems with solar and wind energy sources," *IEEE Trans. Energy Convers.*, vol. 25, no. 2, pp. 535–545, Jun. 2010.

[60] M. C. Kisacikoglu, B. Ozpineci, and L. M. Tolbert, "Examination of a PHEV bidirectional charger system for V2G reactive power compensation," in *Applied Power Electronics Conference and Exposition (APEC), 2010 Twenty-Fifth Annual IEEE*, Feb. 2010, pp. 458–465.

[61] A. Leite da Silva, L. C. de Resende, L. A. da Fonseca Manso, and R. Billinton, "Well-being analysis for composite generation and transmission systems," *IEEE Trans. Power Syst.*, vol. 19, no. 4, pp. 1763–1770, Nov. 2004.

[62] G. Li, P. Zhang, P. B. Luh, W. Li, Z. Bie, C. Serna, and Z. Zhao, "Risk analysis for distribution systems in the northeast U.S. under wind storms," *IEEE Trans. Power Syst.*, vol. 29, no. 2, pp. 889–898, Mar. 2014.

[63] C. Liu, K. T. Chau, D. Wu, and S. Gao, "Opportunities and challenges of vehicle-to-home, vehicle-to-vehicle, and vehicle-to-grid technologies," *Proc. IEEE*, vol. 101, no. 11, pp. 2409–2427, Nov. 2013.

[64] Z. Liu, F. Wen, and G. Ledwich, “Optimal planning of electric-vehicle charging stations in distribution systems,” *IEEE Trans. Power Del.*, vol. 28, no. 1, pp. 102–110, Jan. 2013.

[65] J. A. P. Lopes, F. J. Soares, and P. M. R. Almeida, “Integration of electric vehicles in the electric power system,” *Proc. IEEE*, vol. 99, no. 1, pp. 168–183, Jan. 2011.

[66] U. K. Madawala and D. J. Thrimawithana, “A bidirectional inductive power interface for electric vehicles in V2G systems,” *IEEE Trans. Ind. Electron.*, vol. 58, no. 10, pp. 4789–4796, Oct. 2011.

[67] M. Merabti, P. Fergus, O. Abuelma’atti, H. Yu, and C. Judice, “Managing distributed networked appliances in home networks,” *Proc. IEEE*, vol. 96, no. 1, pp. 166–185, Jan. 2008.

[68] A. R. Metke and R. L. Ekl, “Security technology for smart grid networks,” *IEEE Trans. Smart Grid*, vol. 1, no. 1, pp. 99–107, Jun. 2010.

[69] MiD-2002. (2002) Mobilität in Deutschland. DIW Berlin & DLR-Institut für Verkehrs-forschung. [Online]. Available: www.clear-ingstelle-verkehr.de

[70] K. Moslehi and R. Kumar, “A reliability perspective of the smart grid,” *IEEE Trans. Smart Grid*, vol. 1, no. 1, pp. 57–64, Jun. 2010.

[71] J. Park, J. Choi, M. Shahidehpour, K. Y. Lee, and R. Billinton, “New efficient reserve rate index of power system including renewable energy generators,” in *Innovative Smart Grid Technologies (ISGT), 2010*, Jan. 2010, pp. 1–6.

[72] A. Pregelj, M. Begovic, and A. Rohatgi, “Recloser allocation for improved reliability of DG-enhanced distribution networks,” *IEEE Trans. Power Syst.*, vol. 21, no. 3, pp. 1442–1449, Aug. 2006.

[73] Z. Qin, W. Li, and X. Xiong, “Generation system reliability evaluation incorporating correlations of wind speeds with different distributions,” *IEEE Trans. Power Syst.*, vol. 28, no. 1, pp. 551–558, Feb. 2013.

[74] C. Quinn, D. Zimmerle, and T. H. Bradley, “The effect of communication architecture on the availability, reliability, and economics of plug-in hybrid electric vehicle-to-grid ancillary services,” *J. Power Sources*, vol. 195, no. 5, pp. 1500–1509, Mar. 2010.

[75] P. Rietveld, "Rounding of arrival and departure times in travel surveys: An interpretation in terms of scheduled activities," *J. Transportation Stat.*, vol. 5, no. 1, pp. 71–82, 2002.

[76] K. M. Rogers, R. Klump, H. Khurana, A. A. Aquino-Lugo, and T. J. Overbye, "An authenticated control framework for distributed voltage support on the smart grid," *IEEE Trans. Smart Grid*, vol. 1, no. 1, pp. 40–47, Jun. 2010.

[77] K. M. Rogers, R. Klump, H. Khurana, and T. J. Overbye, "Smart-grid-enabled load and distributed generation as a reactive resource," in *Innovative Smart Grid Technologies (ISGT), 2010*, Jan. 2010, pp. 1–8.

[78] B. D. Russell and C. L. Benner, "Intelligent systems for improved reliability and failure diagnosis in distribution systems," *IEEE Trans. Smart Grid*, vol. 1, no. 1, pp. 48–56, Jun. 2010.

[79] H. Salehfar and A. D. Patton, "Modeling and evaluation of the system reliability effects of direct load control," *IEEE Trans. Power Syst.*, vol. 4, no. 3, pp. 1024–1030, Aug. 1989.

[80] C. Singh and A. Lago-Gonzalez, "Reliability modeling of generation systems including unconventional energy sources," *IEEE Trans. Power App. Syst.*, vol. PAS-104, no. 5, pp. 1049–1056, May 1985.

[81] E. Sortomme and M. A. El-Sharkawi, "Optimal charging strategies for unidirectional vehicle-to-grid," *IEEE Trans. Smart Grid*, vol. 2, no. 1, pp. 131–138, Mar. 2011.

[82] ——, "Optimal scheduling of vehicle-to-grid energy and ancillary services," *IEEE Trans. Smart Grid*, vol. 3, no. 1, pp. 351–359, Mar. 2012.

[83] P. Stopher, C. FitzGerald, and M. Xu, "Assessing the accuracy of the Sydney Household Travel Survey with GPS," *Transportation*, vol. 34, no. 6, pp. 723–741, Jun. 2007.

[84] J. Tomić and W. Kempton, "Using fleets of electric-drive vehicles for grid support," *J. Power Sources*, vol. 168, no. 2, pp. 459–468, Jun. 2007.

[85] D. P. Tuttle and R. Baldick, "The evolution of plug-in electric vehicle-grid interactions," *IEEE Trans. Smart Grid*, vol. 3, no. 1, pp. 500–505, Mar. 2012.

[86] U.S. Department of Transportation, Federal Highway Administration. (2009) National Household Travel Survey (NHTS). [Online]. Available: http://nhts.ornl.gov/download.shtml

[87] C. Walsh, S. Carroll, A. Eastlake, and P. Blythe. (2010) Electric vehicle driving style and duty variation performance study. [Online]. Available: http://www.cenex.co.uk/

[88] L. Wang, "The effects of uncertainties in forced outage rates and load forecast on the loss-of-load probability (LOLP)," *IEEE Trans. Power App. Syst.*, vol. 96, no. 6, pp. 1920–1927, Nov. 1977.

[89] W. Wangdee and R. Billinton, "Bulk electric system well-being analysis using sequential Monte Carlo simulation," *IEEE Trans. Power Syst.*, vol. 21, no. 1, pp. 188–193, Feb. 2006.

[90] B. D. Williams and K. S. Kurani, "Commercializing light-duty plug-in/plug-out hydrogen-fuel-cell vehicles: Mobile electricity technologies and opportunities," *J. Power Sources*, vol. 166, no. 2, pp. 549–566, Apr. 2007.

[91] S. G. Wirasingha, N. Schofield, and A. Emadi, "Plug-in hybrid electric vehicle developments in the US: Trends, barriers, and economic feasibility," in *Vehicle Power and Propulsion Conference, 2008. VPPC '08. IEEE*, Sep. 2008, pp. 1–8.

[92] D. Wu, D. C. Aliprantis, and K. Gkritza, "Electric energy and power consumption by light-duty plug-in electric vehicles," *IEEE Trans. Power Syst.*, vol. 26, no. 2, pp. 738–746, May 2011.

[93] D. Wu, D. C. Aliprantis, and L. Ying, "Load scheduling and dispatch for aggregators of plug-in electric vehicles," *IEEE Trans. Smart Grid*, vol. 3, no. 1, pp. 368–376, Mar. 2012.

[94] N. Z. Xu and C. Y. Chung, "Well-being analysis of generating systems considering electric vehicle charging," *IEEE Trans. Power Syst.*, vol. 29, no. 5, pp. 2311–2320, Sep. 2014.

[95] Y. Xu and C. Singh, "Power system reliability impact of energy storage integration with intelligent operation strategy," *IEEE Trans. Smart Grid*, vol. 5, no. 2, pp. 1129–1137, Mar. 2014.

[96] ——, "Adequacy and economy analysis of distribution systems integrated with electric energy storage and renewable energy resources," *IEEE Trans. Power Syst.*, vol. 27, no. 4, pp. 2332–2341, Feb. 2012.

[97] H. M. Yang, C. Y. Chung, and J. H. Zhao, "Application of plug-in electric vehicles to frequency regulation based on distributed signal acquisition via limited communication," *IEEE Trans. Power Syst.*, vol. 28, no. 2, pp. 1017–1026, May 2013.

[98] W. Yao, J. Zhao, F. Wen, Y. Xue, and G. Ledwich, "A hierarchical decomposition approach for coordinated dispatch of plug-in electric vehicles," *IEEE Trans. Power Syst.*, vol. 28, no. 3, pp. 2768–2778, Aug. 2013.

[99] H. Yu, C. Y. Chung, K. P. Wong, and J. H. Zhang, "A chance constrained transmission network expansion planning method with consideration of load and wind farm uncertainties," *IEEE Trans. Power Syst.*, vol. 24, no. 3, pp. 1568–1576, Aug. 2009.